TECHNICAL REPORT STANDARD TITLE PAGE

1. Report No.	2. Government Accession No.	3. Recipient's Catalog No.
FHWATX78-1882F		

4. Title and Subtitle	5. Report Date
STRENGTH AND BEHAVIOR OF STAGE-CAST INVERTED T-BEAMS	August 1978
	6. Performing Organization Code

7. Author(s)	8. Performing Organization Report No.
Richard W. Furlong	Research Report 188-2F

9. Performing Organization Name and Address	10. Work Unit No.
Center for Highway Research The University of Texas at Austin Austin, Texas 78712	11. Contract or Grant No. Research Study 3-5-75-188
	13. Type of Report and Period Covered
12. Sponsoring Agency Name and Address Texas State Department of Highways and Public Transportation; Transportation Planning Division P. O. Box 5051 Austin, Texas 78763	Final
	14. Sponsoring Agency Code

15. Supplementary Notes

Study conducted in cooperation with the U. S. Department of Transportation, Federal Highway Administration. Research Study Title: "Failure Criteria for Precast Elements of Composite Inverted T-Beams"

16. Abstract

On the basis of tests involving both positive moment and negative moment loading on inverted T-beams, the performance and strength of monolithically cast specimens and stage-cast specimens were compared. Variables included the ratio between flange depth and overall beam depth and the amount of tensile reinforcement used in negative moment specimens. It can be concluded that the positive moment behavior of the stage-cast beams was just as strong, and actually stiffer and more ductile than the behavior of monolithic cast specimens under service load forces. At service load forces the negative moment stage-cast specimens displayed the same stiffness and ductility as monolithic cast specimens, and they were just as strong as monolithic cast specimens only for the beams with a flange thickness to beam depth ratio of 0.41. Specimens with the flange thickness to beam depth ratio equal to 0.27 did not possess in the stage-cast specimens as much strength or ductility as did the monolithic cast beams. It was also observed that undesirable cracking can remain in the stage-cast beams if crack sizes on the flanges during construction are allowed to reach the limit size (0.004 in.) before web concrete is cast and cured.

17. Key Words	18. Distribution Statement
T-beams, inverted, stage-cast, behavior, strength, variables, stiffness, ductility, cracking	No restrictions. This document is available to the public through the National Technical Information Service, Springfield, Virginia 22161.

19. Security Classif. (of this report)	20. Security Classif. (of this page)	21. No. of Pages	22. Price
Unclassified	Unclassified	102	

Form DOT F 1700.7 (8-69)

STRENGTH AND BEHAVIOR OF STAGE-CAST INVERTED T-BEAMS

by

Richard W. Furlong

Research Report 188-2F

Project 3-5-75-188

Failure Criteria for Precast Elements of Composite Inverted T-Beams

Conducted for

Texas
State Department of Highways and Public Transportation

In Cooperation with the
U. S. Department of Transportation
Federal Highway Administration

by

CENTER FOR HIGHWAY RESEARCH
THE UNIVERSITY OF TEXAS AT AUSTIN

August 1978

The contents of this report reflect the views of the author who is responsible for the facts and accuracy of the data presented herein. The contents do not necessarily reflect the views or policies of the Federal Highway Administration. This report does not constitute a standard, specification, or regulation.

There was no invention or discovery conceived or first actually reduced to practice in the course of or under this contract, including any art, method, process, machine, manufacture, design, or composition of matter, or any new and useful improvement thereof, or any variety of plant which is or may be patentable under the patent laws of the United States of America or any foreign country.

S U M M A R Y

On the basis of tests involving both positive moment and negative moment loading on inverted T-beams, the performance and strength of monolithically cast specimens and stage-cast specimens were compared. Variables included the ratio between flange depth and overall beam depth and the amount of tensile reinforcement used in negative moment specimens. It can be concluded that the positive moment behavior of the stage-cast beams was just as strong, and actually stiffer and more ductile than the behavior of monolithic cast specimens under service load forces. At service load forces the negative moment stage-cast specimens displayed the same stiffness and ductility as monolithic cast specimens, and they were just as strong as monolithic cast specimens only for the beams with a flange thickness to beam depth ratio of 0.41. Specimens with the flange thickness to beam depth ratio equal to 0.27 did not possess in the stage-cast specimens as much strength or ductility as did the monolithic cast beams. It was also observed that undesirable cracking can remain in the stage-cast beams if crack sizes on the flanges during construction are allowed to reach the limit size (0.004 in.) before web concrete is cast and cured.

I M P L E M E N T A T I O N

Inverted T-beams can be cast in stages with the flange cast first and used thereafter to support stringers while the web of the T beam is formed for casting integrally with the stringers and even the deck slab. With only one precaution, the service load and the ultimate strength performance of such stage-cast inverted T-beams will be as satisfactory as the performance and strength to be expected from the same members cast monolithically. The single precaution involves negative moment regions of members for which the flange is less than 40 percent as thick as the overall composite member. The flexural cracks that are created by construction loading may lead to service load cracks larger than those which can be tolerated for exterior exposure of the structure. The service load strength and ductility for "thin" flange negative moment regions is adequate, but not as good as that of the same members cast monolithically.

Strength design criteria are acceptably accurate for stage-cast members subjected either to positive moment or negative moment. In positive moment regions most service load response characteristics of stage-cast inverted T-beams are actually better than such characteristics for the same beams cast monolithically.

C O N T E N T S

LIST OF TABLES

L I S T O F F I G U R E S

CHAPTER 1

INTRODUCTION

1.1 General

A beam is said to be stage-cast if one or more components of the beam are cast and cured before the remaining parts are cast. Stage-casting of reinforced concrete or prestressed concrete members permits economies in the construction process if one component of a member can be used in lieu of falsework or even field formwork while additional components of the member are cast. The use of precast stringers to support formwork during the casting of a composite slab for the stringers represents perhaps the most familiar form of a stage-cast member.

It has been found expedient and economical to use a cast-in-place flange of a highway bridge bent cap girder to support the weight of stringers while the web of the bent cap girder is formed and cast with the stringers in place. The use of a stage-cast inverted T-beam bent cap girder, as illustrated in Fig.1.1 eliminates the need for forming and casting separate end diaphragms for the stringers.

1.2 Behavior

In the cantilevered portion of a bent cap, the bottom portion of the flange is put into compression as it supports the stringers, formwork, its own weight, and the weight of the deck slab and web before the web gains strength. Although these stresses (and strains) may be quite high in magnitude because of the comparatively small depth of the flange, they are never relieved before traffic loads are permitted to create still more compression in the flange which now acts compositely with the web. The flange portion which was in tension during construction may provide some compression reserve, but only if the neutral axis of the composite section

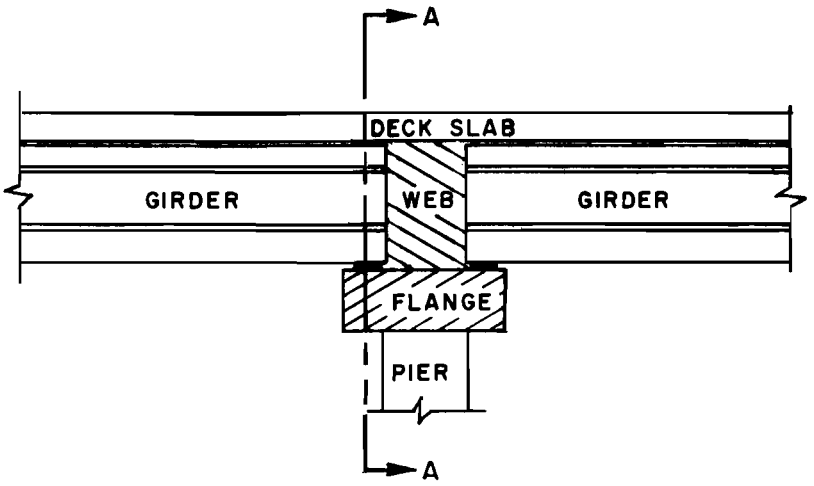

(a) SIDE VIEW

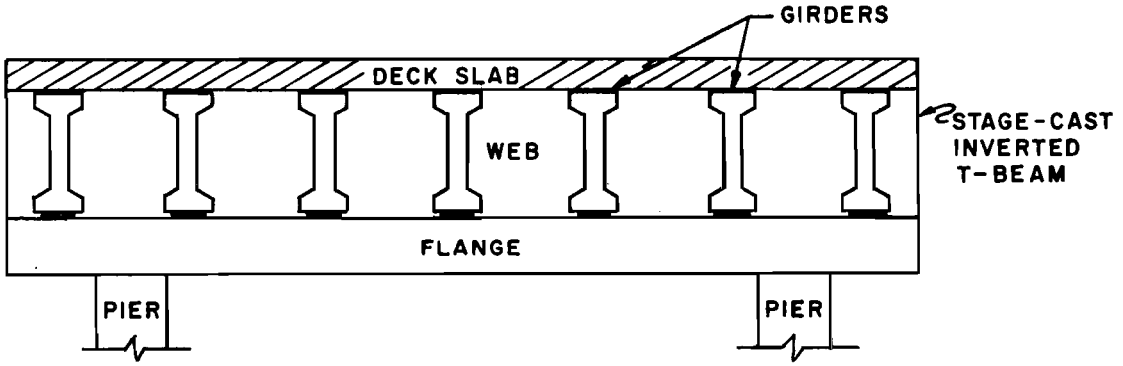

(b) SECTION A-A

Fig. 1.1 Highway bridge bent cap

at ultimate load is farther from the compression face than the neutral axis of the flange during the first stage (construction) loading.

In positive moment regions the bottom steel is required to resist the stresses due to construction loads prior to hardening of the web. As the lever arm of the flange section is much smaller than that of the T-section, the high tensile strain in the steel will permit flexural cracks in the flange. These cracks are never relieved before the traffic loads are permitted to cause additional tension in the same steel when it acts as the reinforcement for the T-section. Since crack width is related more to steel strain and concrete cover than to strain gradient, it is possible that live loads on the stage-cast T-section may extend and widen the already large dead load cracks to unacceptable sizes. However, the precompressed zone of concrete in the flange may help in restraining the further extension of dead load cracks when the precompressed upper portion of the flange becomes a part of the tension zone of the composite T-section. The extent and size of web cracks in a stage-cast inverted T-beam may also be affected by the thickness of the flange. The precompressed zone of a thicker flange would be closer to the neutral axis of the composite T-section and may restrain the size and extent of web cracks more effectively.

In negative moment regions the construction loads create compression in the bottom part of the flange, while significant tensile forces and concrete cracking occur at the top of the flange. After the web is cast and web concrete hardens, the flexural response is changed because the neutral axis of the overall cross section is raised to a new position. Even though live loading on the bridge stringers will increase compressive stress at the bottom of the web, the gradient of flexural stress is reduced significantly from the gradient that existed when the flange acted alone.

The shrinkage of web concrete on the precast web should tend to reduce the size of tension cracks at the top of the preloaded flange, but conversely, the flange restraint to shrinkage of web concrete as it cures

would encourage the formation of vertical cracks in the web. As live loads are added to the composite stage-cast member, there is some question about the gross capacity of the flange concrete that is continually in compression. It is possible that the total compression zone necessary to force flexural steel to yield in tension may involve concrete fibers that were in tension before the stage-cast web was cast. The question arises whether or not a nominal surface strain of 0.3 percent and a rectangular stress block approximation of concrete at ultimate remain applicable. A related question arises involving changes in the overall ductility of stage-cast members in flexure prior to failure.

For both positive and negative moment regions of stage-cast members, the nonplanar distribution of strains may modify the usual assumptions that should be used for flexural stiffness of members after cracking. Flexural stiffness may be influenced also by the creep displacements that may occur in the flange during construction. Dead load forces that create creep in the flange are never removed, and it is known[1,2] that after some creep has occurred there is a stiffened response to subsequent application of load. Will stage-cast members possess more stiffness to live load than monolithic-cast members of the same proportions?

1.3 Purpose of Study

The purpose of this study was to investigate the performance of stage-cast inverted T-beams as they support construction loads as the web concrete cures, and thereafter as "live" load is superimposed on the composite stage-cast member. The capacity of the stage-cast members is to be studied also as "live" loads are increased well beyond service load levels.

Service load performance of reinforced concrete in flexure is reflected most vividly by the pattern of cracks that develop under applied load. Therefore, for positive moment and for negative moment, test specimens were proportioned such that the neutral axis of the composite stage-cast specimen either would be moved from the flange into the web, or it would remain in the flange.

Specific objectives of the study involve a search for answers to the following questions:

(1) Are crack widths in stage-cast members larger or smaller than crack widths in monolithically cast members?

(2) Can a close spacing of cracks in a precast flange propagate and create a closer spacing of cracks in the web of stage-cast beams?

(3) How does stage-casting affect live load flexural stiffness?

(4) How does stage-casting affect ultimate load flexural ductility?

(5) In the flanges of a negative moment region of an inverted T beam, does the rectangular stress block analysis of concrete capacity continue to give an accurate estimate of flexural capacity?

(6) Should there be a special construction load design condition for proportioning stage-cast inverted T beams?

CHAPTER 2

SPECIMENS AND LOADING

2.1 General

The study of physical specimens involved a matrix of eight specimens that were constructed and tested at the Civil Engineering Structures Research Laboratory of The University of Texas at Austin. The sketch of Fig. 2.1 illustrates the three categories that were considered for the design of specimens, the casting method (stage-cast or monolithic), the loading method (positive bending or negative bending), and the relative flange size (thick or thin).

The specimen marking system evolved largely from the loading requirements of each specimen. A general beam symbol BM was used as a prefix followed by the beam type for the loading category, S for simply supported positive moment and C for cantilevered negative moment. A fourth letter symbol P was used to identify those specimens for which the flange was preloaded for stage-casting, but no fourth letter was used to identify monolithically cast members. Thin-flanged members were cast and loaded before the thick-flanged members, and the numerical sequence number 1 identifies thin-flanged members, while 2 identifies thick-flanged members as indicated in Fig. 2.1. The specimen marked BMCP2 is a beam with negative moment cantilever loading. It is preloaded for stage-casting and it is proportioned for the thicker flange.

2.2 Design Criteria

Stage-cast specimens were designed such that stresses in the tensile steel of the first stage would reach the 40 to 45 ksi range before the concrete of the second stage could cure and modify subsequent strain gradients as loads were increased on the composite stage-cast specimens. The stress of 45 ksi was considered to be the highest likely construction

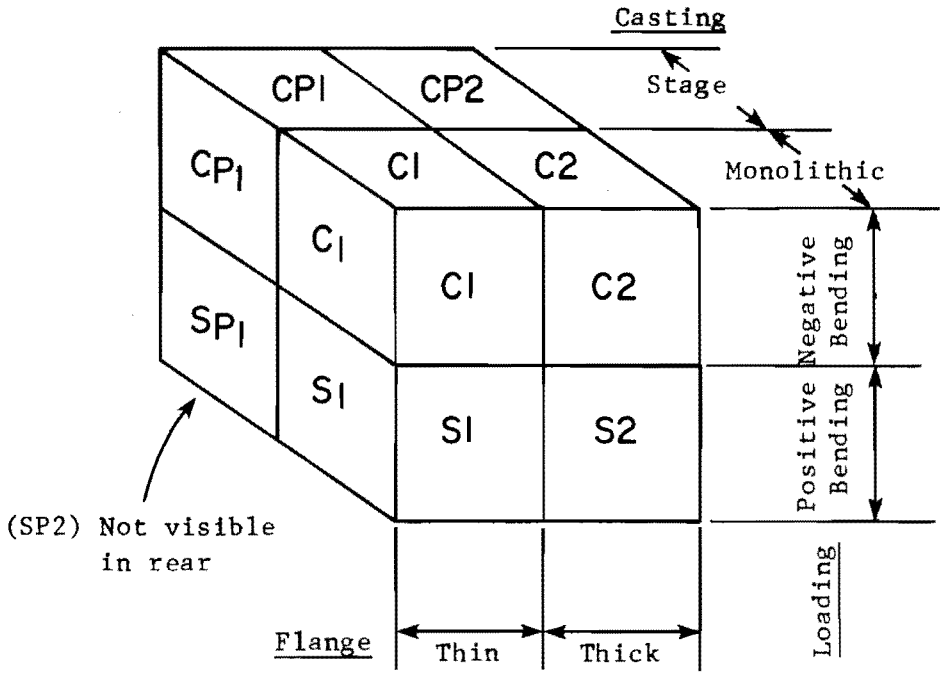

Fig. 2.1 Categories and specimen marking

load stress consistent with the proportioning of the flange according to the strength design method. Under AASHTO criteria, a net load factor of 1.30 can exist when only dead loads are significant for member design, as is the case for the construction loads of stage-cast members. With the flexural capacity reduction factor φ taken as 0.9, the product of 0.9 x 60 ksi divided by 1.30 produces a possible stress near 42 ksi.

Positive moment specimens were proportioned with a web width and height such that the tensile steel of the flange should equal about 60 percent of the balanced steel ratio for the composite inverted T-beam. The use of less ductile ratios of tensile steel should be discouraged, and the 60 percent value is considered to be near an upper limit for practical purposes. The same tension bars that support flexural load on positive moment specimens must also support flexural forces on the composite cross sections subjected to positive moment.

Flexural tension bars on the stage-cast flange of negative moment specimens could not provide effective tension resistance when flexural loads were applied to the negative moment specimens. A second set of tension reinforcement was used for negative bending specimens. The amount of tensile reinforcement at the top of the web for one end of each negative moment specimen was selected to be consistent with design live load requirements of the composite member if live load were considered to be almost the same as dead load. At the opposite end of each negative moment specimen, the tensile reinforcement at the top of the web was made large enough to force the neutral axis of the composite cross section to be located in the web of the member above the flange.

Stirrup reinforcement and transverse steel for the flanges was proportioned to resist with a comfortable margin of reliability the shear forces that were necessary to cause flexural failure. Design of such reinforcement was made in accordance with recommendations of Ref. 8.

Grade 60 reinforcement and 4000 psi concrete were assumed for the design of all specimens.

2.3 Specimen Details

The details of member dimensions with the size, length, and location of all reinforcement for each specimen are given in Figs. 2.2 through 2.5. Duplicate specimens were constructed for each of the four configurations of beam specimens; one of each pair was cast monolithically and the other was stage-cast.

Horizontal bars that were placed across the top of the flanges perpendicular to the web were welded to U-shaped stirrup bars across the bottom of the flanges. The welded assembly assured the development of anchorage for cantilever flexural action of the bars at the top of the flanges, and provided also a closed stirrup for the flange itself.

Measured dimensions of each specimen are given in Table 2.1. The values that are listed represent the average of measurements that were made prior to each test. Four or more measurements were made in order to establish each average value listed.

2.4 Forms

Plywood forms were used for the construction of all specimens. The monolithic-cast specimens could be constructed from one set of forms. The stage-cast specimens have to be constructed with two separate sets of forms. Since the same 16 in. web height was used for all specimens, the thickness of flanges could be controlled in the forms simply by changing the side forms attached to a common bottom form. Monolithic-cast specimens were constructed with the flange on top, inverted from the position of each specimen for physical testing.

The flanges of stage-cast specimens were cured and then load was applied to represent construction forces on each flange before the web concrete was cast. The loads that were applied to the flanges caused deflections of the flanges, and it was necessary to use a polystyrene fill material of varying thickness in order to permit a variation in the depth of stage-cast members. The top of the web of stage-cast members was

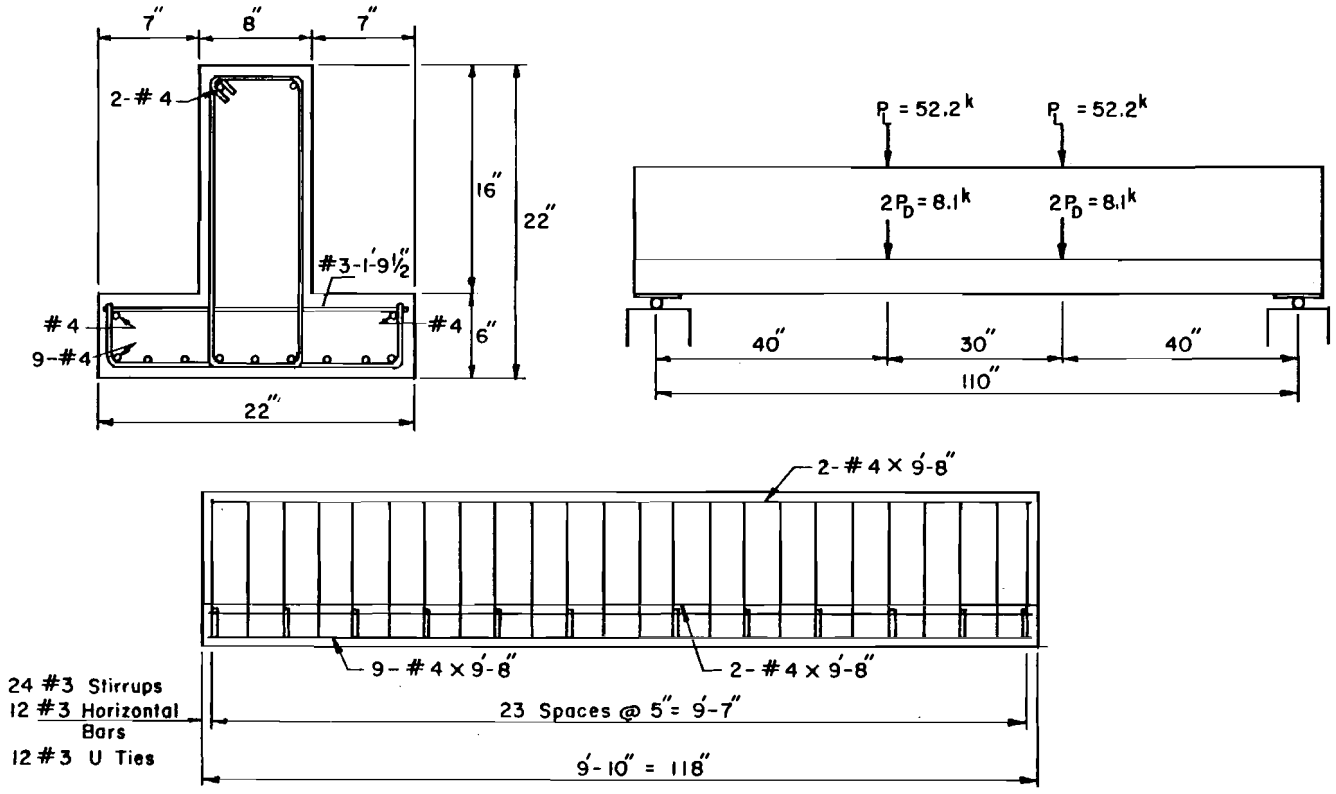

Fig. 2.2 Dimensions, reinforcement, and predicted maximum loads for Beams BMS1 and BMSP1

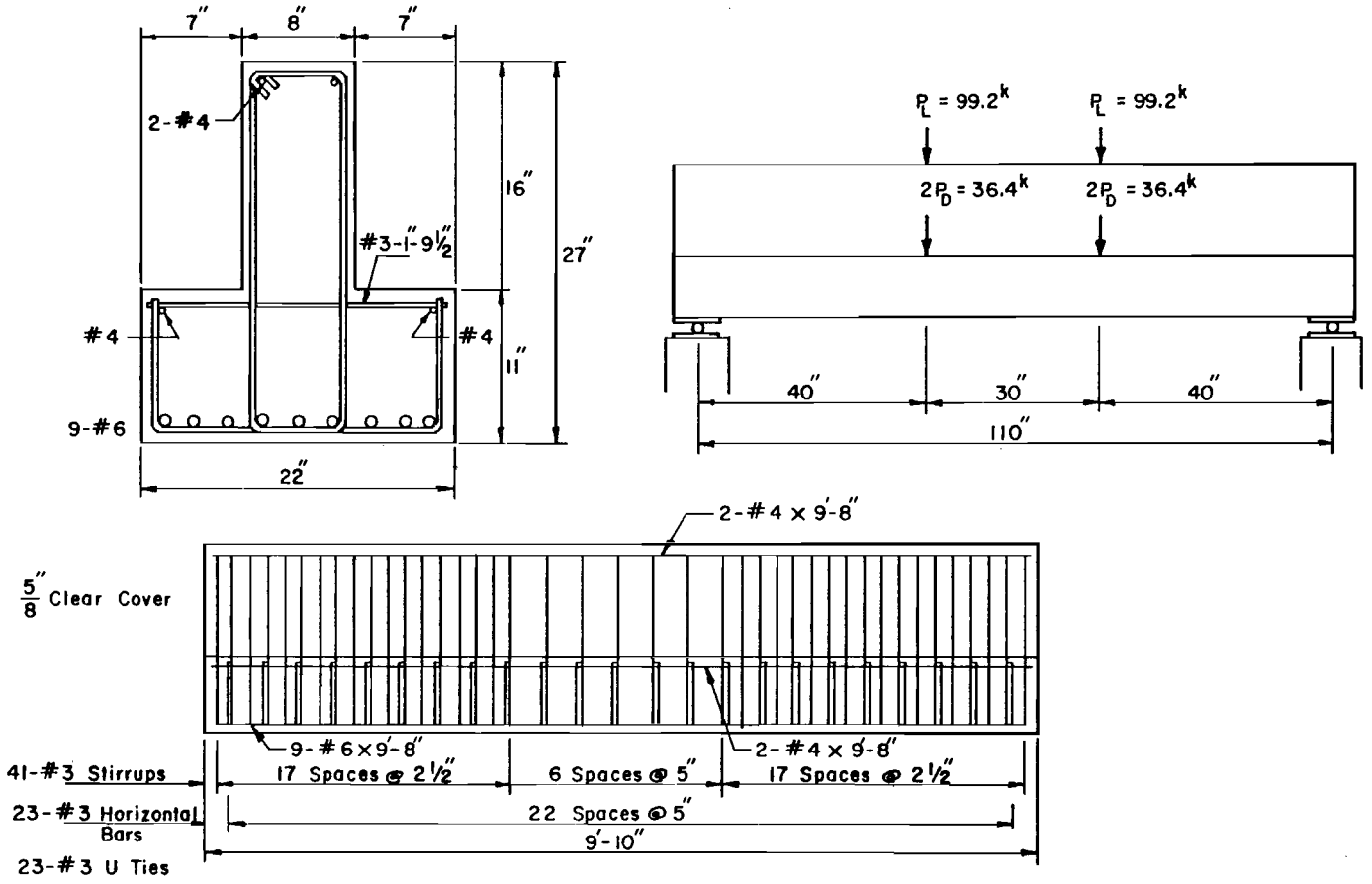

Fig. 2.3 Dimensions, reinforcement, and predicted maximum loads for Beams BMS2 and BMSP2

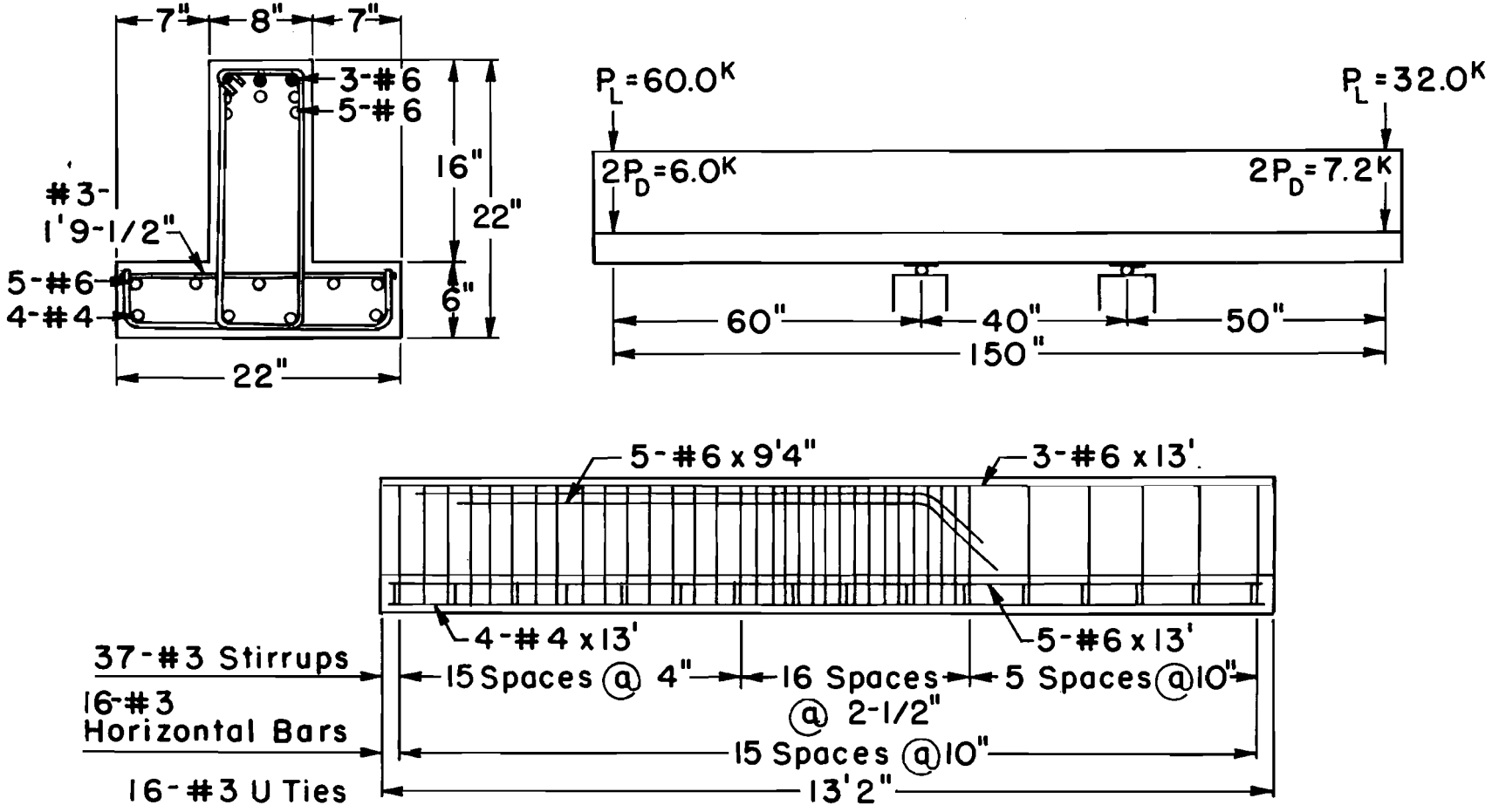

Fig. 2.4 Dimensions, reinforcement, and predicted maximum loads for Beams BMC1 and BMCP1

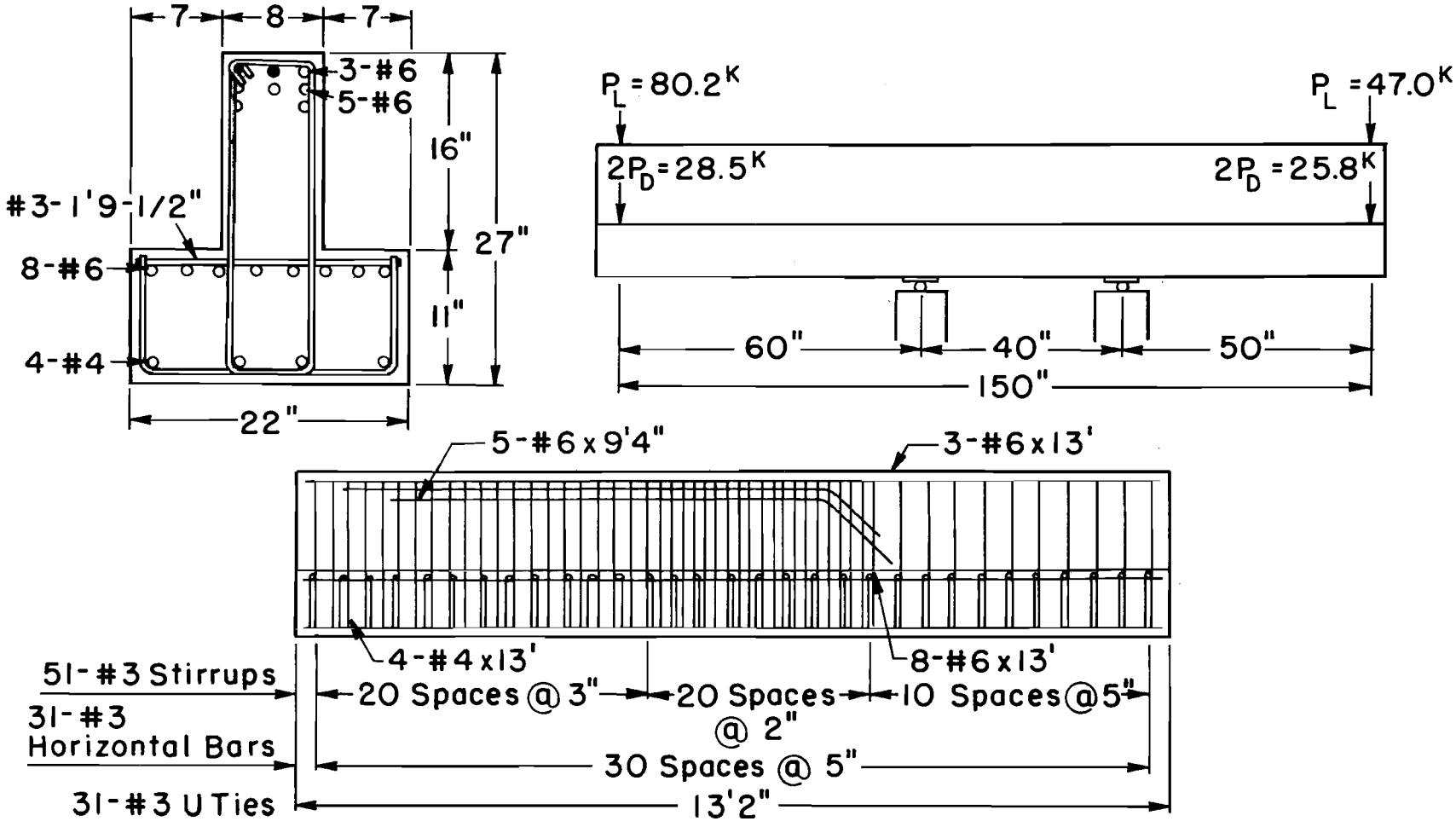

Fig. 2.5 Dimensions, reinforcement, and predicted maximum loads for Beams BMC2 and BMCP2

TABLE 2.1 ACTUAL DIMENSIONS OF SPECIMENS

(a)

Specimen	Avg. breadth of web in constant moment region b_w(in.)	Avg. width of flange in constant moment region b_f(in.)	Avg. depth of web in constant moment region d_w(in.)	Avg. thickness of flange in constant moment region t_f(in.)
BMS1	8.25	22.13	16.16	6.09
BMSP1	9.05	22.19	16.91	6.19
BMS2	8.313	22.29	16.28	11.14
BMSP2	7.875	21.88	16.56	11.08

Span of all beams = 110 in.

(b)

Specimen	Avg. breadth of web at supports b_w (in.)	Avg. width of flange at supports b_f (in.)	Avg. depth of web at supports d_w (in.)	Avg. thickness of flange at supports t_f (in.)
BMC1	8.19	22.00	16.14	6.20
BMCP1	8.03	22.03	16.41	6.25
BMC2	8.22	22.28	16.22	11.11
BMCP2	7.97	22.91	16.31	11.27

Span of all beams = 150 in.

maintained as a straight line. The photographs of Fig. 2.6 illustrate the attachment of web forms for the stage-cast members.

2.5 Material

2.5.1 Concrete. A concrete mix was designed according to Texas State Department of Highway and Public Transportation specifications for achieving a compressive strength of 4000 to 5000 psi. A maximum aggregate size of 3/4 in. was used, and ready mix concrete with a desired slump of 4 in. was delivered to the laboratory. High early strength cement was specified only for the webs of stage-cast specimens. Listed below are typical proportions of the concrete mix used per cubic yard of material.

Cement (Type I or Type III)	564 lbs
Coarse Aggregate	1820 lbs
Fine Aggregate	1450 lbs
Water	230 lbs
Septer Additive	2 oz
Airsene Additive	30 oz

Concrete was placed in the forms and hand held vibrators were used during the casting of each specimen. Forms were removed from specimens after two days, and the specimens were left in the air of the laboratory to cure for at least two more weeks before they were moved and any loads were added.

Control cylinders were made during the casting of each specimen and the average of observed properties for each specimen are listed in Table 2.2. Control cylinders were tested for material strength on the day each specimen was tested.

2.5.2 Reinforcing Steel. Reinforcing steel with a nominal yield strength of 60 ksi was specified for use in all beams. A typical stress-strain curve for the #6 bar longitudinal steel is shown in Fig. 2.6. The average yield strength of the flexural steel for each specimen is listed also in Table 2.2. Tensile strength specimens of reinforcement were

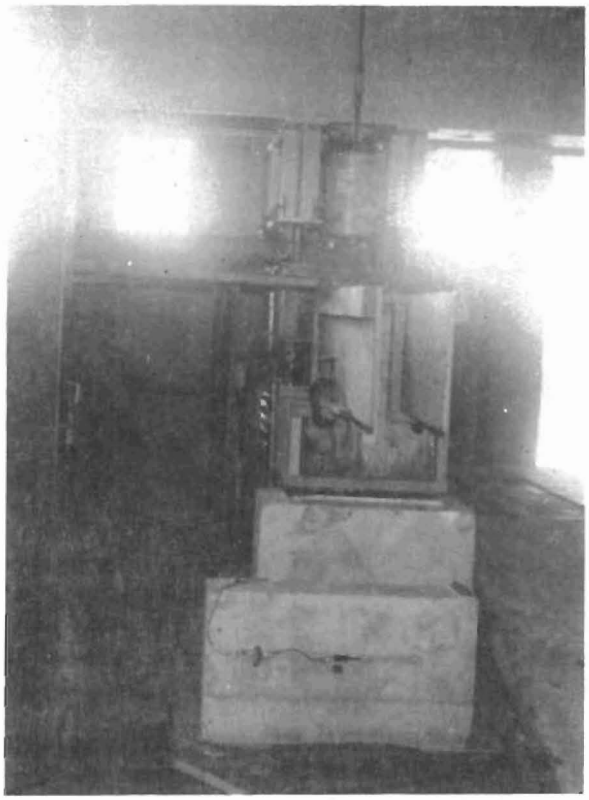

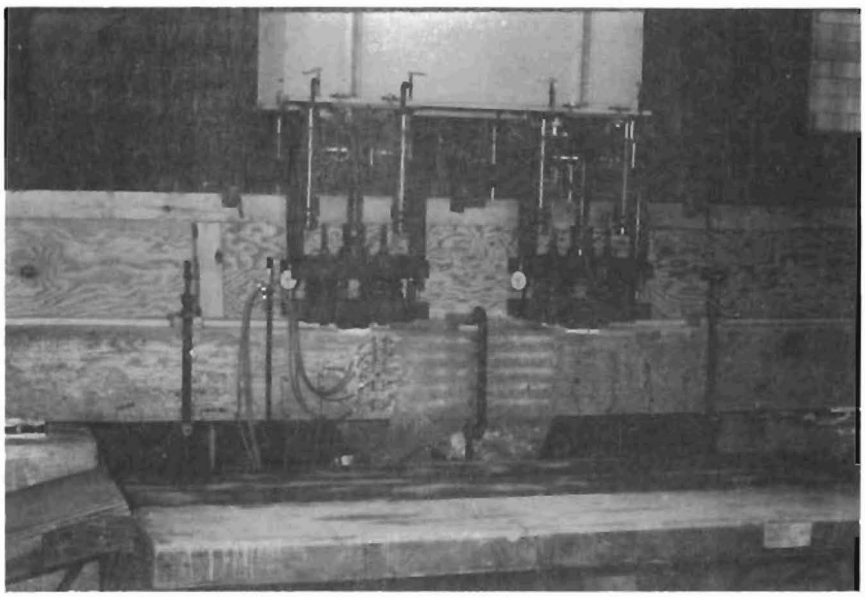

Fig. 2.6 Forming stage-cast web segments

TABLE 2.2 PROPERTIES OF SPECIMENS

Specimen	Avg. yield Stress for tension steel f_y, ksi	f'_c		f_r	
		For flange psi	For web psi	For flange psi	For web psi
BMS1	65.5	4846	4846	515	515
BMSP1	65.5	5540	4004	612	455
BMS2	60.7	5208	5208	553	553
BMSP2	60.7	5173	5540	553	612
BMC1	60.7	4776	4776	451	451
BMCP1	60.7	4776	5047	451	498
BMC2	60.7	4923	4923	429	429
BMCP2	60.7	4923	3927	429	400

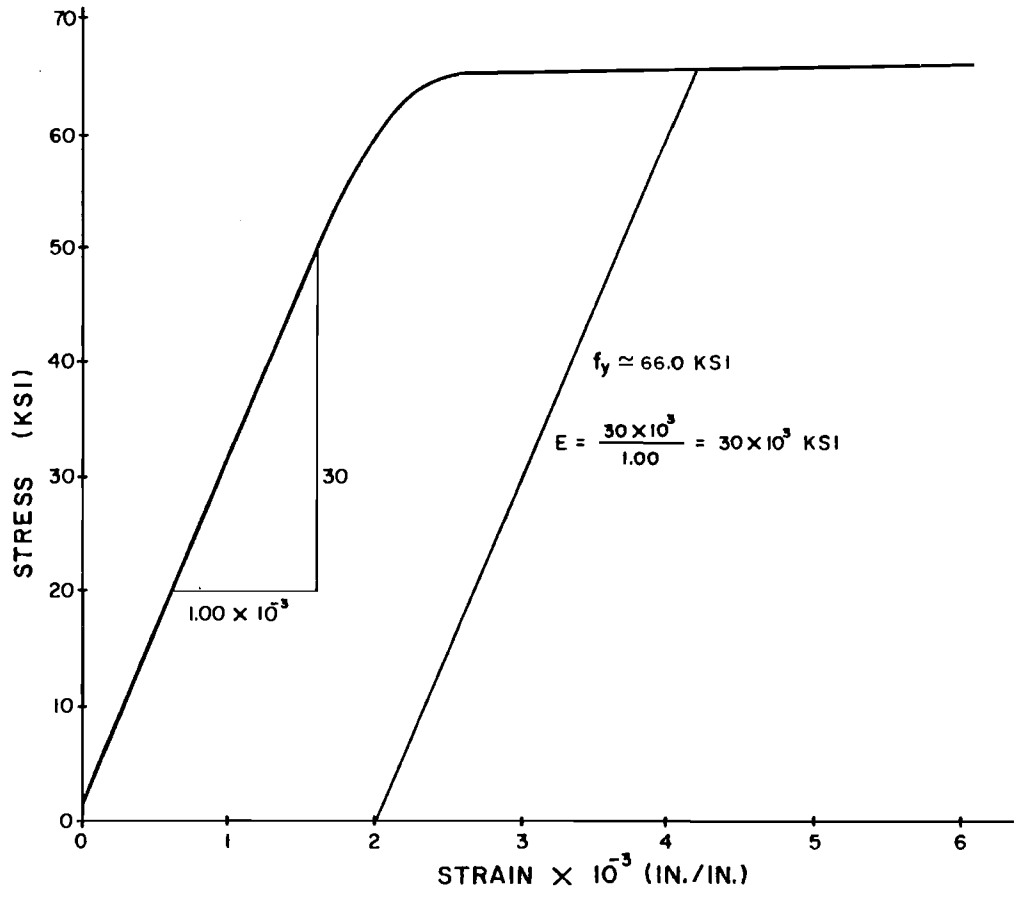

Fig. 2.7 Typical stress-strain curve for steel

tested before the specimens were cast. The average yield strength of four #3 bars that were used for stirrups was 67 ksi and the average yield strength of #4 bars used was 65.5 ksi.

2.6 Loading

Diagrams of Fig. 2.8 and Fig. 2.9 display the arrangement of loads and supports for each of the beams that were used in this study. Loads that were intended to represent dead loads on the flanges were applied at opposite positions on each side of the web of each beam. Additional loads that were applied to the composite member were applied at the top of the flange in the same longitudinal position as flange loads.

For the stage-cast members, the flanges were loaded symmetrically on both sides, as indicated in Fig. 2.8 and in Fig. 2.9. The flange loads were applied to spring assemblies in order that the loads could be maintained with relatively little sensitivity to deformations that might occur due to the creep of concrete under the sustained loads. The spring assemblies were calibrated such that dial indicators revealed the amount of force on each spring assembly. The mechanical jacks that were used to apply load to the spring assemblies could be altered in order that applied loads could be maintained at a constant level during the flange loading period. The forces on spring assemblies were checked and adjusted almost daily.

Forces were applied on top of the webs of specimens by means of hydraulic rams acting against steel loading plates set against the concrete in hydrastone bearings. As the web loads were applied, the flange loads were maintained by means of the mechanical jacks against spring assemblies on the flanges.

The loading sequence for monolithic-cast specimens and for stage-cast specimens tested to failure involved the application of loads in increments initially approximately 1/10 of the estimated failure load for the specimen. As the observed response of each specimen indicated

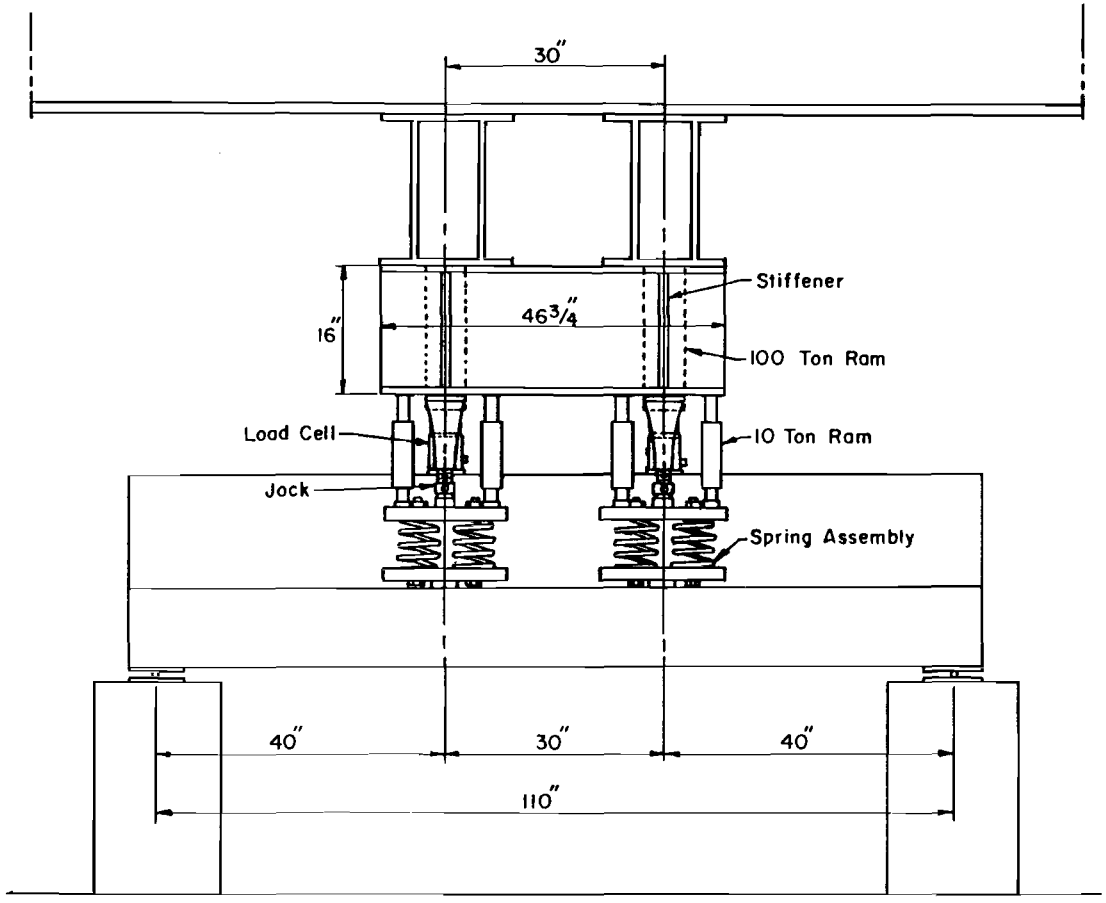

Fig. 2.8 Loading system for simply supported beam

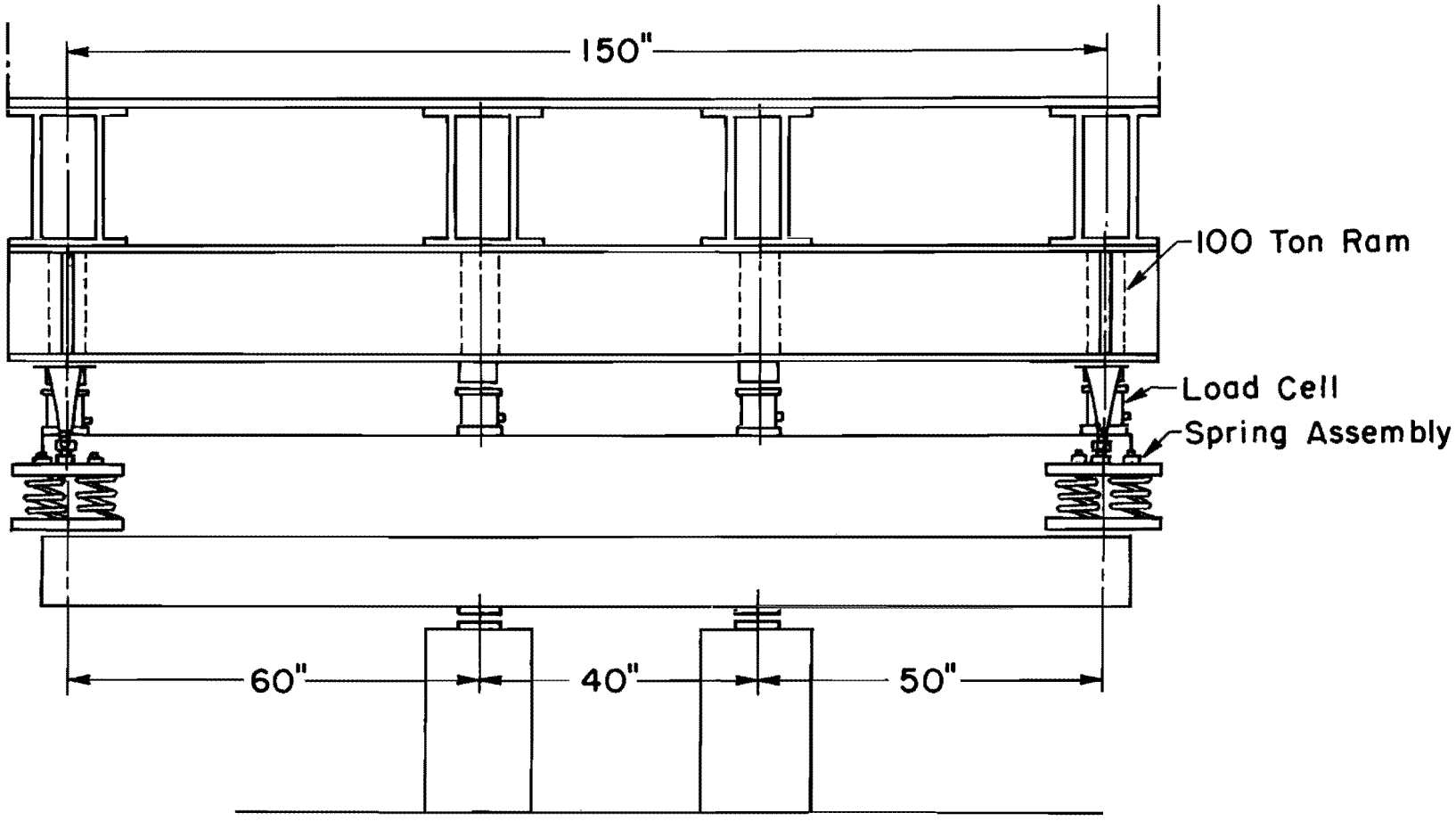

Fig. 2.9 Loading system for cantilever span beam

nonlinear deformations with respect to the magnitude of load, the size of each load increment was reduced.

The magnitude of each load was monitored by means of calibrated spring assemblies, as already indicated. The magnitude of load on hydraulic rams was monitored by load cell and also by hydraulic pressure gages.

2.7 Strain and Displacement Measurements

Strain meters were constructed for the measurement of surface displacements through the height of each member. A surface strain meter is shown in Fig. 2.10. The ends of the strain meter were attached to bolts connected to the sides of the specimen by means of epoxy glue. As the ends of the strain meter distort, strain gages at the center of the meter reveal the amount of change in position between the ends of the strain meter. The use of the electrical signals from these strain meters permitted the research staff to acquire numerous readings in a very short period of time during each test. It was felt that the reading of flexural strength near failure would be enhanced if remote reading equipment were employed for the tests. The research staff calibrated each of the strain meters, and the calibration was checked after each test that involved large measured deformations at the surface of a member.

Strain meters were attached to the sides of the specimens at approximately 2 in. intervals throughout the height of each specimen. The strain meters were located at midspan for positive moment specimens, and the strain meters were located over the supports of negative moment specimens.

Vertical displacements were measured both by dial indicators attached to the floor of the laboratory and by linear displacement transducers that provided an electrical signal for remote recording.

Crack sizes were measured as each test proceeded. The width of the cracks was measured at four to eight stations on each specimen. The stations were located at the more prominent cracks which occurred early in

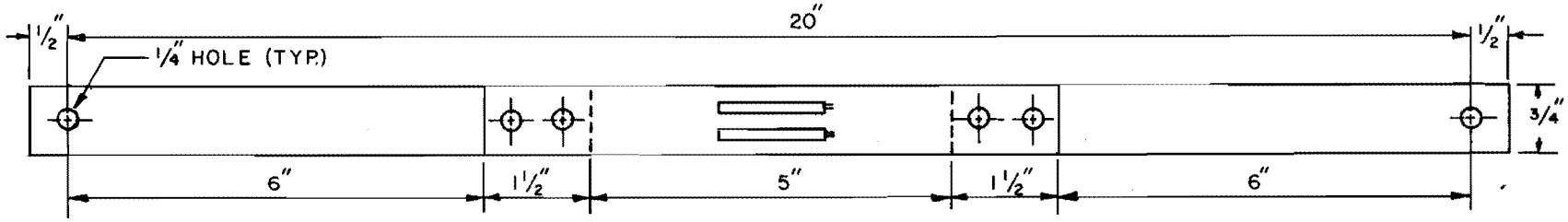

TOP VIEW

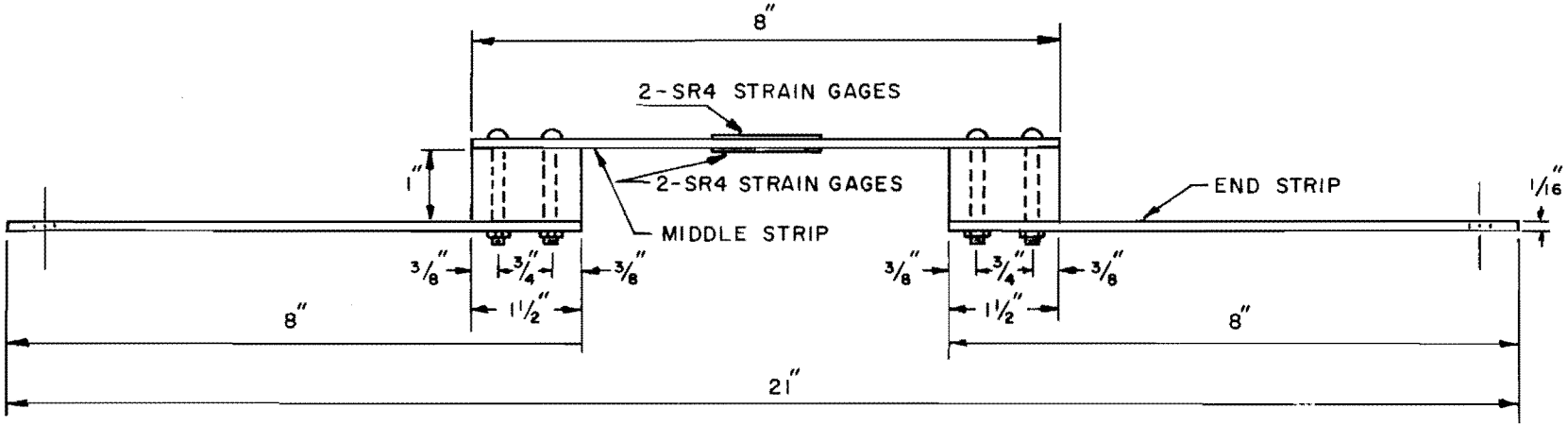

SIDE VIEW

Fig. 2.10 Strain meter

the testing. If new cracks appeared and seemed to be growing at fast rates, the size of the new cracks also was monitored. A magnifying comparator was used in order to estimate the size of cracks that were measured.

CHAPTER 3

TEST RESULTS

The measured responses that were observed for each pair of identical specimens will be displayed together for comparisons of the influence of stage-casting. Positive moment specimens will be discussed before negative moment specimens and each of the three types of response--strain profile, deflection, and crack width--will be presented separately.

3.1 Positive Moment Specimens

Two of the beams, BMS1 and BMSP1, that were simply supported and loaded only for positive moment had "thin" flanges of 6-in. depth, and the other two, BMS2 and BMSP2, had "thick" flanges of 11-in. depth.

3.1.1 Strain Profiles. The variation of strain through the depth of the precast and loaded flanges that were used for the stage-cast members are illustrated in Figs. 3.1 and 3.2. For each of the beam flanges three strain profiles are presented: (1) the strains at half the total applied flange load, (2) the strains immediately after the full flange load had been applied, and (3) the strains after several weeks of sustained loading on the flange. In all cases the strain profiles exhibited a tendency toward nonlinear variation of strain, with tension strains larger than linear variations would indicate. The actual neutral axis was lower than the position predicted by linear strain cracked transformed section theory. The dashed lines of Fig. 3.1 and Fig. 3.2 indicate the theoretical distribution of strains for which steel would be at a stress of 45 ksi. It is of some interest to note that the actual amount of compressed concrete was larger than that which corresponded with elastic cracked section theory, even for the initial loading before creep occurred.

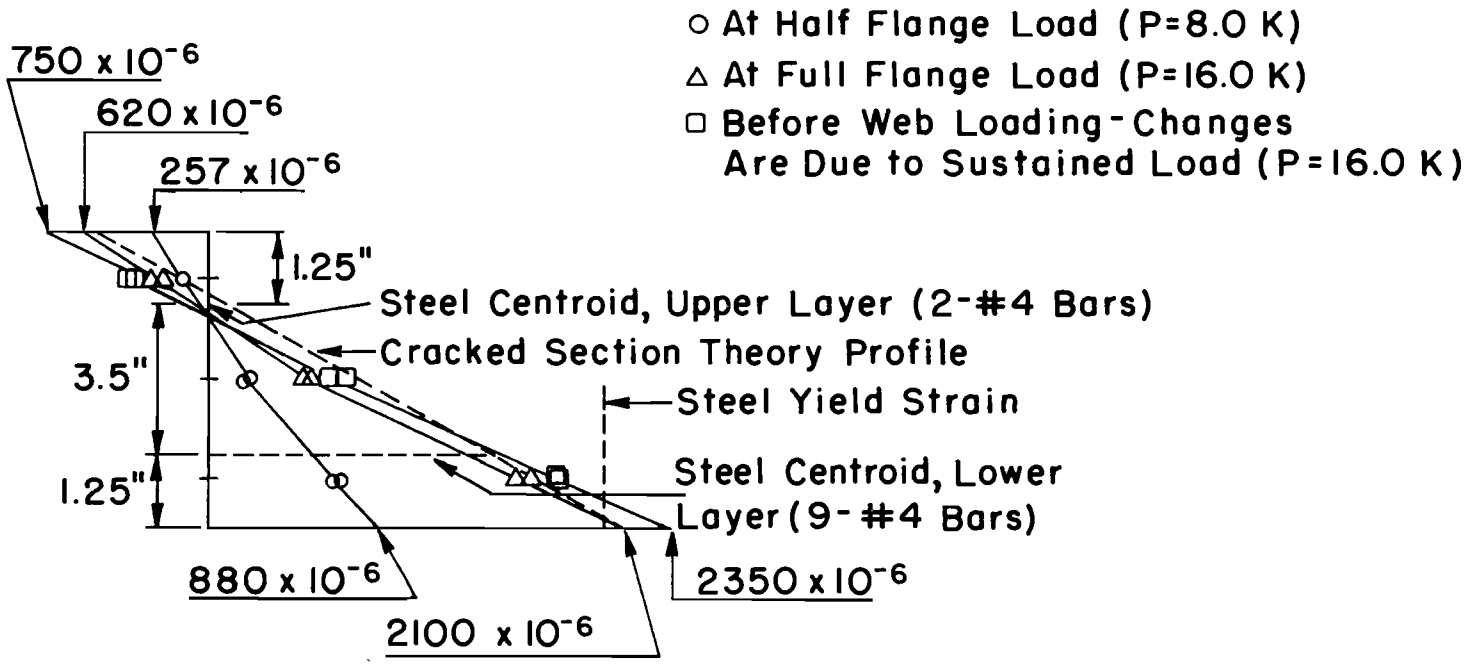

Fig. 3.1 Strain profiles for flange of BMSP1

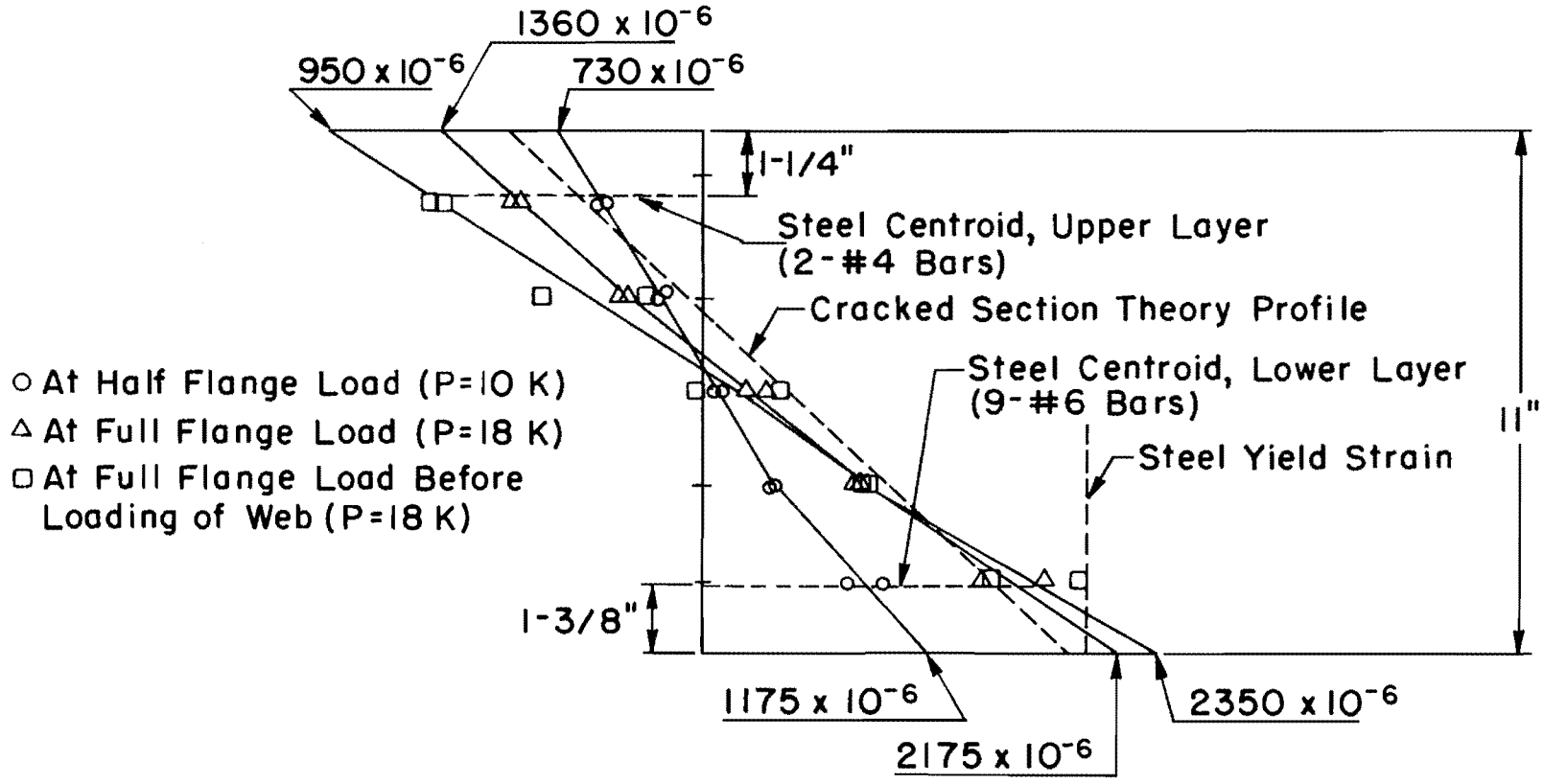

Fig. 3.2 Strain profiles for flange of BMSP2

After creep occurred under the sustained flange loading, maximum flange strains shown in Figs. 3.1 and 3.2 were reached. Under the sustained load there was some increase in tensile strains at the level of reinforcement even though reinforcement is always assumed not to creep. The concrete that surrounds tensile reinforcement may deform (stretch) slightly under sustained load. Figure 3.2 clearly shows considerably more creep strain in compression at the top of the flange than in tension at the bottom of the flange.

The "thin" flange specimens BMS1 and BMSP1 were subjected to positive moment loading until each failed. Strain profiles at three different load levels are displayed for each specimen in Figs. 3.3 and 3.4. The load levels that are displayed represent half the load at which flexural reinforcement first yielded, the yield load for flexural reinforcement, and the maximum (last) load for which strains could be measured.

As loads were increased to the yield load of the steel in the stage-cast specimens, the tensile steel experienced an increase of about 16 ksi stress, and Fig. 3.3 indicates very little change from a linear distribution of strain through the full depth of the stage-cast composite cross section. In some contrast, the strain profiles of Fig. 3.4 for the monolithic cast specimen BMS1 display nonlinear strain profiles for the half-yield and full-yield load conditions during which tensile reinforcement experienced a 60 ksi stress increase. In contrast to the strain profile for the (wide beam) stage-cast flanges, the (narrow beam) web regions of inverted T-beams developed strain gradients with maximum values at the compression face. Before failure took place, the apparent upper limit to tensile strain could be a measurement error, because strain meters could not stretch as far as the tensile region of the specimens.

Strain profiles at half-yield load, yield load, and ultimate load are displayed for the thick flange specimens BMSP2 and BMS2 in Figs. 3.5 and 3.6. Strain profiles for these thicker flange specimens were more nearly linear than were those for the thinner flanges. Elastic cracked

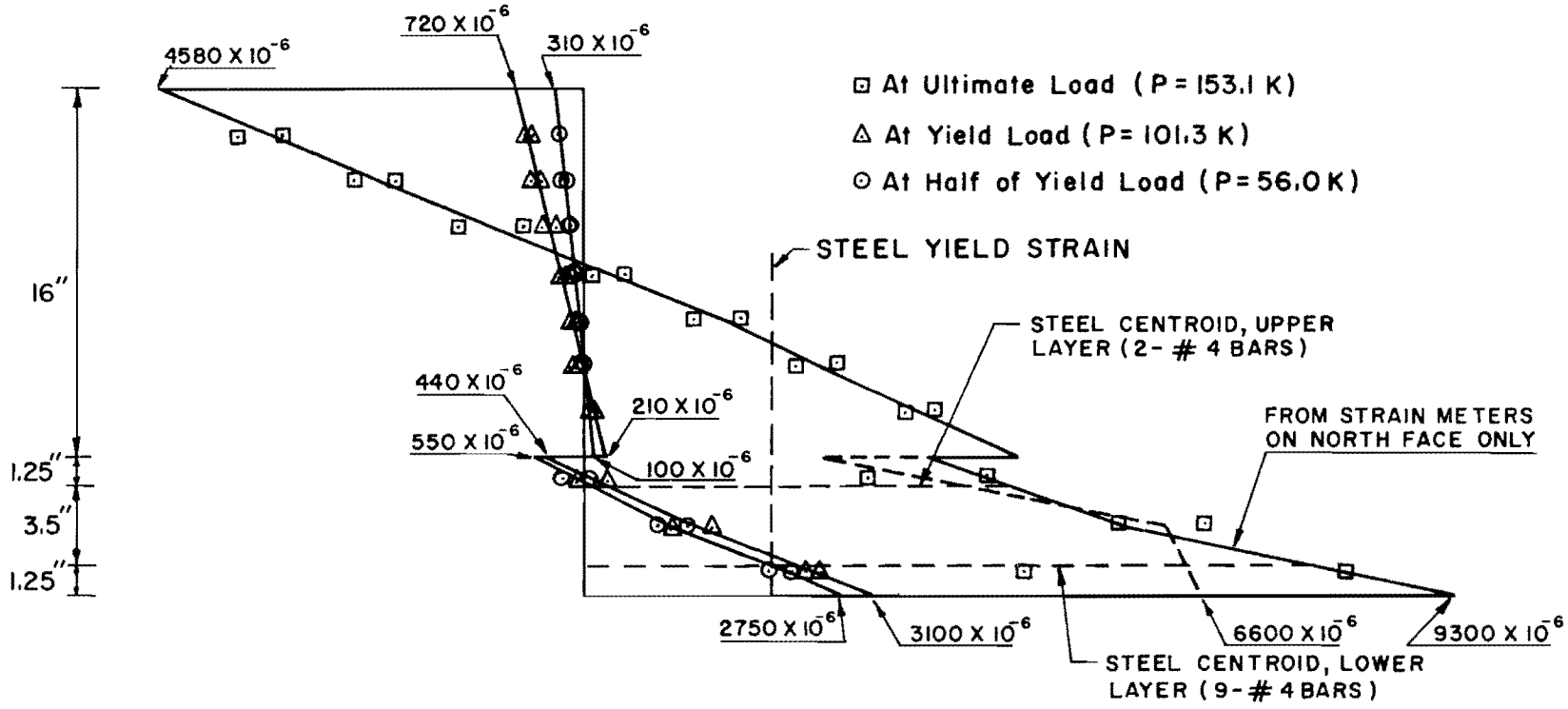

Fig. 3.3 Strain profiles for BMSP1 (composite section)

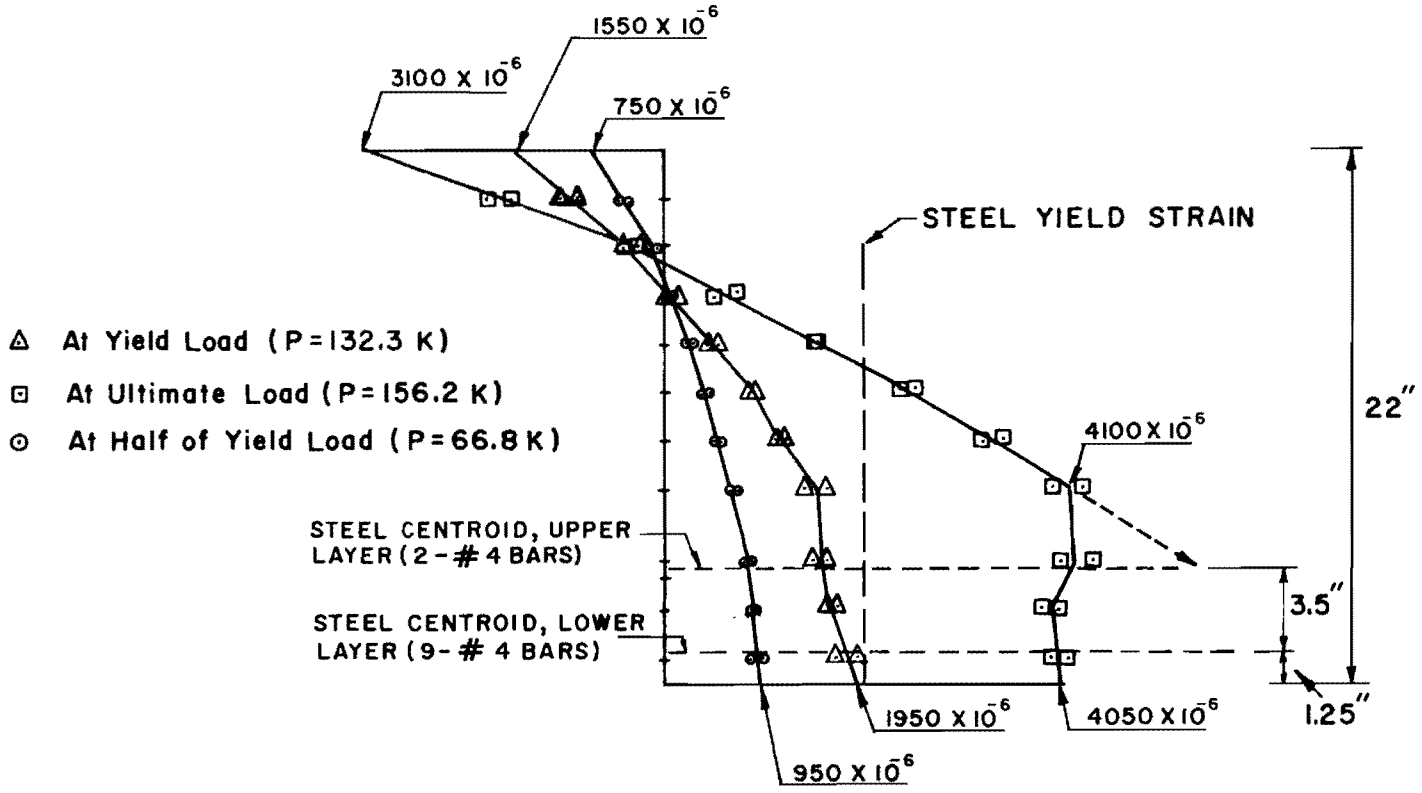

Fig. 3.4 Strain profiles for BMS1

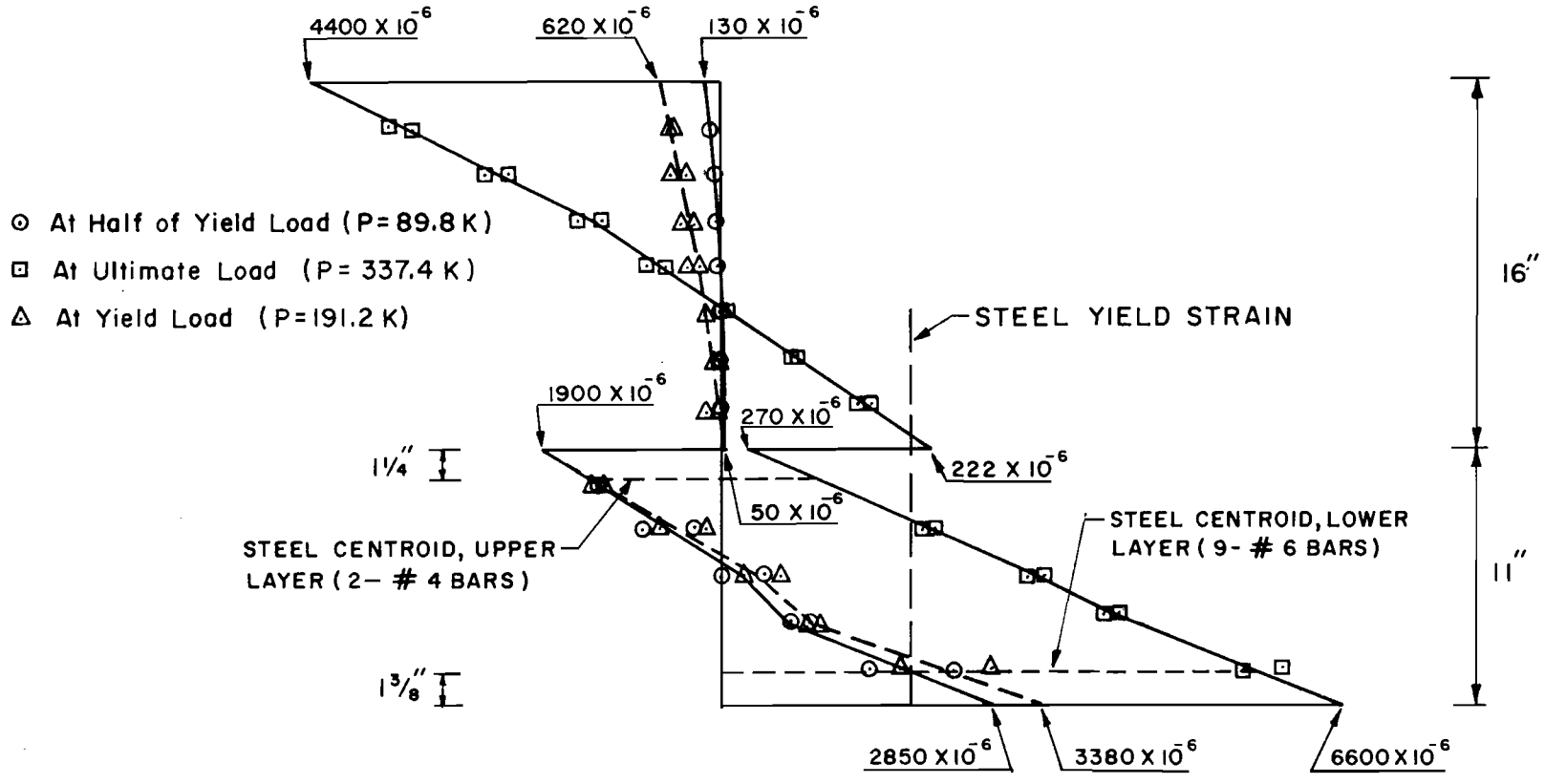

Fig. 3.5 Strain profiles for BMSP2 (composite section)

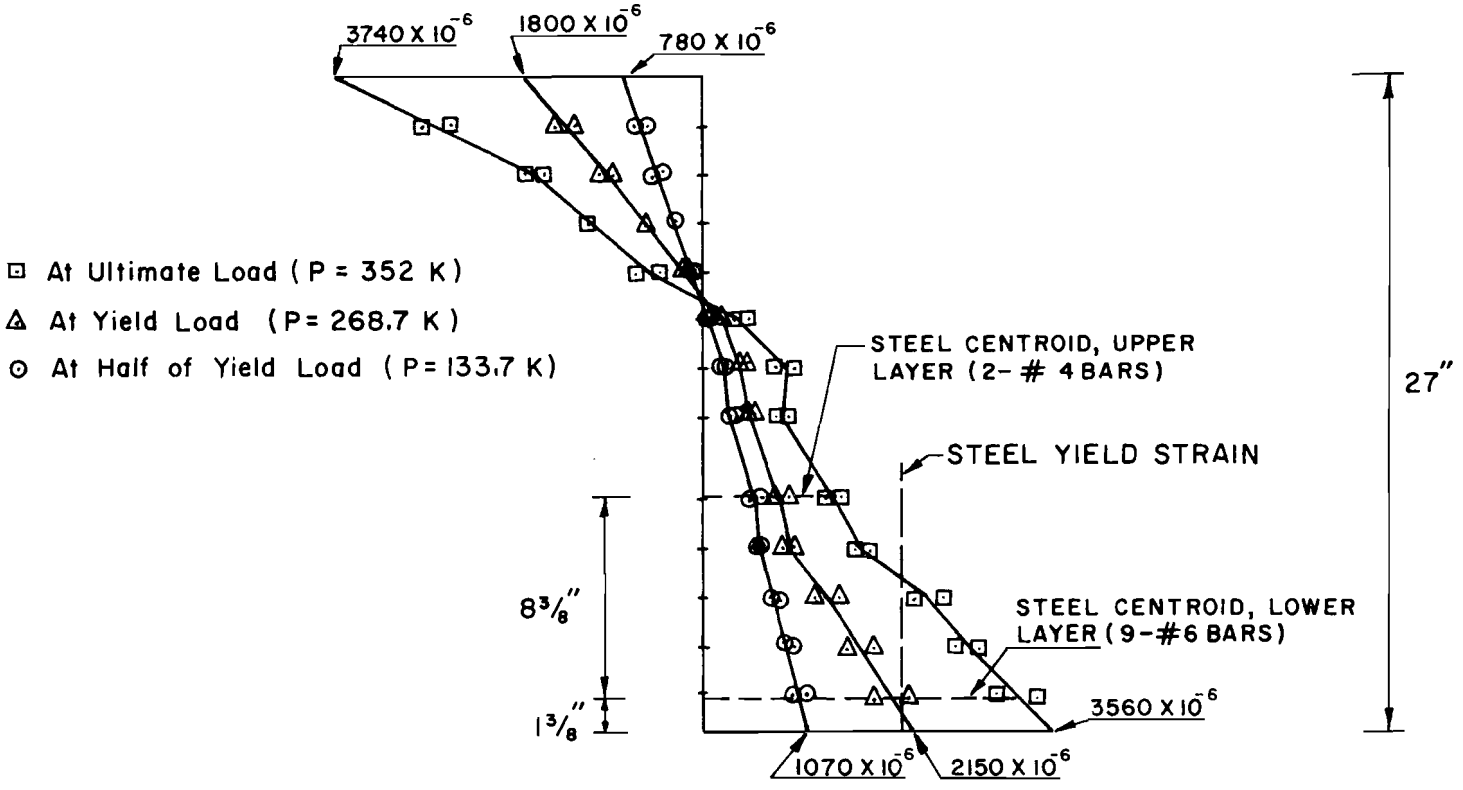

Fig. 3.6 Strain profiles for BMS2

section theory for the monolithic cast beam BMS2 in Fig. 3.6 shows that the actual neutral axis was higher than theory predicted. Again, maximum strain gradients appeared in the compression flanges except for the total strain gradient of the precast flanges shown in Fig. 3.5. Before steel yielded there was very little release of precompressed concrete strain at the top of the stage-cast thick flange; but as loads were increased until tensile flexural steel could yield, the top of the flange eventually experienced only compressive stress before failure.

The almost parallel strain profiles at flanges of stage-cast beams shown in Figs. 3.3 and 3.5 indicate that there was very little alteration of strain distribution due to shrinkage and/or creep after web concrete hardened. After stage-cast webs hardened, the composite member behaved largely as a monolithic member.

The discontinuity of strains between stage-cast flanges and webs have been removed in the strain profiles displayed in Figs. 3.7 and 3.8. These strain profiles illustrate only the change in strain after "live" loads (web loads) were added to each specimen. The profiles were constructed for load cases at which measured curvatures of stage-cast and monolithic-cast companion specimens were almost identical and near the yield load for the monolithic-cast member. The profiles show that linear strain profiles were maintained before yielding on the stage-cast specimens, but not on the monolithic-cast specimens. The webs of stage-cast specimens had to resist considerably lower stresses before steel yielded than did the webs of monolithic-cast specimens. The steeper observed strain profile of monolithic-cast specimens imply that tensile cracking should be larger for these specimens than for stage-cast members.

3.1.2 Deflections. Deflection at midspan was measured by two dial gages. Load-deflection curves plotted in Figs. 3.9 and 3.10 show that the total midspan deflection of stage-cast specimens at ultimate was approximately twice as much as that of the control specimens and that the ultimate load of stage-cast specimens was slightly less than that for control specimens. It may also be interesting to observe that for the

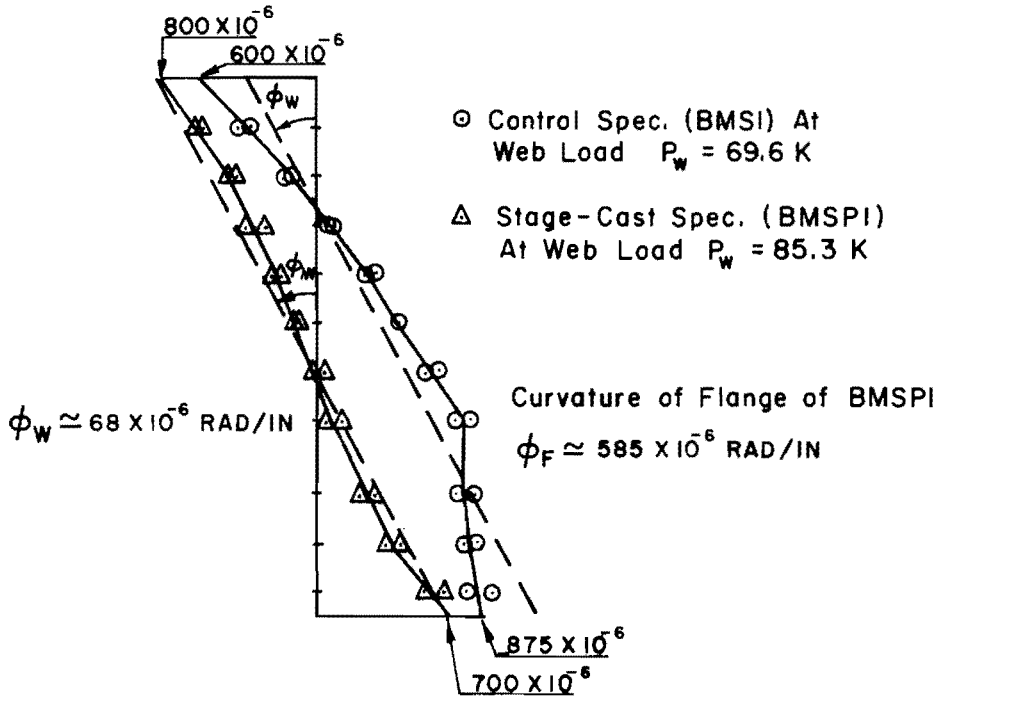

(a) At ϕ_w (Curvature Due to Web Load) $\simeq 68 \times 10^{-6}$ Rad/In

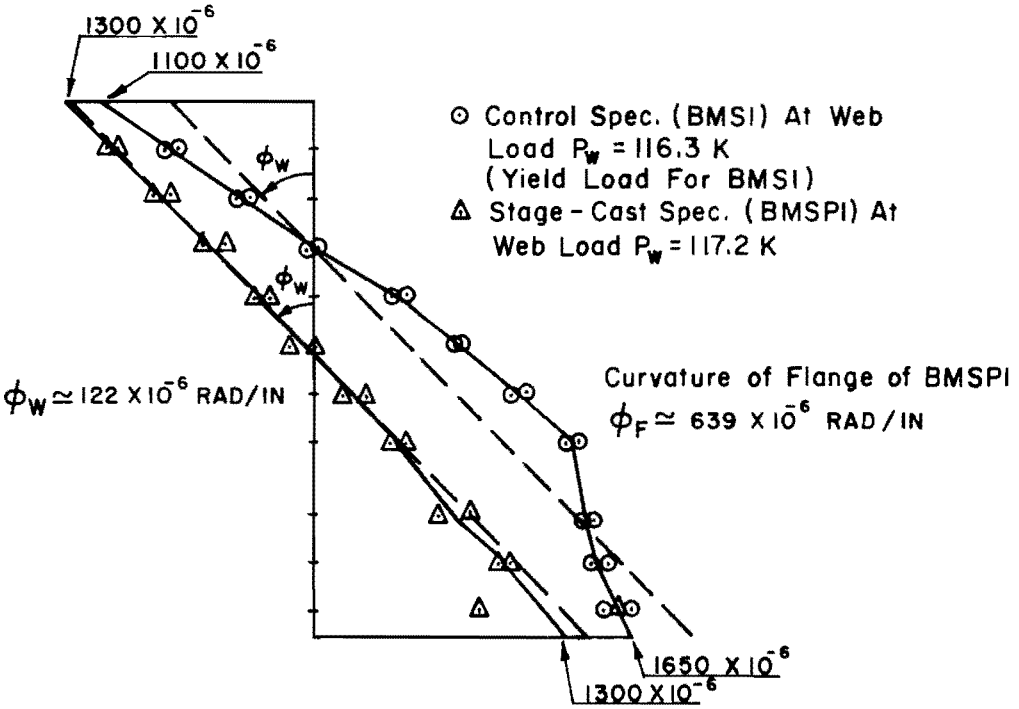

(b) At ϕ_w (Curvature Due to Web Load) $\simeq 122 \times 10^{-6}$ Rad/In

Fig. 3.7 Comparison of live load strain profiles of specimens BMS1 and BMSP1

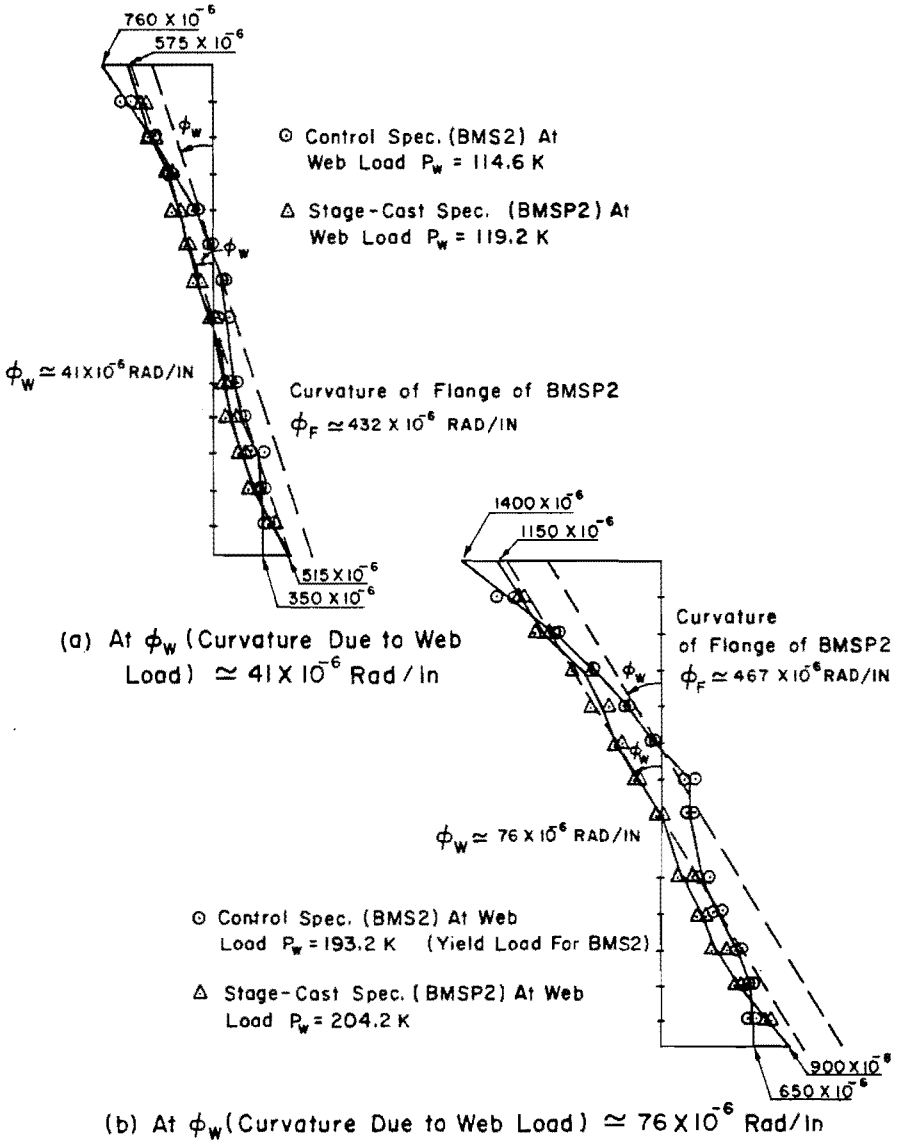

Fig. 3.8 Comparison of live load strain profiles of specimens BMS2 and BMSP2

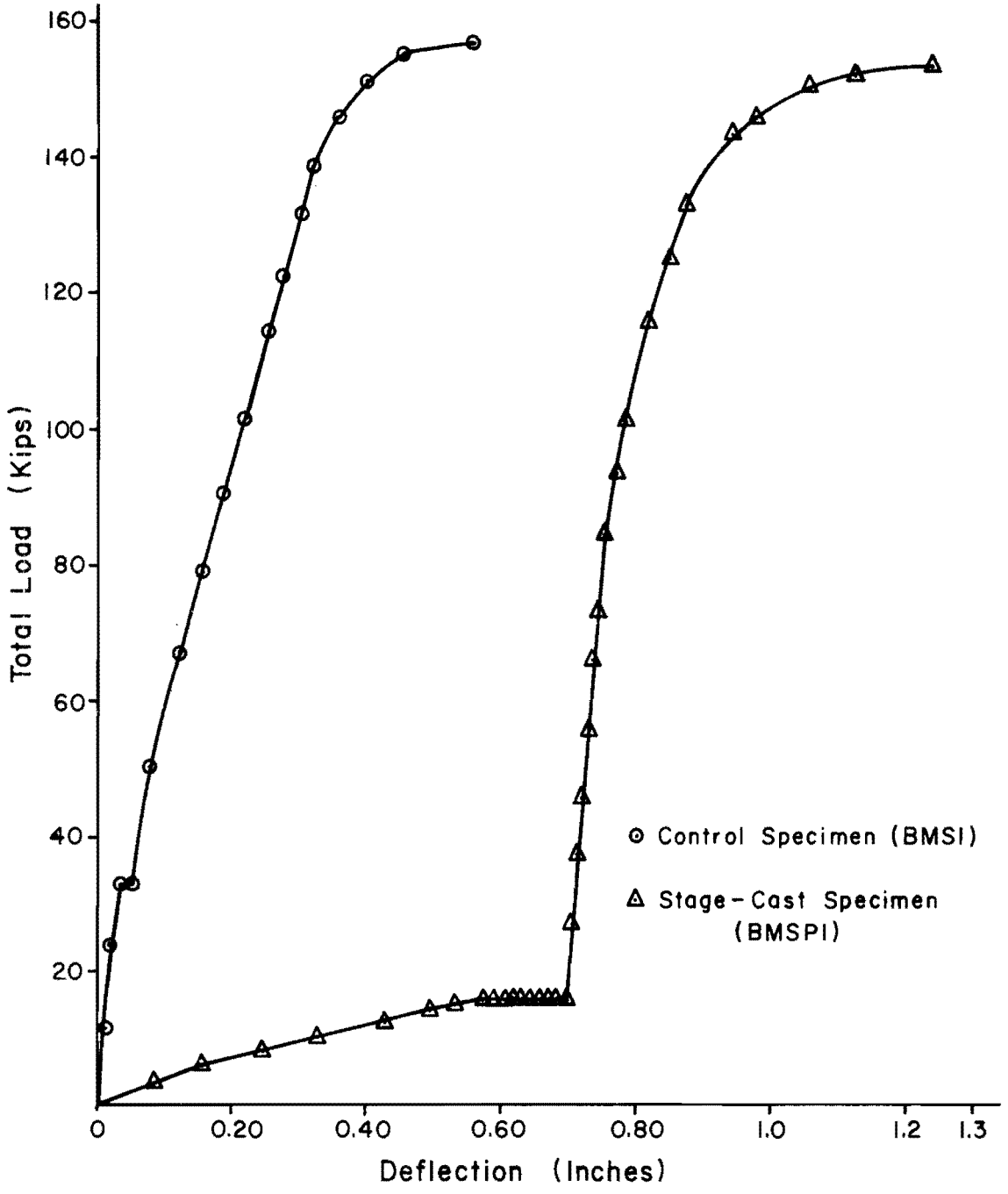

Fig. 3.9 Load-deflection curves for BMS1 and BMSP1

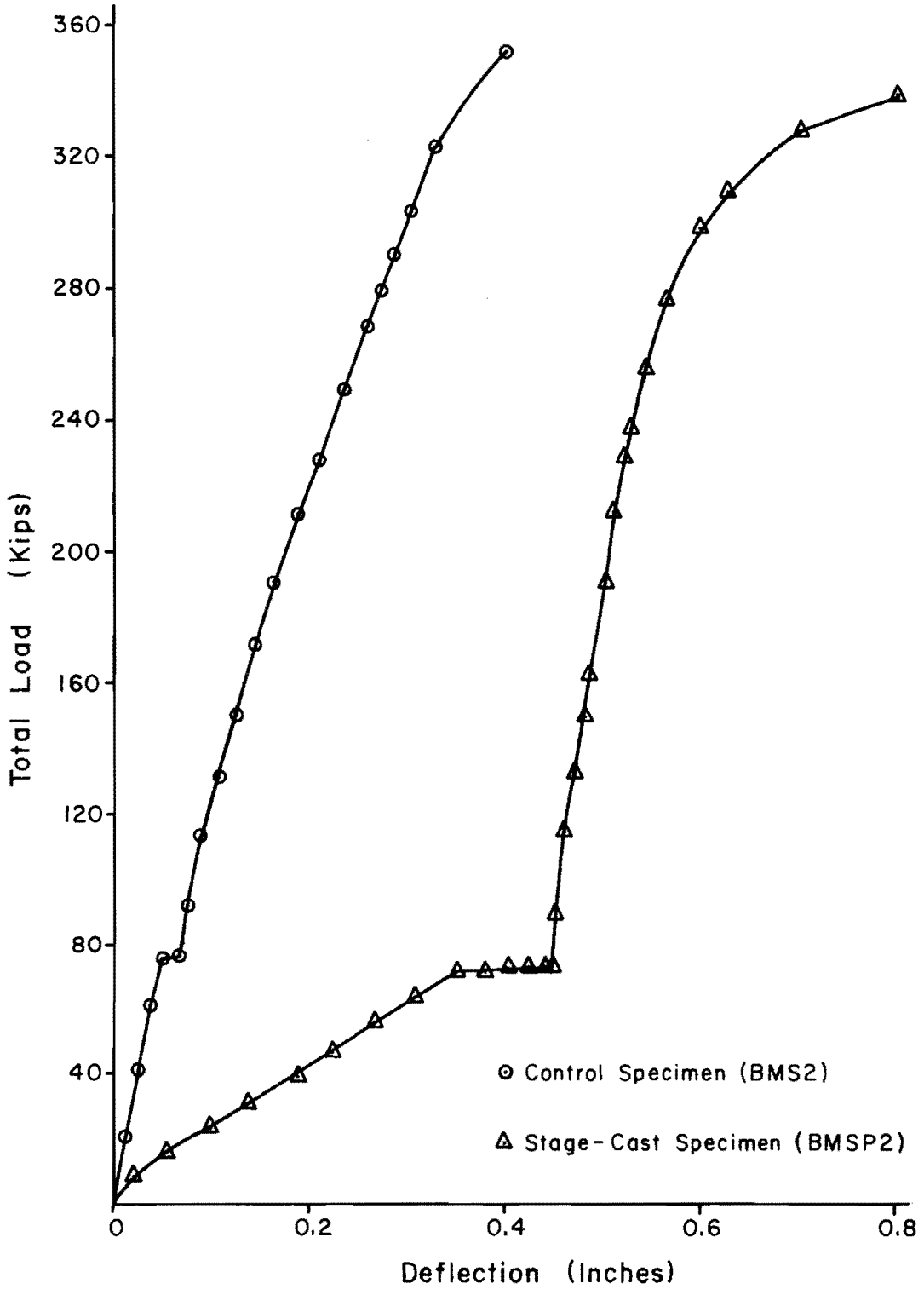

Fig. 3.10 Load-deflection curves for BMS2 and BMSP2

beams tested, approximately half of the total ultimate deflection in stage-cast specimens was due to the instantaneous and creep deflection of the flange caused by preloading of the flange.

Throughout this report the term live load will be used to represent any load which was applied to a stage-cast beam after the stage-cast web had cured sufficiently to support the load in composite action with the precast flange. For control specimens the term live load will mean the total applied load minus the flange load of the corresponding stage-cast specimen. Monolithic beams are frequently called control specimens.

Live load-deflection curves for the specimens are shown in Figs. 3.11 and 3.12. These curves display only those deflections which occurred after web loads were applied.

Stage-cast specimens appeared to be about two times as stiff as control specimens subjected to the same change in service live loads. The uncracked precompressed portion of flange resulted in a greater apparent moment of inertia and a greater stiffness for the stage-cast specimens at service live loads. As the load increased, the stiffness of stage-cast specimens reduced, due to the propagation of cracks into the precompressed zone of the flange. The stiffness of control specimens, however, remained almost constant over a wide range of live load, as shown by the live load-deflection curves in Figs. 3.11 and 3.12. Stage-cast specimens reached yield stress in tension reinforcement at live loads 27 to 40 percent lower than those resisted by control specimens before yielding took place. After yielding, the stiffness of stage-cast specimens decreased at a greater rate. The stiffnesses of stage-cast and control specimens were found to be equal at the load at which the tension steel of the control specimens reached yield stress. Beyond this load, stage-cast specimens were less stiff than the control specimens.

The total live load deflection prior to collapse was virtually the same for both the stage-cast and the control specimens.

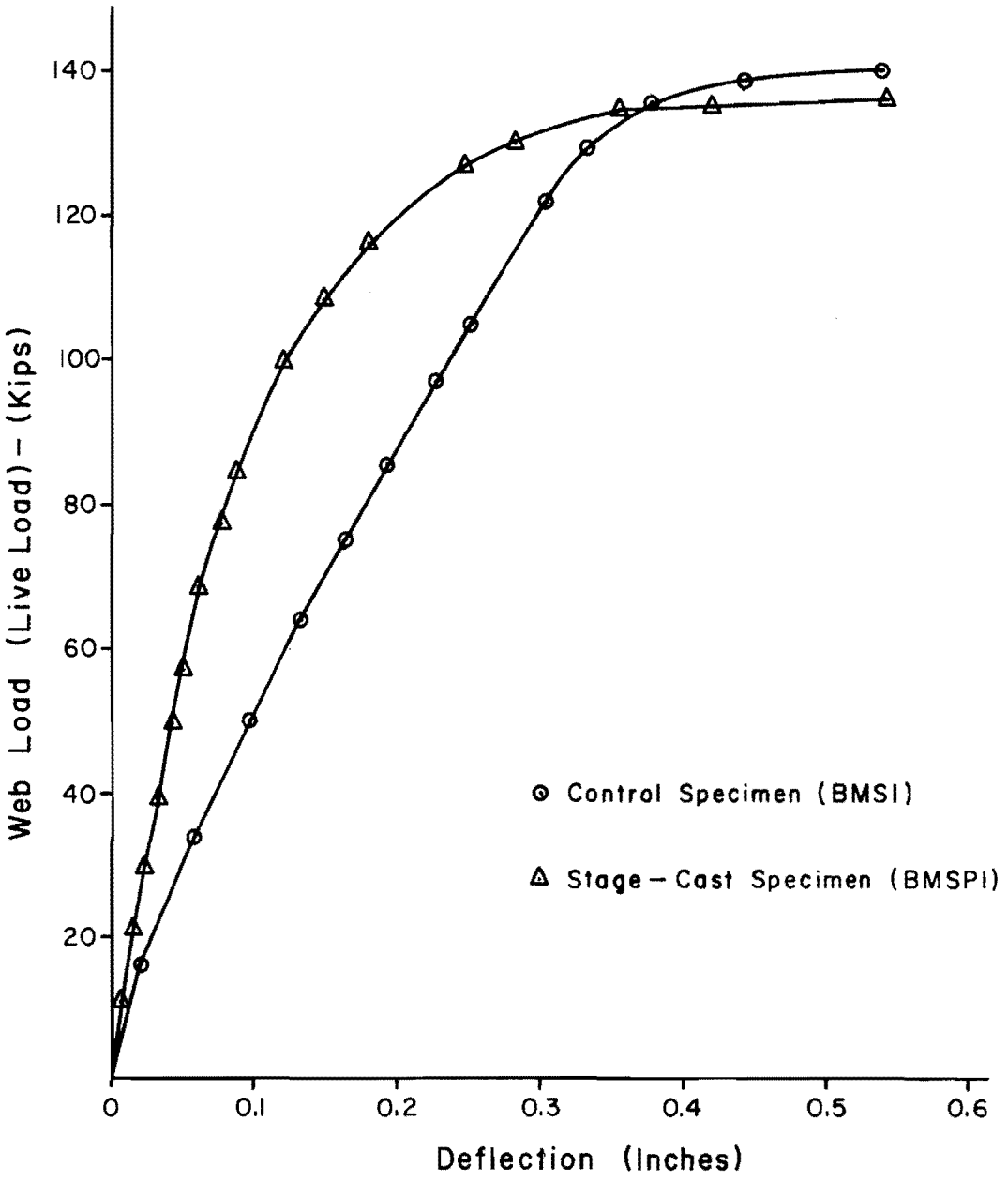

Fig. 3.11 Comparison of live load-deflection curves for BMS1 and BMSP1

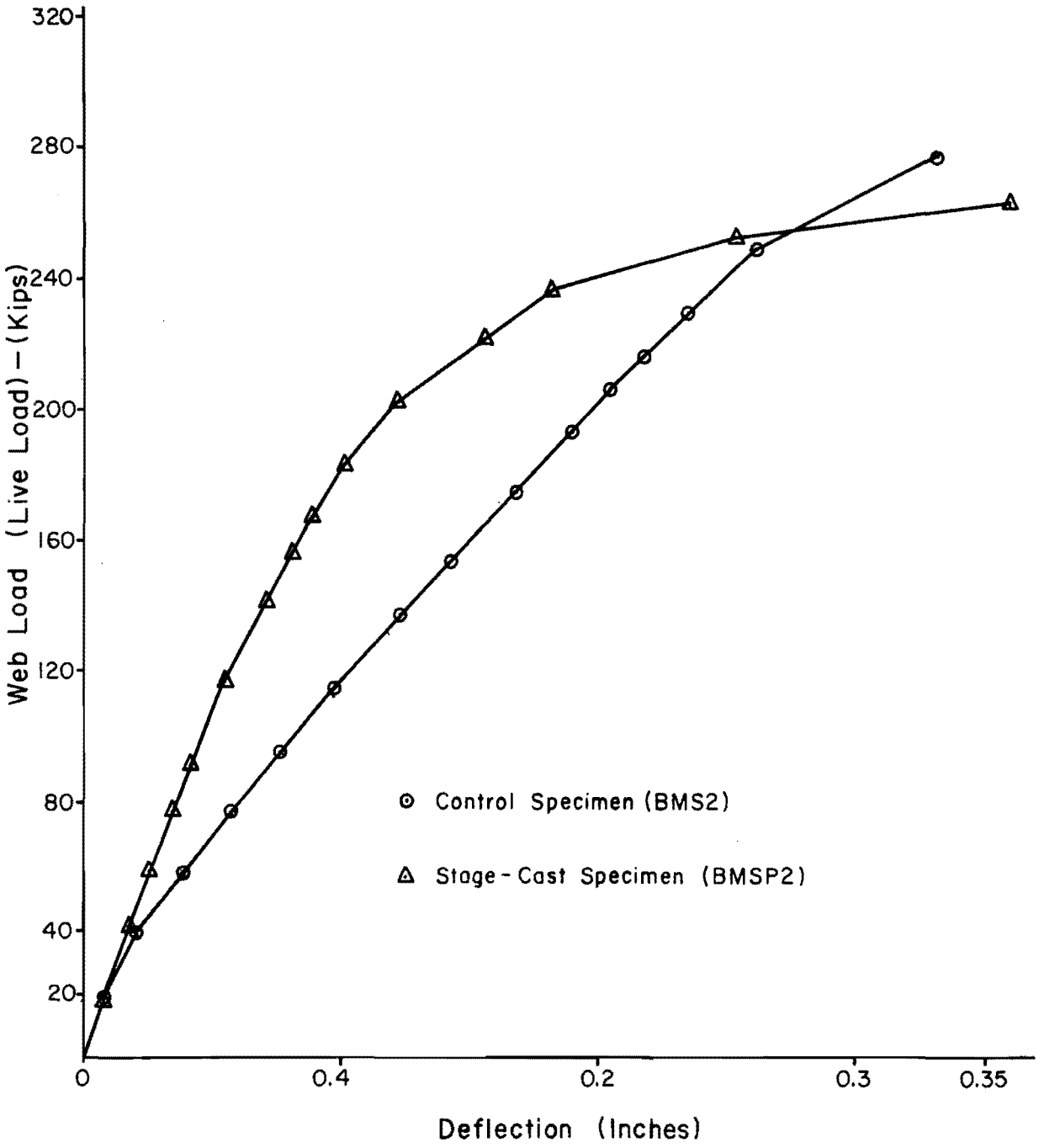

Fig. 3.12 Comparison of live load-deflection curves for BMS2 and BMSP2

Stage-cast specimens possessed more apparent ductility than the control specimens because yielding of steel of stage-cast specimens took place at a lower live load and live load deflection, but flexural failure of stage-cast specimens took place virtually at the same ultimate load and deflection at which the control specimens failed.

3.1.3 Crack Width. Crack width was measured at eight stations located on comparatively wide cracks so that the maximum crack width could be measured. The size of other wide cracks was also checked frequently to make sure that new cracks were not wider than the ones being measured. When new cracks became the largest cracks, another location for crack size measurement was established at the widest observed crack.

Figures 3.13 and 3.14 show the maximum crack widths at various load stages. Despite the care taken to locate the crack of maximum size, the widest crack in BMSP2 near ultimate load went unnoticed as it developed very suddenly before failure. This crack was located right below the flange load point and it widened rapidly near the final load stages to a width of 0.08 in. at ultimate.

Control specimens cracked at full flange load (cracks were visible one day after the loading). The crack width at this stage was less than 0.001 in., as shown in Table 3.1. The least count of the comparator used for crack size measurement was 0.001 in., hence the actual width of these cracks could not be recorded. Maximum crack width in BMSP1 was 0.004 in., and in BMSP2 was 0.001 in. at full flange load, just before loads were applied on the web--flange loads equivalent to 45 ksi of stress in tension steel were maintained on the flange of BMSP1 for seven days before casting of the web and for an additional period of 38 days before application of the web load; flange loads on BMSP2 were maintained for 13 days before and 27 days after the casting of the web. Due to wider cracks created by the flange load, maximum crack width in stage-cast specimens was greater in the usual range of everyday load. Wider cracks existed in BMSP1 and BMSP2 up to a live load equal to 86 percent and 50 percent of that at full service load, respectively (see Figs. 3.13 and 3.14). For higher

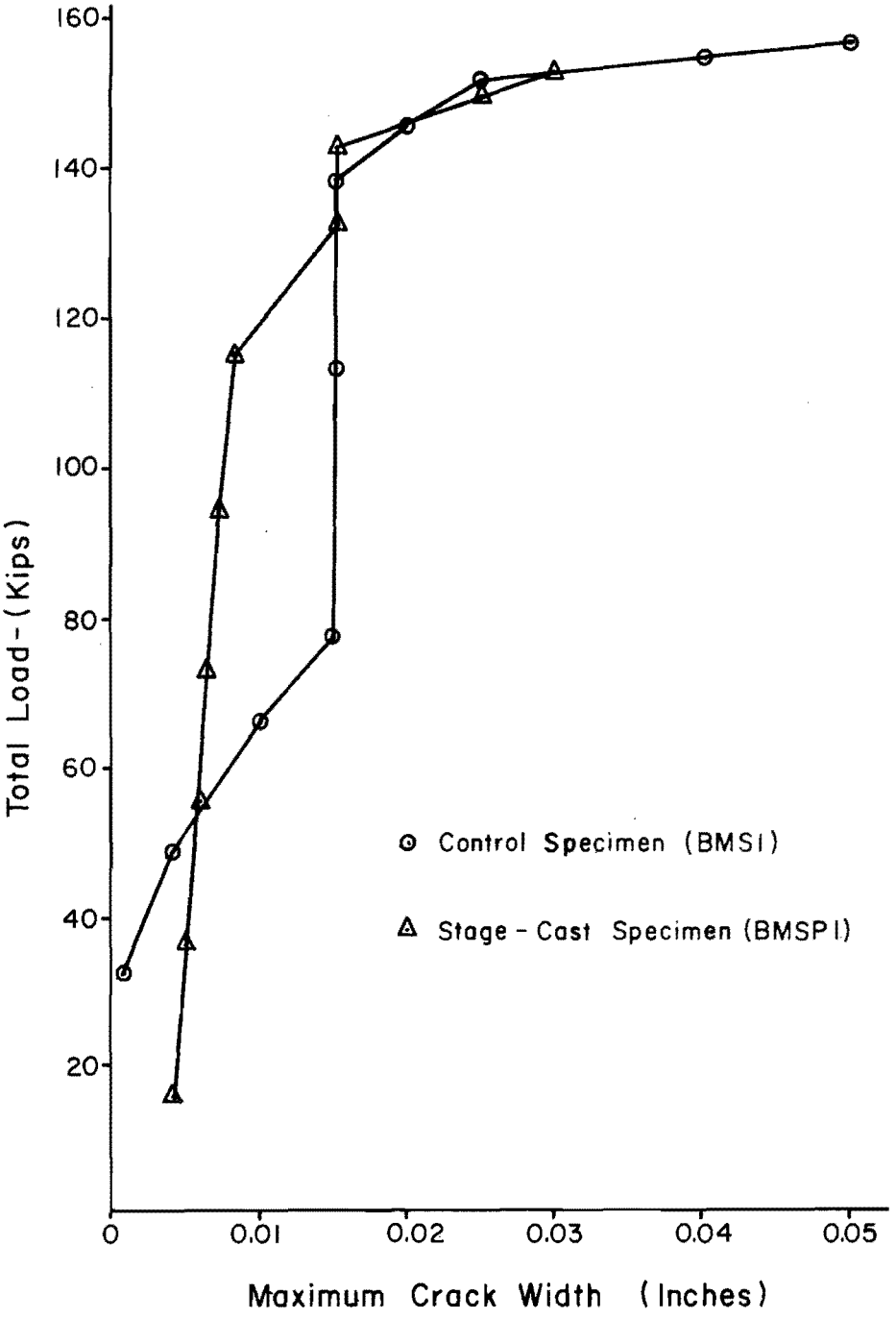

Fig. 3.13 Load-crack size relation for BMS1 and BMSP1

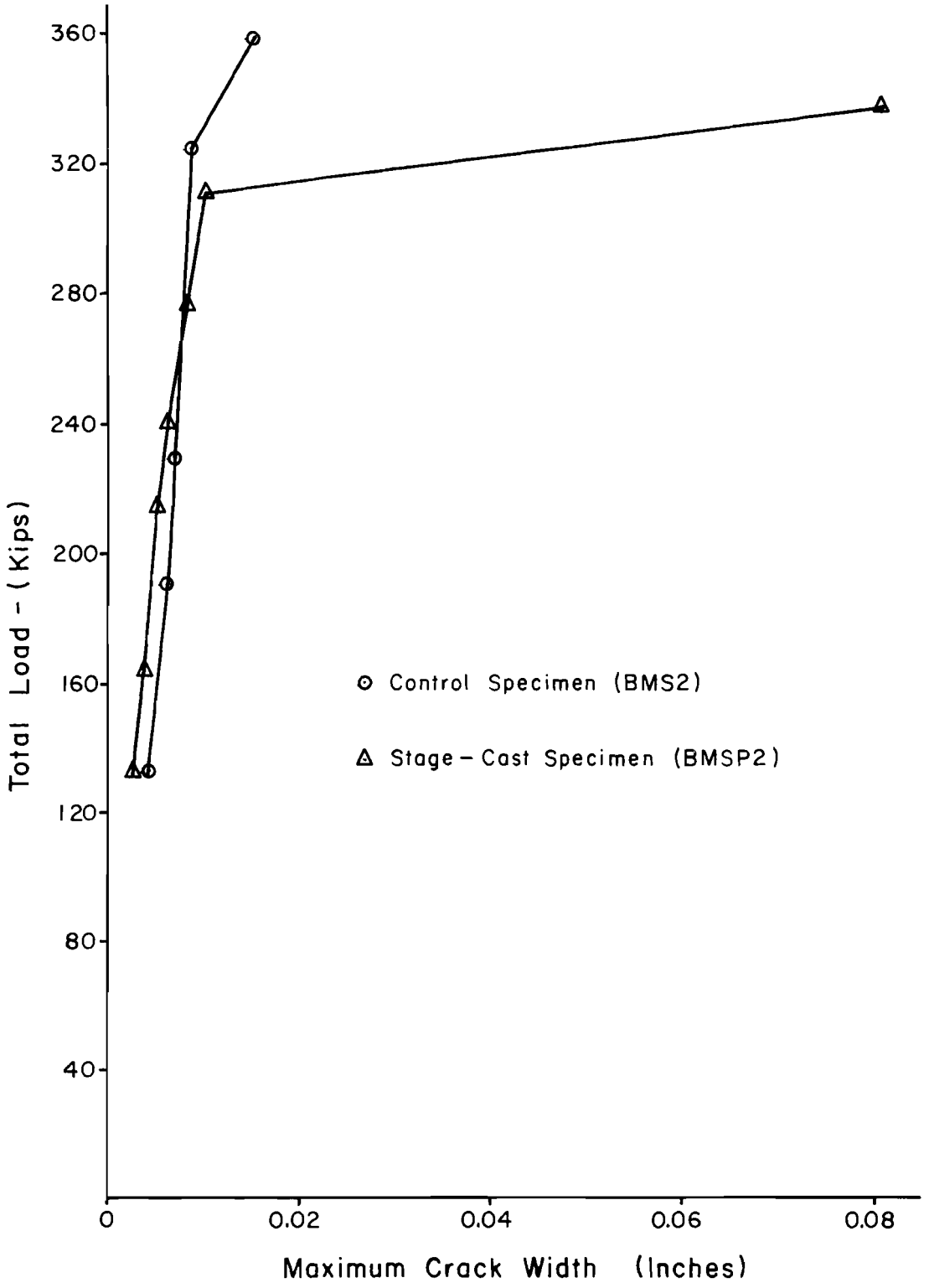

Fig. 3.14 Load-crack size relation for BMS2 and BMSP2

TABLE 3.1 MAXIMUM MEASURED CRACK WIDTHS FOR SPECIMENS

Specimen	Desired depth d (in.)	Span-flange thick-ness ratio L/t_f	p	Total service load (from AASHTO load factors) (kips)	Yield load for stage-cast specimen (kips)	Yield load for control specimen (kips)	Ultimate load (kips)	Maximum measured crack width, at: Full DL (zero LL) (in.)	Service load (in.)	Yield load of stage-cast spec. (in.)	Yield load of control specimen (in.)	Ultimate load (in.)	Total load at which the maximum crack width is: 0.004" (kips)	0.008" (kips)	0.012" (kips)
BMS1	20.75	18.3	0.0135	60.0	101.3	132.3	156.2	<0.001	0.008	0.015	0.015	0.050	49.0	60.0	71.0
BMSP1	20.75	18.3	0.0135	60.0	101.3	132.3	153.1	0.004	0.006	0.0075	0.015	0.030	16.0	116.0	126.0
BMS2	25.625	10.0	0.0218	148.4	191.2	268.7	346.0	<0.001	0.005	0.006	0.008	0.015	135.0	268.7	341.0
BMSP2	25.625	10.0	0.0218	148.4	191.2	268.7	337.4	<0.001	0.003	0.005	0.008	0.080	164.0	268.7	312.0

loads, cracks in control specimens were wider until the yielding of steel of control specimens. After yielding, crack width was found to be greater in the control specimen of 22-in. deep beam, but was found to be more in the stage-cast specimen of 27-in. keep beam.

Even though comparatively wider cracks existed in stage-cast beams at service live loads, these cracks were small enough to be permitted according to the recommendations of CEB (European Committee on Concrete), shown in Table 3.2. A maximum crack width of 0.004 in. in BMSP1 at full flange load (i.e., at full dead load and no live load) seems to be permissible as the major portion of creep due to flange (or dead) load had already taken place in the flange and cracks were not expected to widen appreciably with the passage of time due to further creep under dead load. However, special protection against corrosion may be necessary if the structure is located in very aggressive atmospheric conditions for beams like BMSP1 with comparatively thin flanges (span-to-flange thickness ratio of BMSP1 = 18.3). Cracks less than 0.005 in. in width are usually considered to be invisible from a distance. For the specimens tested, crack size in similar stage-cast and control specimens was found to exceed 0.005 in. at approximately equal loads. Maximum crack width reached 0.008 in. in BMSP1 at a load of 116 kips and at a load of 60 kips (maximum service load) in BMS1. Both BMS2 and BMSP2 had 0.008 in. wide cracks at a load of 268.7 kips (yield load for BMS2). Load for a crack width of 0.012 in. was much higher for BMSP1 than that for BMS1. Loads for this crack size were close to ultimate load in the case of BMS2 and BMSP2.

TABLE 3.2 CEB RECOMMENDATIONS FOR DEFORMED BARS

	Members Exposed to Very Aggressive Condition	Ordinary Structural Members	
		Unprotected	Protected
Maximum crack width (w_{max}), in.	0.004	0.008	0.012

It is interesting to note that crack width in a stage-cast beam at a certain load depends not only on the depth of the composite section but also on the depth of the flange. At low live loads maximum crack width depends on the span-flange thickness ratio, i.e., at low live loads specimens with thin flanges are expected to have wider cracks. The increase in crack width due to live loads depends more on the depth of the composite section than that of the flange. An increase in crack width due to live load is slower in stage-cast beams because live load moments are partially resisted by the increase in lever arm, while the increase in steel strain is comparatively small.

In short, the test results show that cracks large enough to be distinctly visible were produced in stage-cast and control specimens approximately at the same load. Cracks wider than permissible limits for prevention of corrosion under ordinary conditions (Table 3.2) were produced in stage-cast specimens at loads equal to (if not greater than) that for similar control specimens. Under highly aggressive atmospheric conditions, stage-cast beams with thin flanges (high span-flange thickness ratio) may need special protection against corrosion.

Cracks widened more rapidly in the shallow beams BMS1 and BMSP1. A crack width of 0.008 in. (maximum permissible crack size under ordinary conditions) was observed in BMS1 at service load, and at 1.93 times the service load in BMSP1. The same crack width was observed in deeper beams BMS2 and BMSP2 only at yield load. Hence, maximum crack width at a certain load was found to depend upon the depth of section more than on the stage-casting sequence. The width of cracks in stage-cast beams at low live loads was found to depend on the depth of the flange and at high loads on the depth of the composite T-section, as already mentioned under the preceding subsection.

Crack widths remained less than 0.01 in. for all beams until loads reached 80 percent of ultimate values. Cracks remained smaller in stage-cast specimens than in control specimens at the same stage of loading. Even with a scale factor of 3, it can be concluded that cracks remained

within acceptably small limits at service live load levels for all four specimens in this study.

3.1.4 Extent of Cracking. Cracking patterns and the extent of cracking as loading progressed are shown in Figs. 3.15 through 3.18. The numbers along each crack indicate the load sequence at which the extent of cracking was marked. A comparatively large number of flexural cracks was observed in the flanges of stage-cast specimens, considerably more than in the flanges of the control specimens.

Table 3.3 shows typical crack spacings and maximum heights to which the cracks extended at different loads.

Typical crack spacing was about 3 in. in BMSP1 and 6 in. in BMS1. Crack spacing was between 4 and 5 in. (5 in. typically) in BMSP2 and 5 in. in BMS2. Cracks at service load extended up to height greater than 0.5d (up to 52 and 65 percent of d) from the bottom fiber in control specimens, but only up to 21 to 29 percent of d in stage-cast specimens. No crack extended into the web of stage-cast specimens at service load.

3.1.5 Ultimate Strength. The specimens were loaded until crushing of concrete was observed near the top of the web near midspan. Crushing of concrete took place gradually as the load was applied, at a top fiber strain of 0.0031 to 0.0046. The crushing zone was found to be 2 to 3 in. deep and it extended 10 to 15 in. along the top surface of the beams.

Ultimate load capacities of the test specimens and a value for ultimate moment adjusted to a reference concrete strength, f'_c = 4000 psi, specimen width b_w = 8.0 in., and specimen depth d = 20.11 in. for BMS1 and BMSP1, or 24.86 in. for BMS2 and BMSP2, are shown in Table 3.4. The corrected value of ultimate moment was obtained by multiplying the actual ultimate moment by a correction factor of $[20.11 - f'_c b_w a/(4000 \times 8.0 \times 2)]/(d - a/2)$ for BMS1 and BMSP1 and $[24.86 - f'_c b_w a/(4000 \times 8.0 \times 2)]/(d - a/2)$ for BMS2 and BMSP2. In each expression, "a" represents the height of

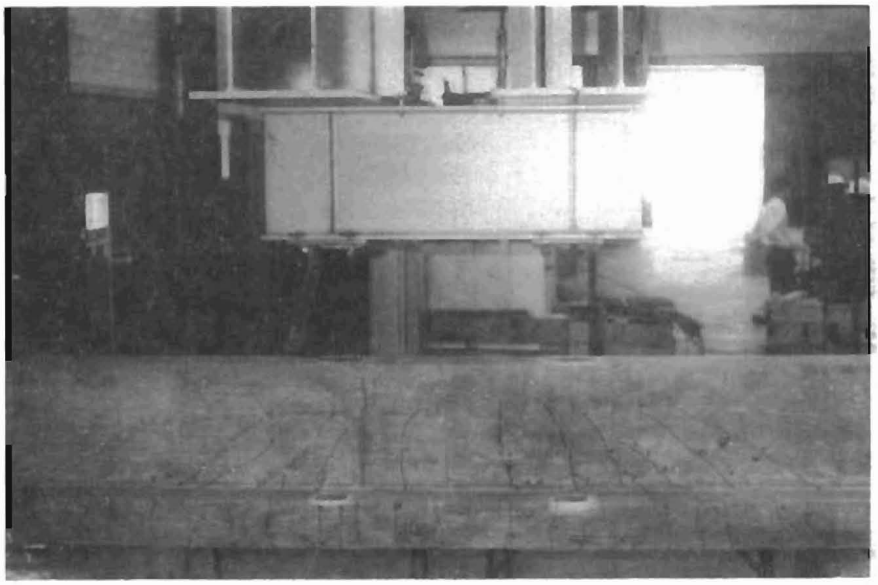

Fig. 3.15 Cracking pattern and extent of cracking in specimen BMS1

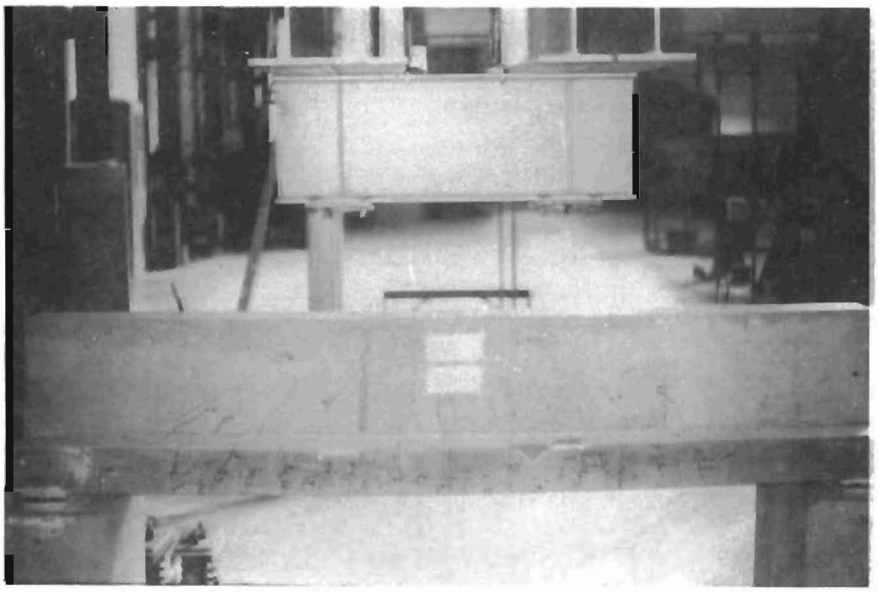

Fig. 3.16 Cracking pattern and extent of cracking in specimen BMSP1

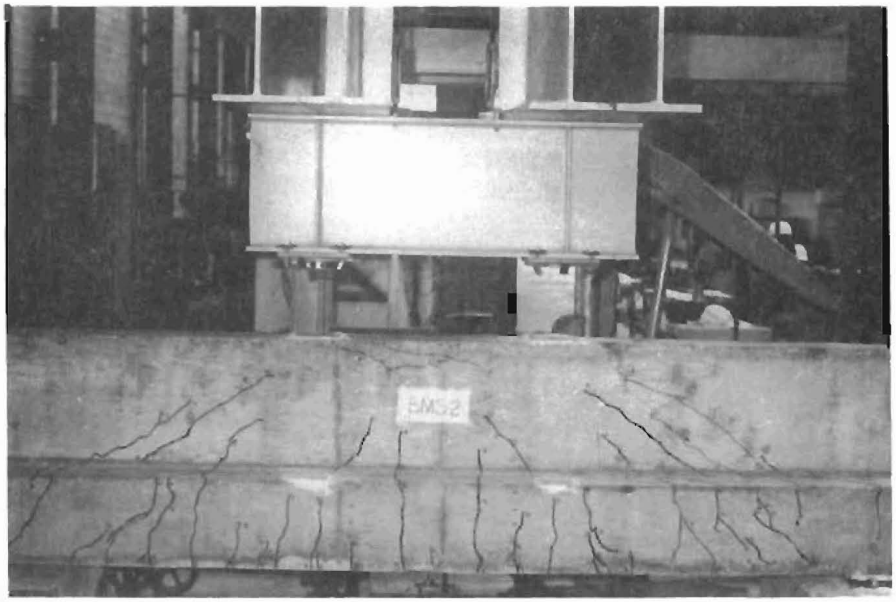

Fig. 3.17 Cracking pattern and extent of cracking in specimen BMS2

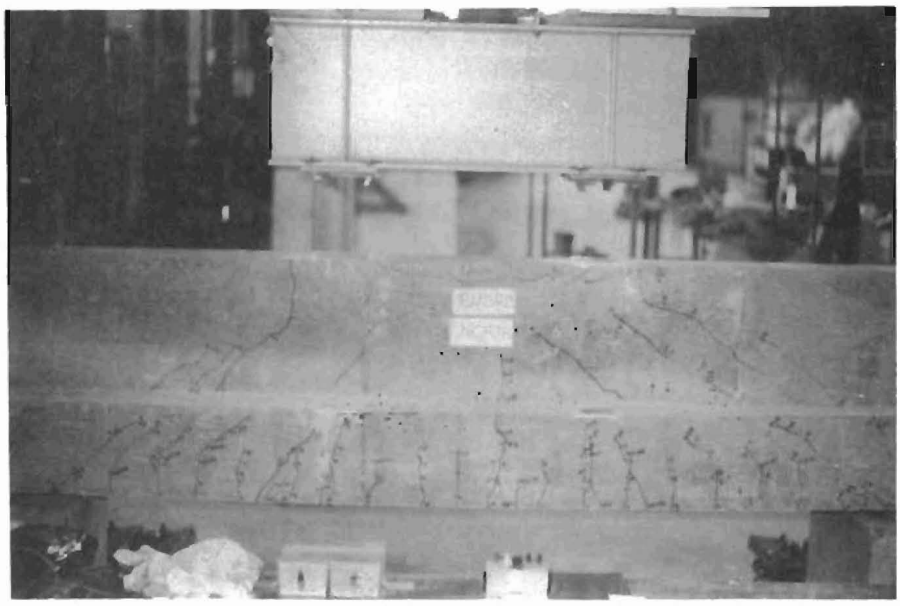

Fig. 3.18 Cracking pattern and extent of cracking in specimen BMSP2

TABLE 3.3 TYPICAL CRACK SPACING AND EXTENT OF CRACKING

Specimen	Typical crack spacing					Maximum height to which the cracks extended (measured vertically from bottom fiber					Total load at which flange top cracked (kips)
	at full DL (zero LL) (in.)	at service load (in.)	at yield load of stage-cast specimen (in.)	at yield load of control specimen (in.)	at ultimate (in.)	at full DL (zero LL) (in.)	at service load (in.)	at yield load of stage-cast specimen (in.)	at yield load of control specimen (in.)	at ultimate (in.)	
BMS1	10.0	6.0	6.0	6.0	6.0	5.0	11.6	17.3	18.0	18.3	49.8
BMSP1	3.0	3.0	3.0	3.0	3.0	3.5	4.25	6" in web* 4.25	12.7	17.7	116.1
BMS2	2 cracks only; below load points	5.0	5.0	5.0	5.0	5.0	16.35	16.6	21.5	24.2	133.2
BMSP2	4 to 5	4 to 5	4 to 5	3 to 5	3 to 5	6.75	7.25	7.5	10.5" in web* 9.5	22.5	337.4

*Measured from top of flange

TABLE 3.4 ULTIMATE MOMENT OF SPECIMENS

Specimen	b_w (in.)	d (in.)	d_f/d	f'_c (psi)	p_w	Ultimate moment from test (k-in.)	Ultimate moment corrected to f'_c=4000 psi, b_w=8.0 in., and d=20.11 in. or 24.86 in.*	(Corr. Ult. Moment of Stage-cast) + (Corr. Ult. moment of control spec.) x 100
BMS1	8.25	20.270	0.236	4846	0.0135	3159	3053	95.3%
BMSP1	9.05	21.208	0.236	4004	0.0135	3099	2908	
BMS2	8.313	25.144	0.387	5208	0.0218	7092	6547	94.9%
BMSP2	7.875	25.503	0.387	5539	0.0218	6798	6215	

*d = 20.11 in. for BMS1 and BMSP1 and d = 24.86 in. for BMS2 and SMSP2.

the rectangular stress block at ultimate. The correction factor was obtained using the rectangular stress block to represent concrete. It was assumed that small changes in steel strain at ultimate did not change the steel stress appreciably.

Corrected ultimate moment capacity for stage-cast specimens was found to be about 5 percent less than that for control specimens for beams of both sizes, as shown in Table 3.4.

Flexural cracks were observed at ultimate load to extend up to the top of the flange of stage-cast specimens, indicating that all of the precompression due to preloading of the flange was lost before ultimate load was applied. Therefore, the internal couple resisting the ultimate moment was provided by compression in web concrete and tension in flange steel, as in the case of control specimens. Thus, the behavior of stage-cast specimens at ultimate was found to be similar to that of control specimens. However, it is possible to have stage-cast inverted T-beams with flange thickness-to-depth ratios large enough to retain some precompression in the flange even at ultimate. In that case, the ultimate moment capacity of stage-cast beams may be considerably less than that of similar monolithic beams. Hence, the ultimate strength of a stage-cast inverted T-beam can be considered as equal to that of a monolithic beam of the same size and reinforcement unless the flange depth to total beam depth ratio exceeds $0.4(d_f/d = 0.4$ for BMS2 and BMSP2).

3.1.6 Yield Moment Capacity. Measured yield moment capacities of the specimens are shown in Table 3.5. The yield moment capacities shown in the table may not be precisely accurate as those values were taken equal to the applied moment at the load stage immediately following the yielding of steel. Yield moment capacity of stage-cast specimens could not be converted easily and accurately to an adjusted capacity for the reference concrete strength $f'_c = 4000$ psi and the nominal specimen dimensions, because a part of the total flexural compression was present in the flange also. Hence, the yield moment capacity of control specimens was adjusted to match the stage cast specimens. The corrected yield moment for

TABLE 3.5 YIELD MOMENT CAPACITY OF SPECIMENS

Specimen	b_w (in.)	d (in.)	d_f/d	f'_c psi	p_w	Yield moment from test (k-in.)	Yield moment of control specimens corrected to f'_c, b_w and d of corresponding stage-cast specimen (k-in.)	(Yield moment of stage-cast) ÷ (Corr. yield moment of control specimen) x 100
BMS1	8.25	20.270	0.236	4846	0.0135	2681	2784	74.1%
BMSP1	9.05	21.208	0.236	4004	0.0135	2063		
BMS2	8.313	25.144	0.387	5208	0.0218	5424	5521	70.2%
BMSP2	7.875	25.503	0.387	5539	0.0218	3873		

control specimens shown in Table 3.5 was obtained by multiplying the actual yield moment of control specimens by a factor of $[d_s - f'_c b_w a/(2f'_{cs} b_{ws})]/(d - a/2)$, in which the subscript "s" indicates that the related quantity pertains to the corresponding stage-cast beam. The correction factor was derived using the rectangular stress block to represent concrete at yield load.

Yield moment capacity of stage-cast specimens BMSP1 and BMSP2 was found to be 26 percent and 30 percent less than that of the corresponding control specimens BMS1 and BMS2. The difference between the yield moment capacities of stage-cast specimens and corresponding control specimens increased slightly with the increase in d_f/d ratio (flange depth to composite section depth ratio), but this increase (in difference between yield moments) was less than 4 percent for a 64 percent increase in d_f/d ratio. Hence, according to the test results, the yield moment for stage-cast beams (with d_f/d ratio between 0.2 and 0.4) does not depend on d_f/d ratio and may be about 30 percent less than that of similar monolithic beams.

A review of the flexural behavior of stage-cast specimens at a load equal to the yield load of similar control specimens may be interesting, since most of the stage-cast beams are designed by neglecting the stresses and strains caused by the preloading of the flange, i.e., by assuming the stage-cast beam to be monolithically cast. Stage-cast specimens were found to be stiffer than the control specimens at all loads less than the yield load of the control specimens. Live load deflection of stage-cast specimens at ultimate load was virtually equal to that of the control specimens; live load deflection of stage-cast specimens was less than that of control specimens at all other loads. The ultimate strength of stage-cast specimens was the same as that of the control specimens. The ductility of stage-cast specimens was more than that of control specimens. Hence, stage-cast beams designed by the common procedure which neglects the effects of preloading of flange are expected to possess sufficient strength and ductility and better serviceability than similar monolithically cast beams.

3.2 Negative Moment Specimens

Two of the beams BMC1 and BMSC1, that were loaded as cantilevers for negative moment had "thin" flanges of 6 in. depth, and the other two BMC2 and BMCP2 had "thick" flanges of 11 in. depth.

3.2.1 Strain Profiles. The variation of strain through the depth of the precast and loaded flanges that were used for the stage-cast members are illustrated in Figs. 3.19 and 3.20. Again, for each of the two stage-cast flanges three strain profiles are presented: (1) the strains at half the total applied flange load, (2) the strains immediately after the full flange load had been applied, and (3) the strains after several weeks of sustained loading had been applied to the flange. The strain profiles for negative moment loading on flanges remained more closely linear than did those of the positive moment specimens. The dashed lines of Fig. 3.19 and Fig. 3.20 indicate the strain profile in accordance with cracked section theory. The measured strain profiles corresponded very closely to the cracked section linear theory. Sustained loads on the flange caused the neutral axis to move away from the compression face of the concrete. Almost no creep or change in strain was observed at the level of tension steel in the negative moment stage-cast flanges.

Negative moment specimens were loaded with two different cantilever spans, one of 60 in. and one of 50 in. Strain profiles from only two conditions of load are displayed for the negative moment specimens. One strain profile illustrates the condition of each specimen at the reading just before yield strains were observed in tensile reinforcement, and the other profile indicates the condition of strain at the last load condition for which strain readings could be made.

Strain profiles for the monolithic cast thin flange specimen BMC1 are shown in Figs. 3.21 and 3.22. The 60 in. cantilevered span was reinforced with eight #6 bars, and the 50 in. cantilevered span was very lightly reinforced with only three #6 tension bars. Just before tensile

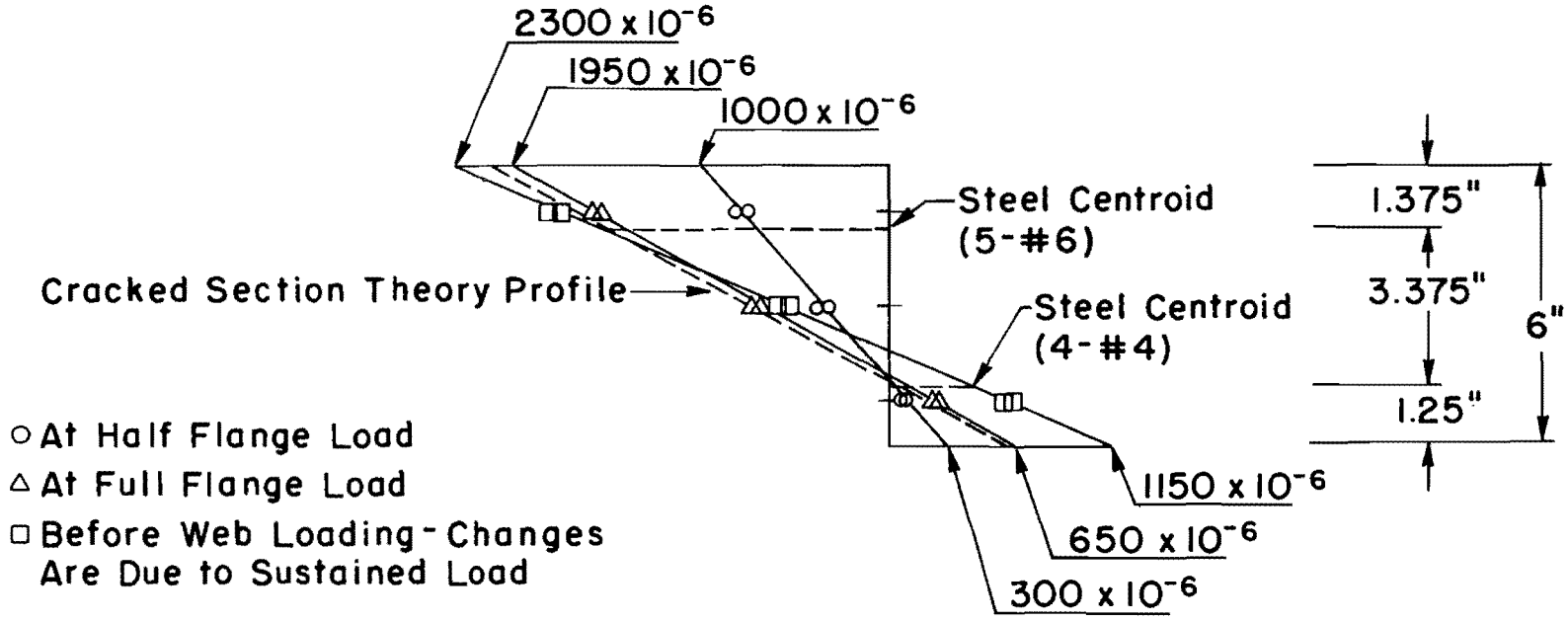

Fig. 3.19 Strain profiles for flange of BMCP1

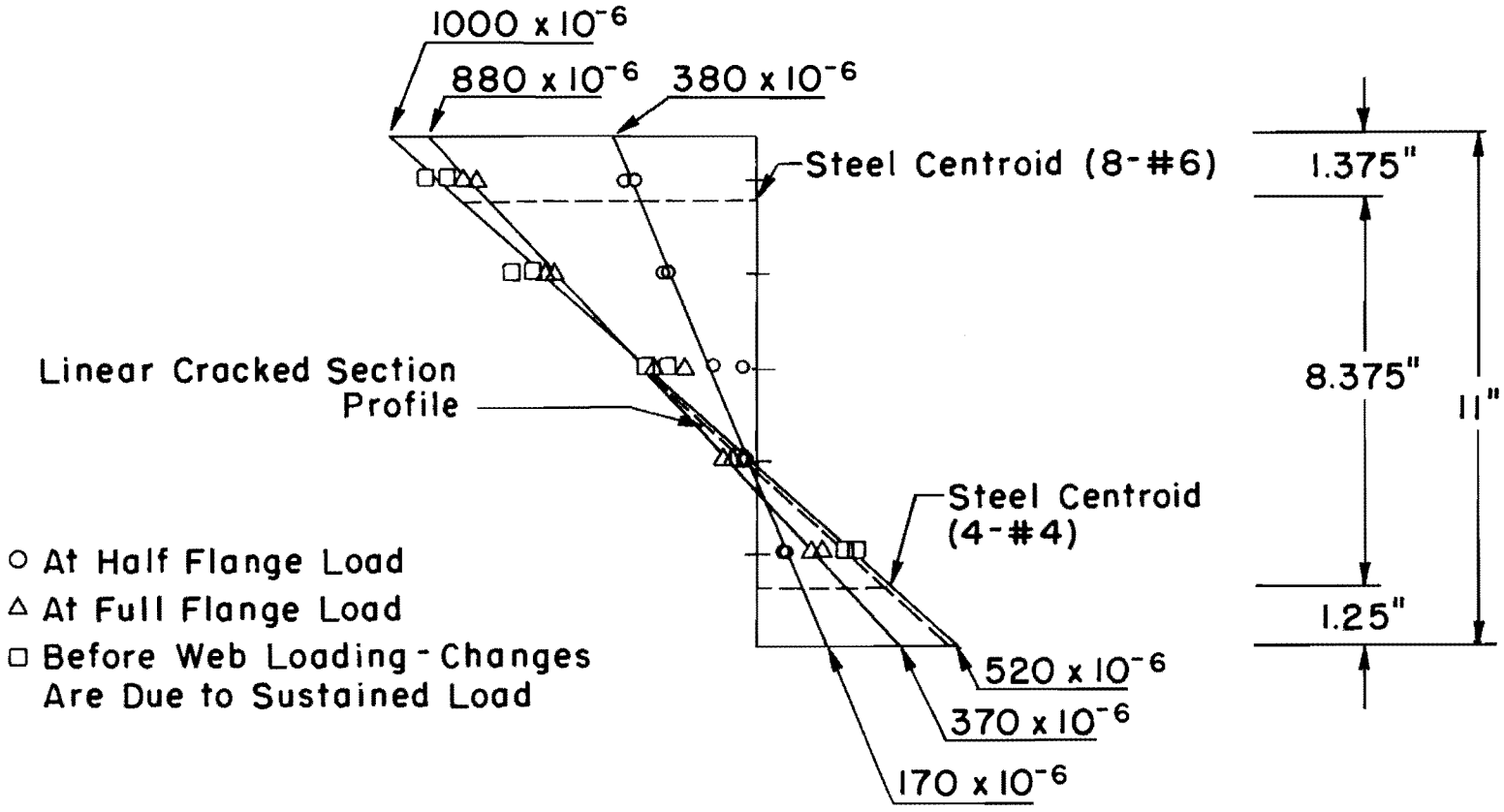

Fig. 3.20 Strain profiles for flange of BMCP2

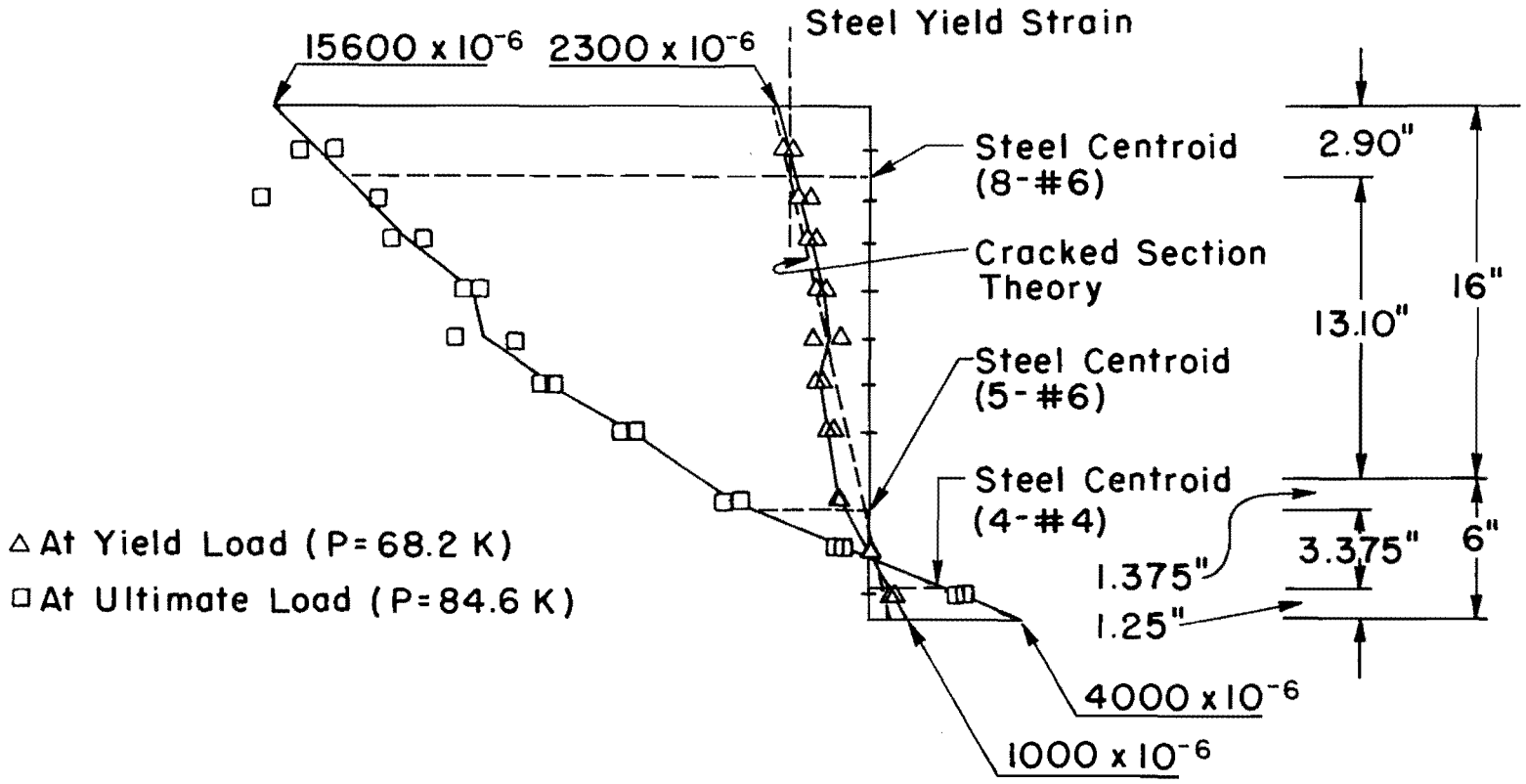

Fig. 3.21 Strain profiles for BMC1, 60-in. cantilever span

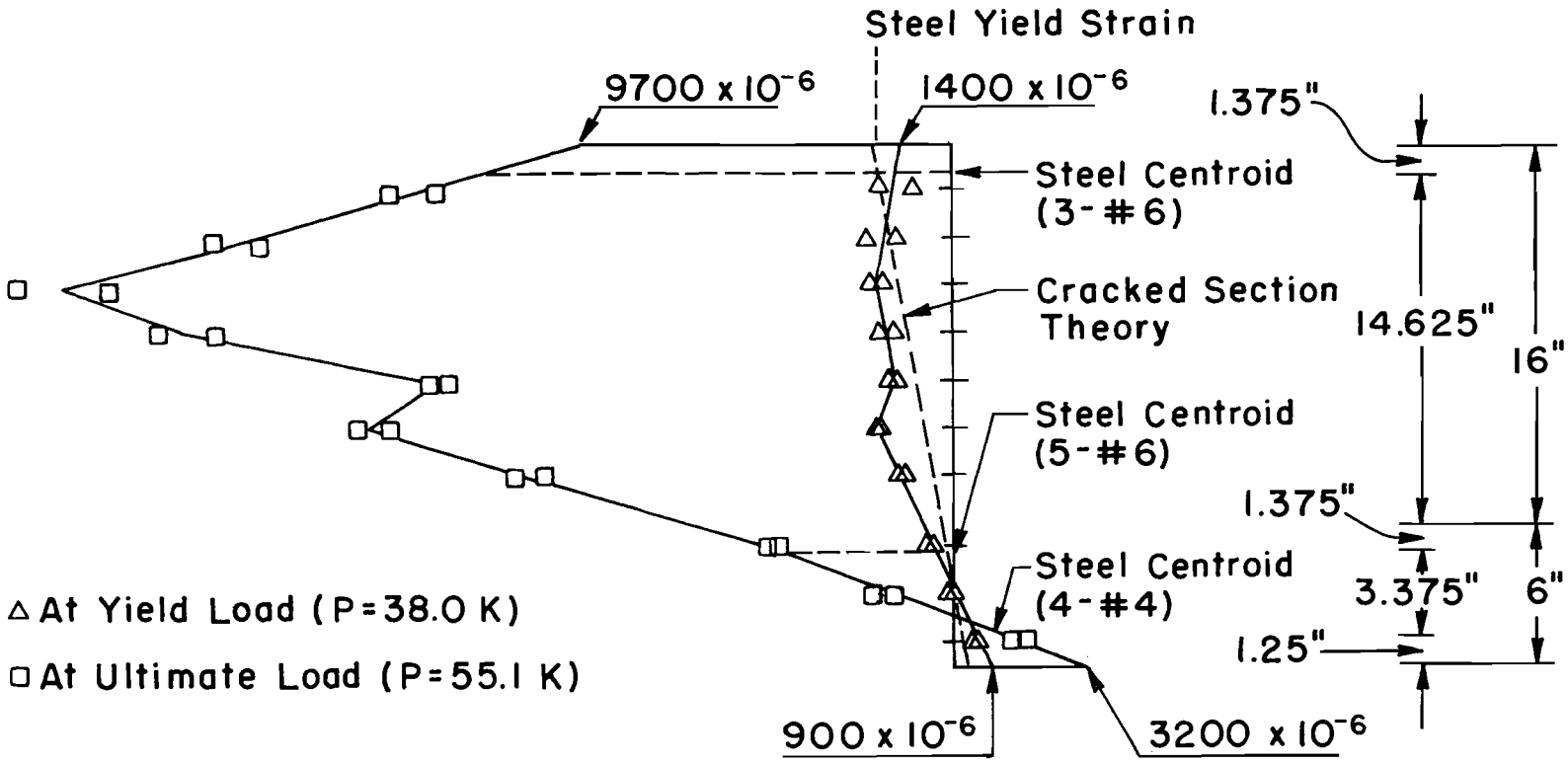

Fig. 3.22 Strain profiles for BMC1, 50-in. cantilever span

steel yielded, the strain profiles for both of the monolithic cast specimens displayed a nonlinear variation of strain through the depth of the member. At the position of flexural tension steel the observed strains of BMC1 were almost the same as the predicted theoretical value of f_y/E_s. The very lightly reinforced region of BMC2 actually had a measure of strain smaller than that at which tensile steel yields. The concrete around the three #6 bars apparently helped resist tensile forces that were nominally adequate to yield the bars.

Near the region of the neutral axis there was evidence of tensile strain in concrete much greater than that suggested by cracked section theory applied to the cross section. The dashed lines of Fig. 3.21 and Fig. 3.22 indicate the strain profile consistent with the cracked section theory. Compressive strains for both the thin flange cantilever yield loads measured almost twice as large as the cracked section theory suggested.

At the ultimate load the strains on compressed concrete decreased almost linearly with distance above the bottom edge, but strains measured in the tension region reflected a strain gradient much less than that of the compression concrete. Possibly a significant component of flexural tension was retained by concrete even after tension steel yielded. In the lightly reinforced end at a location 4 to 6 in. away from the tension bars, cracks in concrete were large enough that the net amount of surface strain was almost double that at the level of the tension bars.

Strain profiles for the deep flange monolithic cast specimens are shown in Figs. 3.23 and 3.24. At the yield load the measured variation of strain was much closer to that predicted by cracked section theory than it was for the thin flange specimen. Again, the compressed concrete reflected higher strains and a strain gradient steeper than that consistent with cracked section theory. At ultimate load near the tension reinforcement the strain gradient was very low, again suggesting that the flexural strains were almost uniform in the exterior 6 to 8 in. of each cross section.

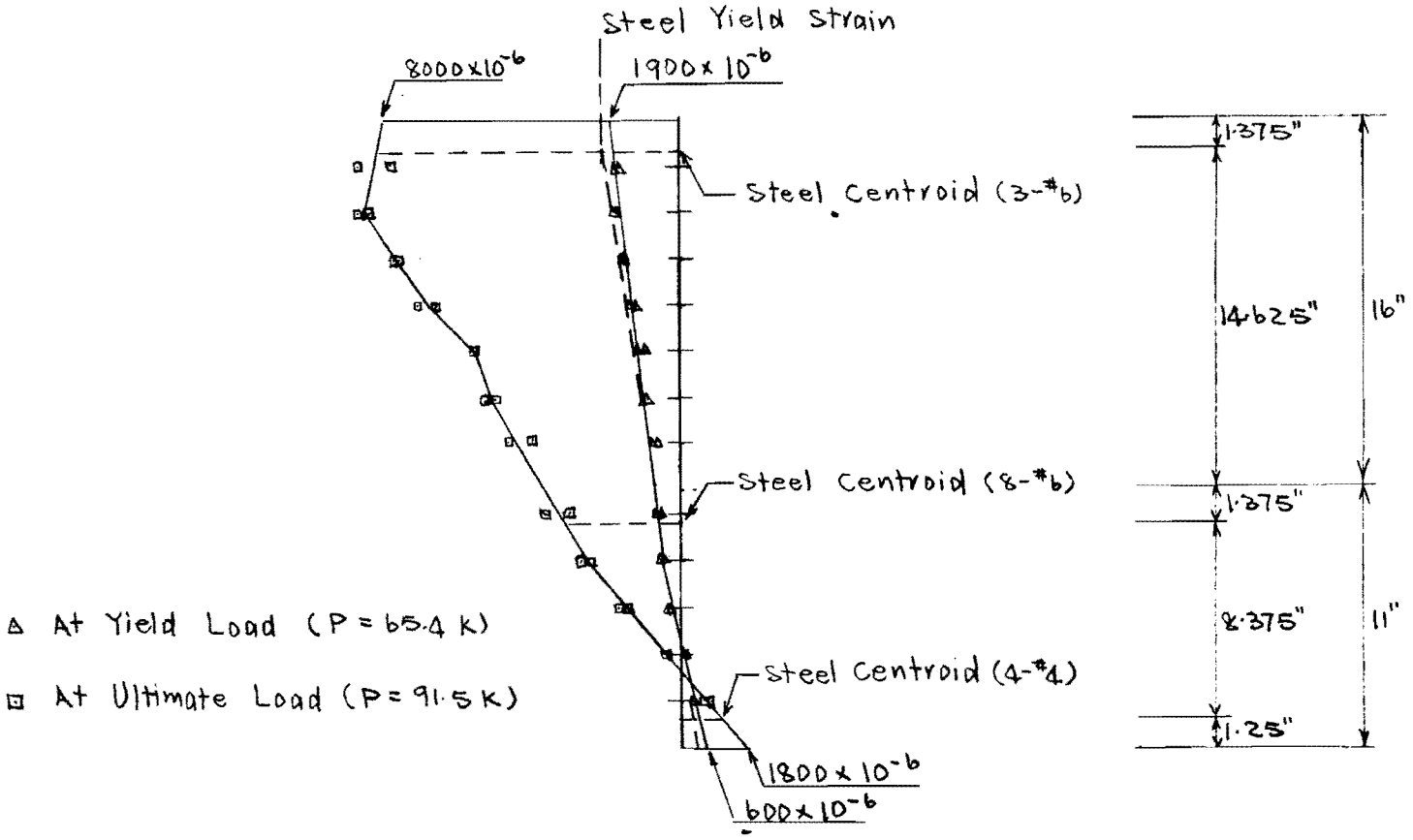

Fig. 3.23 Strain profiles for BMC2, 50 in. cantilever span

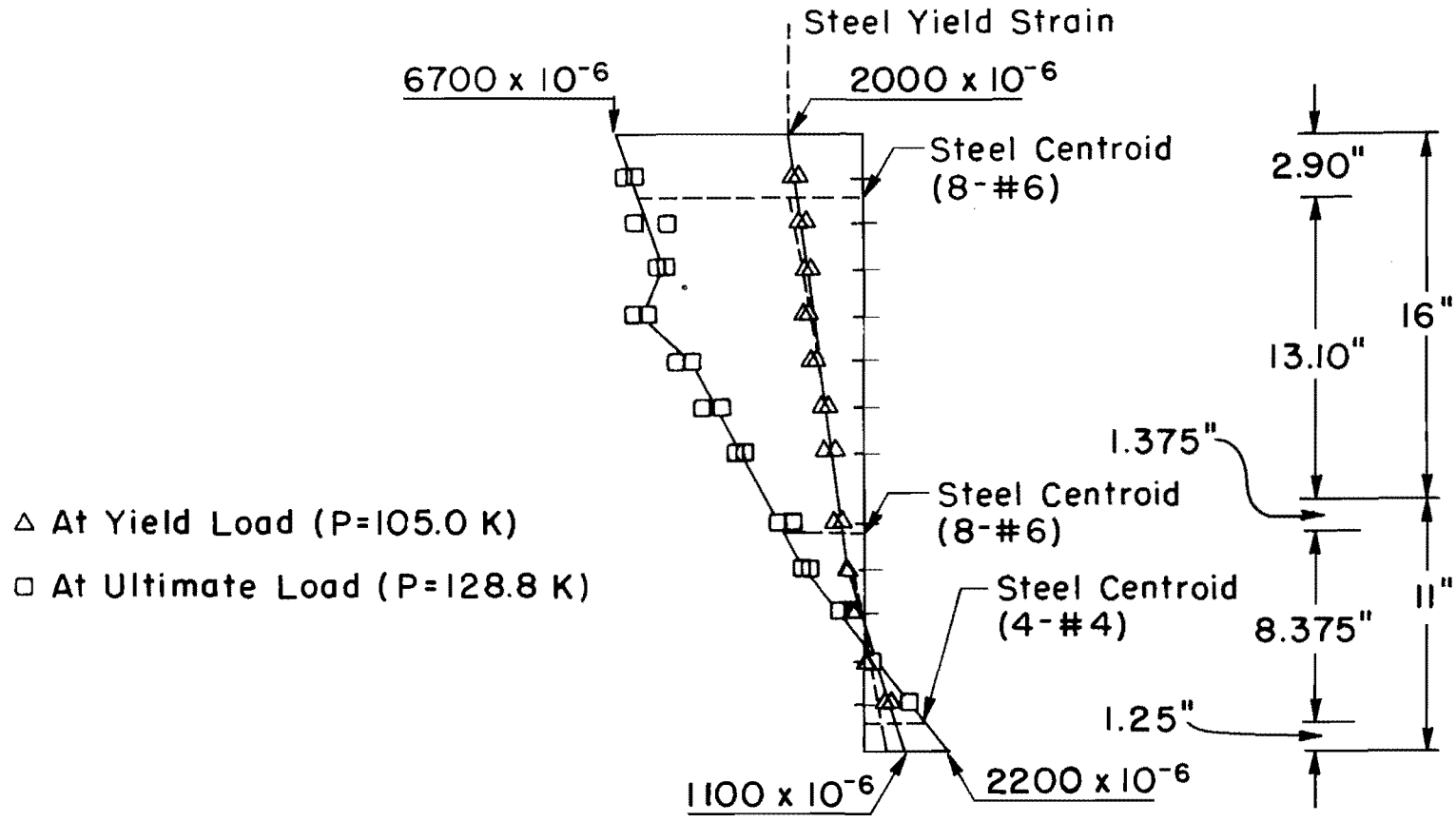

Fig. 3.24 Strain profiles for BMC2, 60-in. cantilever span

The strain profiles for full depth response of stage-cast shallow flange specimens are shown in Figs. 3.25 and 3.26. The changes in strain through the depth of the stage-cast members exhibited the same general response as that already observed for the monolithic cast beams. Maximum strain gradients appeared near the compression surface and minimum gradients were detected near flexural steel.

Deep flange specimens gave strain profiles very similar to those of shallow flange stage-cast composite beams, as indicated by the diagrams of Figs. 3.27 and 3.28. There was evidence of tensile force in concrete helping to resist flexural tension near the neutral axis, more so in stage-cast than in monolithic cast deep flange specimens (Figs. 3.23 and 3.24), and the rather constant amount of strain in the outer 6 to 8 in. of the tension flange was more obvious in the deep flange than in the shallow flange beams.

Strain profiles at or near the same "live" loads on monolithic and corresponding stage-cast specimens are displayed in Figs. 3.29 and 3.30. Within the accuracy of the measuring system used, there were no significant differences in the solid line (monolithic cast) and dotted line (stage-cast) strain responses for shallow flange specimens shown in Fig. 3.29. In contrast, for deep flange beams there was a smaller change in strain on stage-cast specimens than in monolithic cast specimens at the same "live" loads shown in Fig. 3.30. The tensile strength of stage-cast concrete in BMCP2 apparently resists a significantly greater portion of overall tensile forces than does the concrete (precracked by dead load) of monolithically cast beams through the same range of loading.

3.2.2 Deflections. The total deflection and total load graphs for all cantilevered specimens are shown in Figs. 3.31 through 3.34. In each figure the behavior of a stage-cast specimen is compared with the behavior of the corresponding monolithic cast specimen. In all cases the ultimate deflection before failure was hardly influenced by stage-casting, but the ultimate strength of stage-cast thin flanged beams was lower

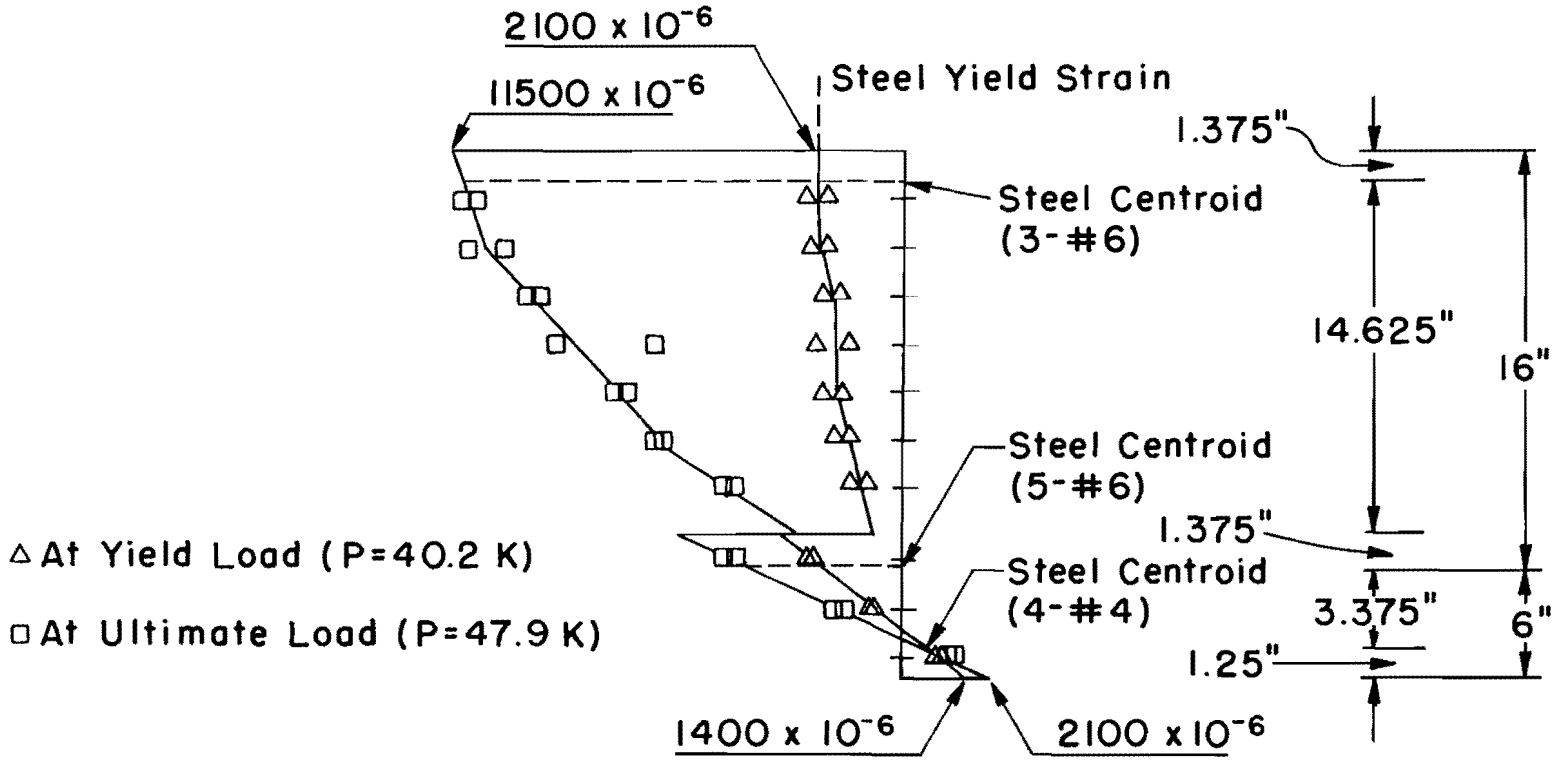

Fig. 3.25 Strain profiles for BMCP1, 50-in. cantilever span

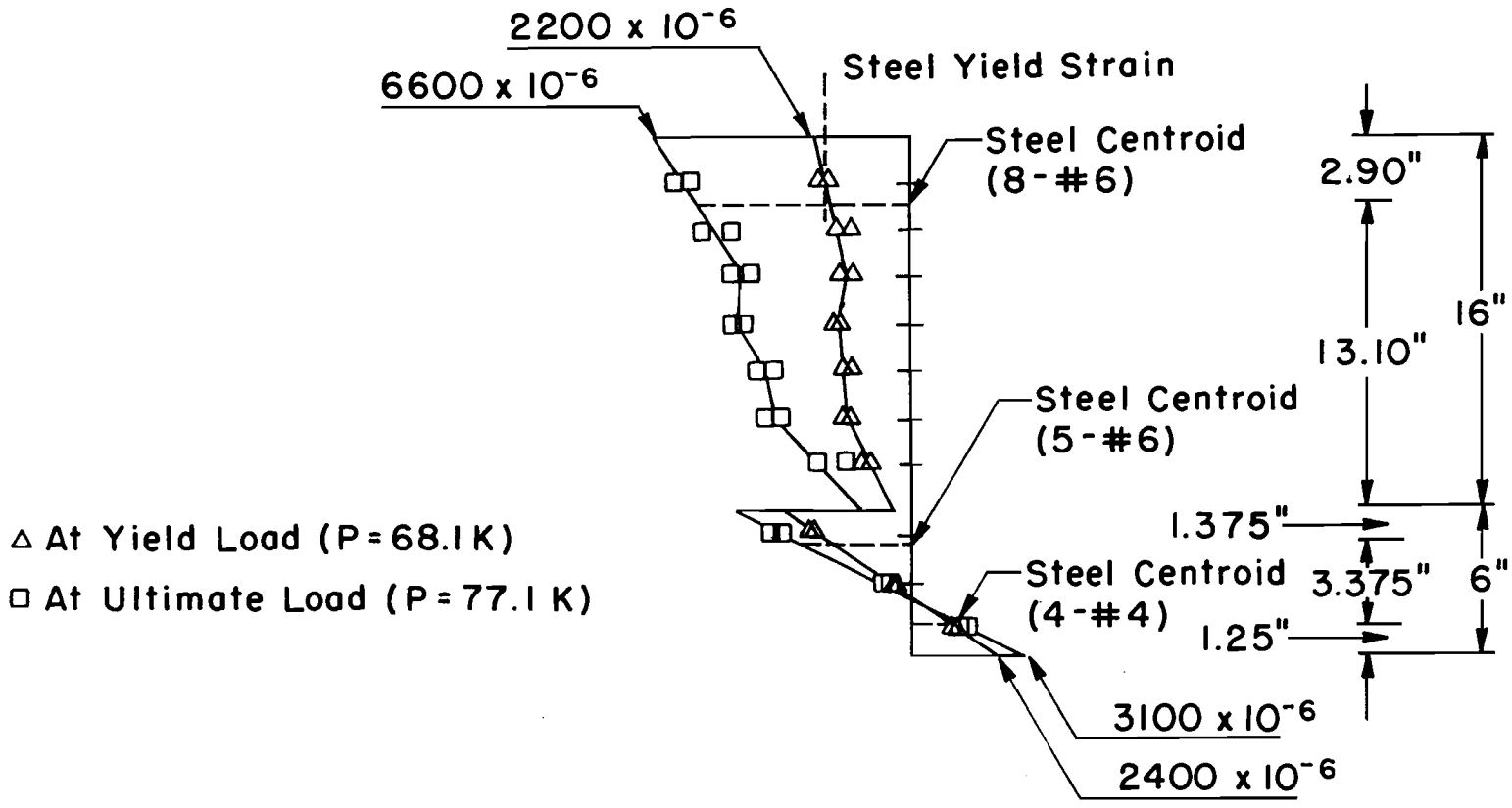

Fig. 3.26 Strain profiles for BMCP1, 60-in. cantilever span

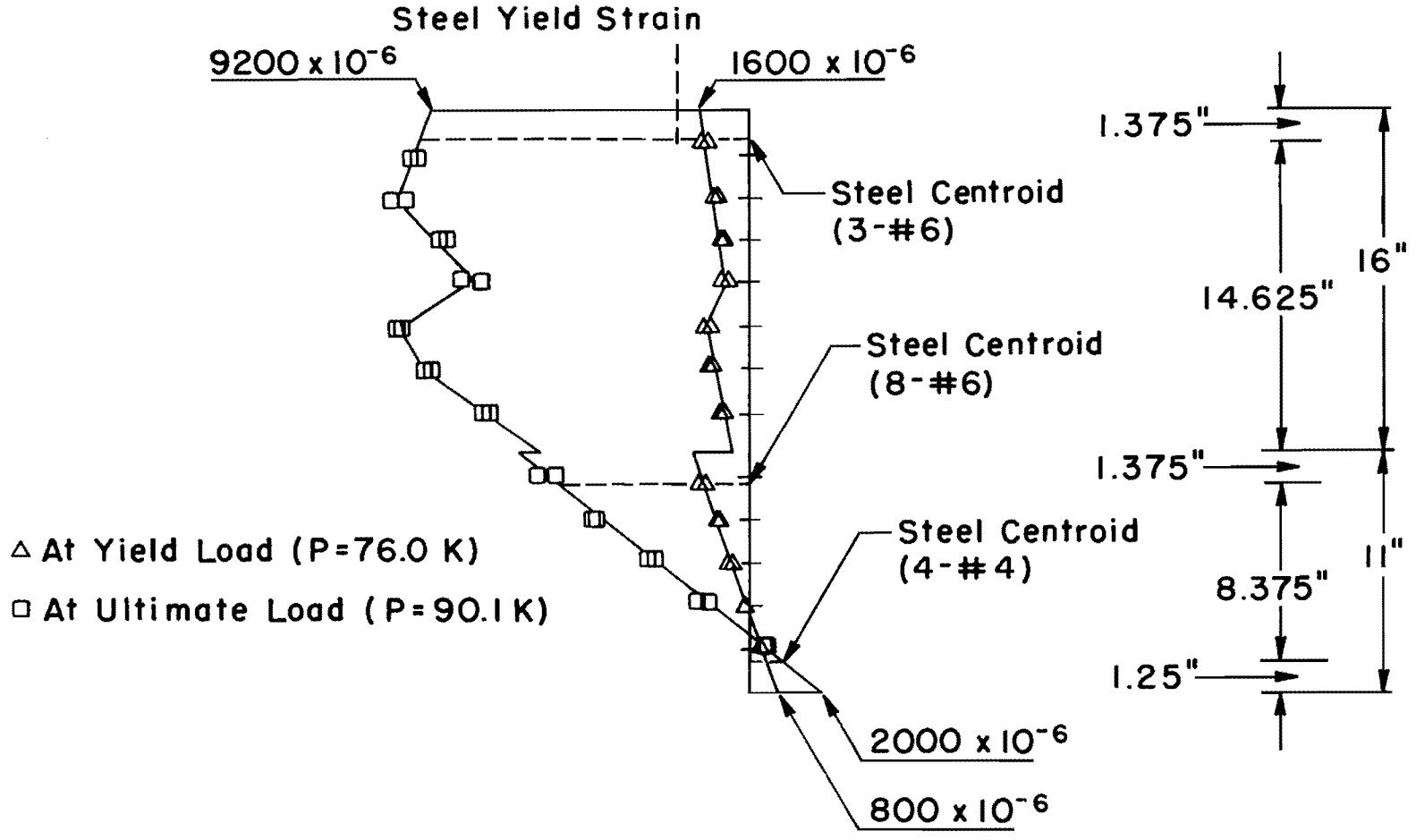

Fig. 3.27 Strain profiles for BMCP2, 50-in. cantilever span

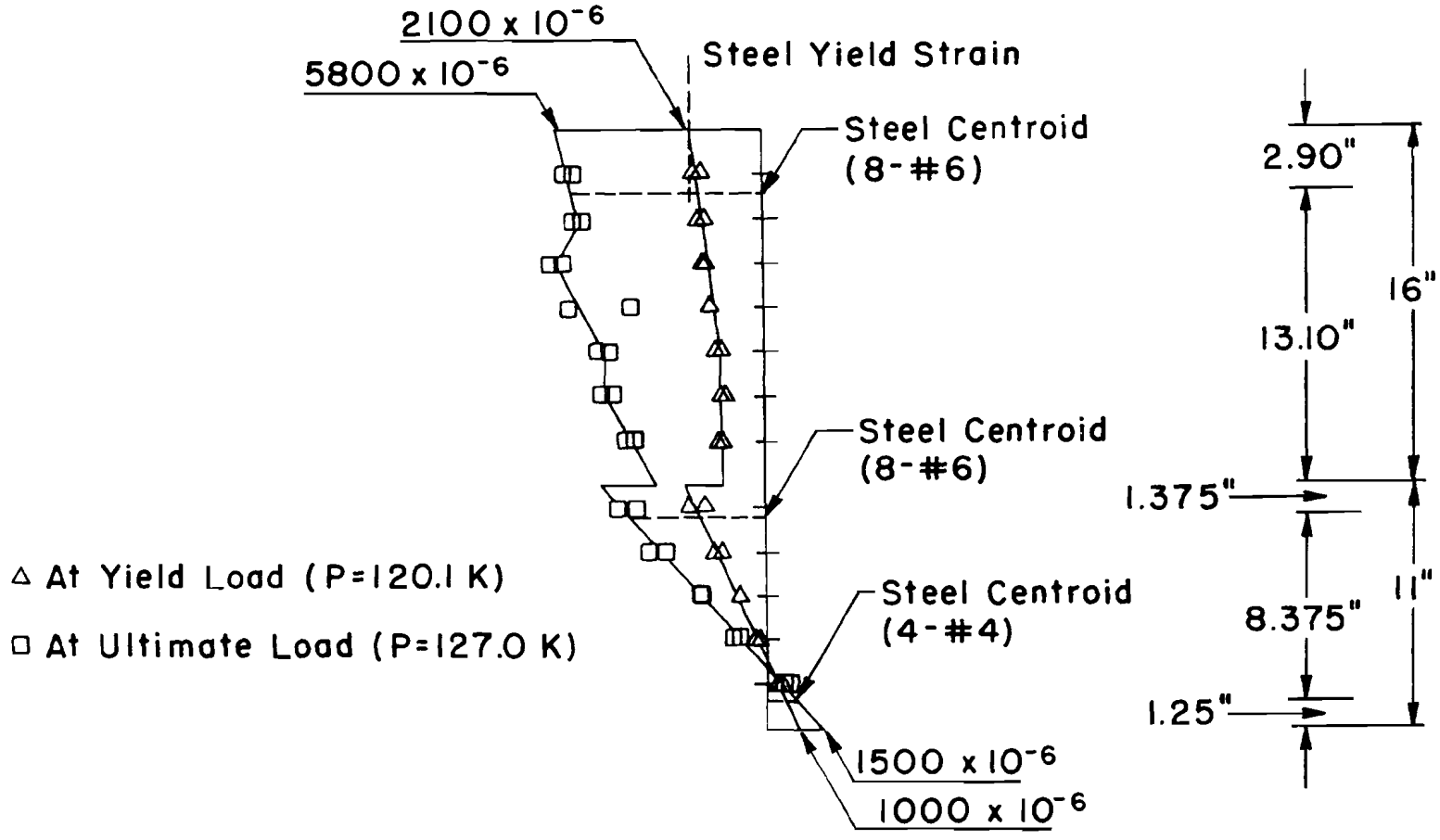

Fig. 3.28 Strain profiles for BMCP2, 60-in. cantilever span

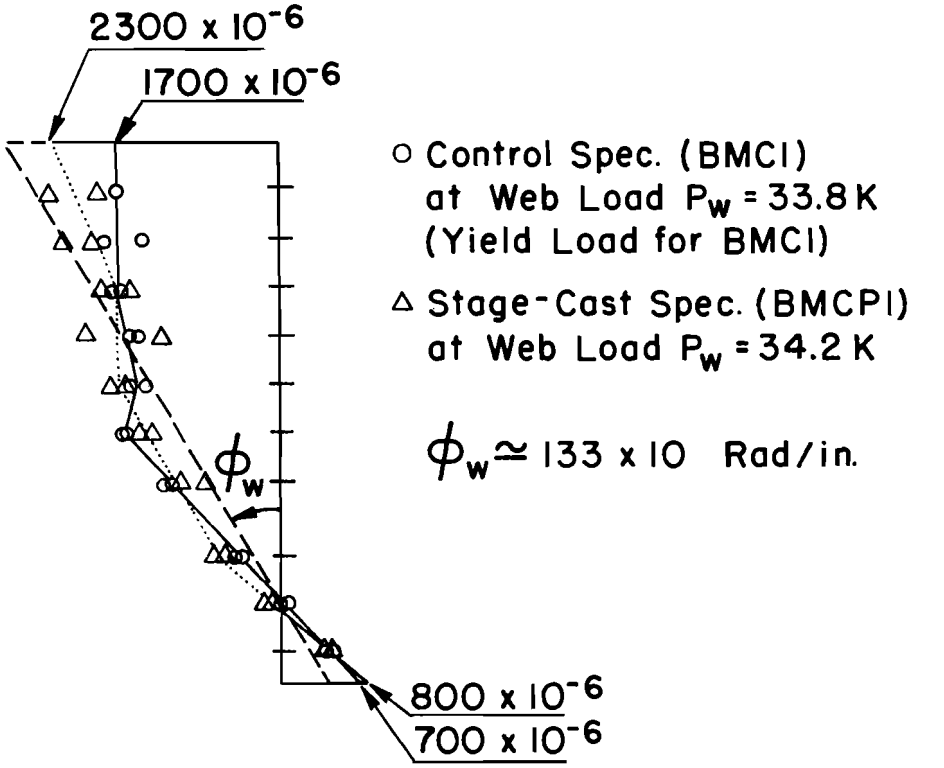

(a) At 50-in. cantilever span

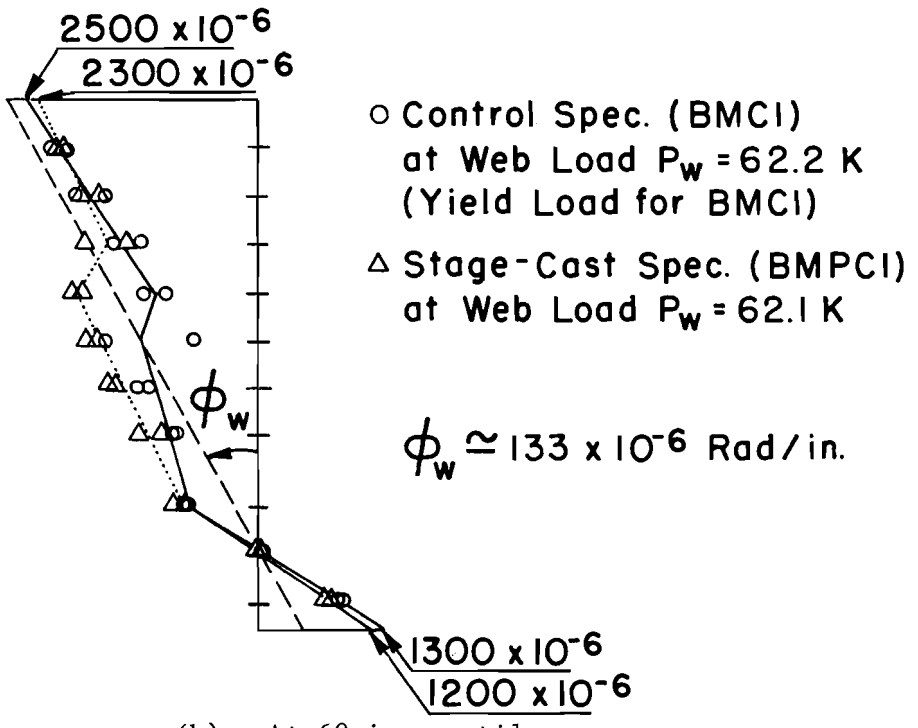

(b) At 60-in. cantilever span

Fig. 3.29 Comparison of strain profiles of specimens BMCl and BMCPl

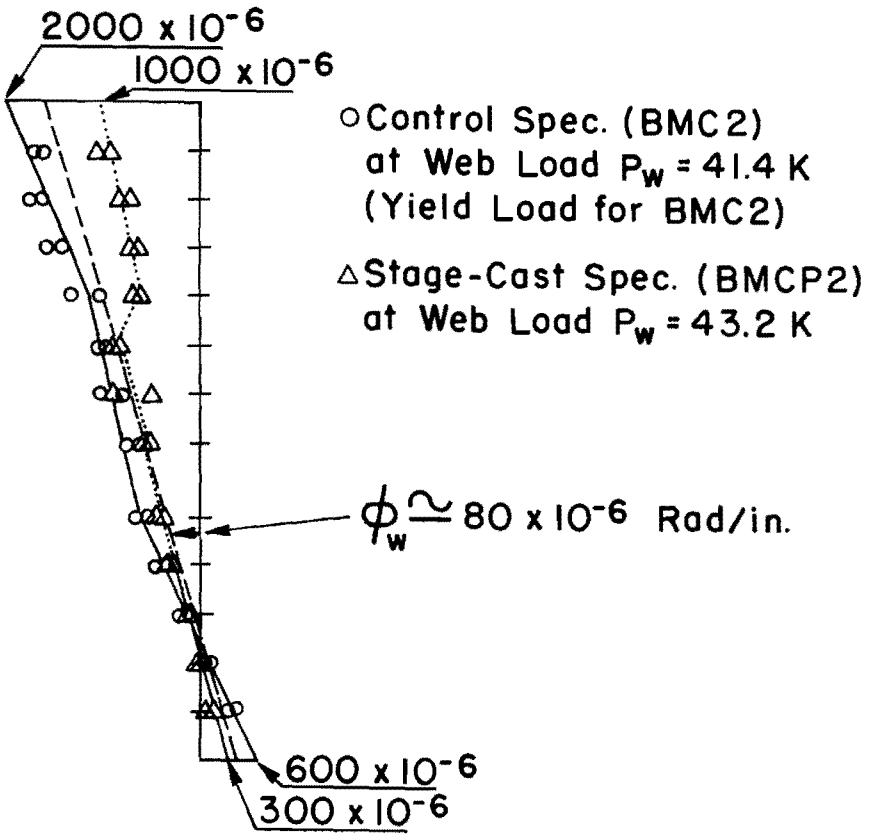

(a) At 50-in. cantilever span

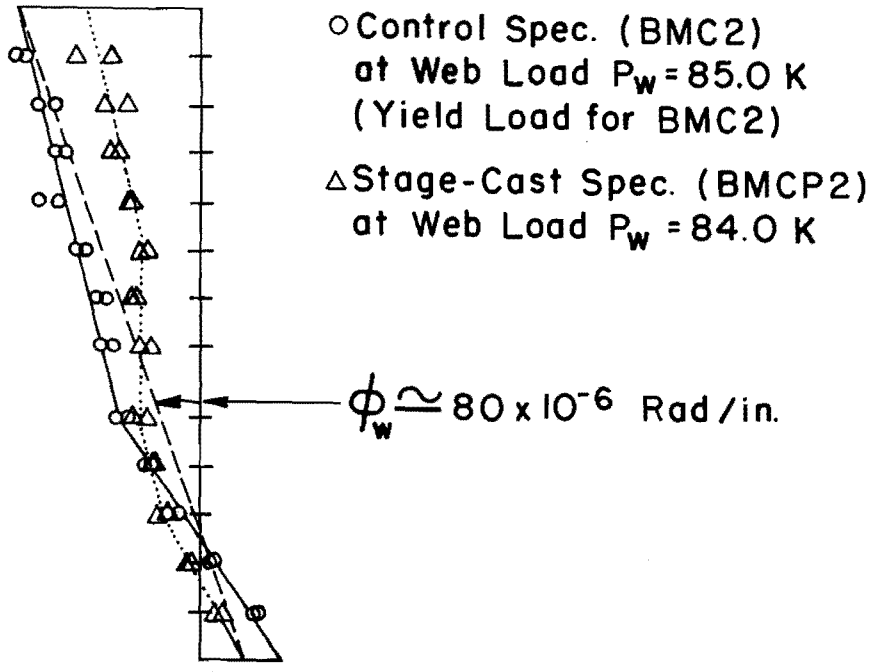

(b) At 60-in. cantilever span

Fig. 3.30 Comparison of strain profiles of specimens BMC2 and BMCP2

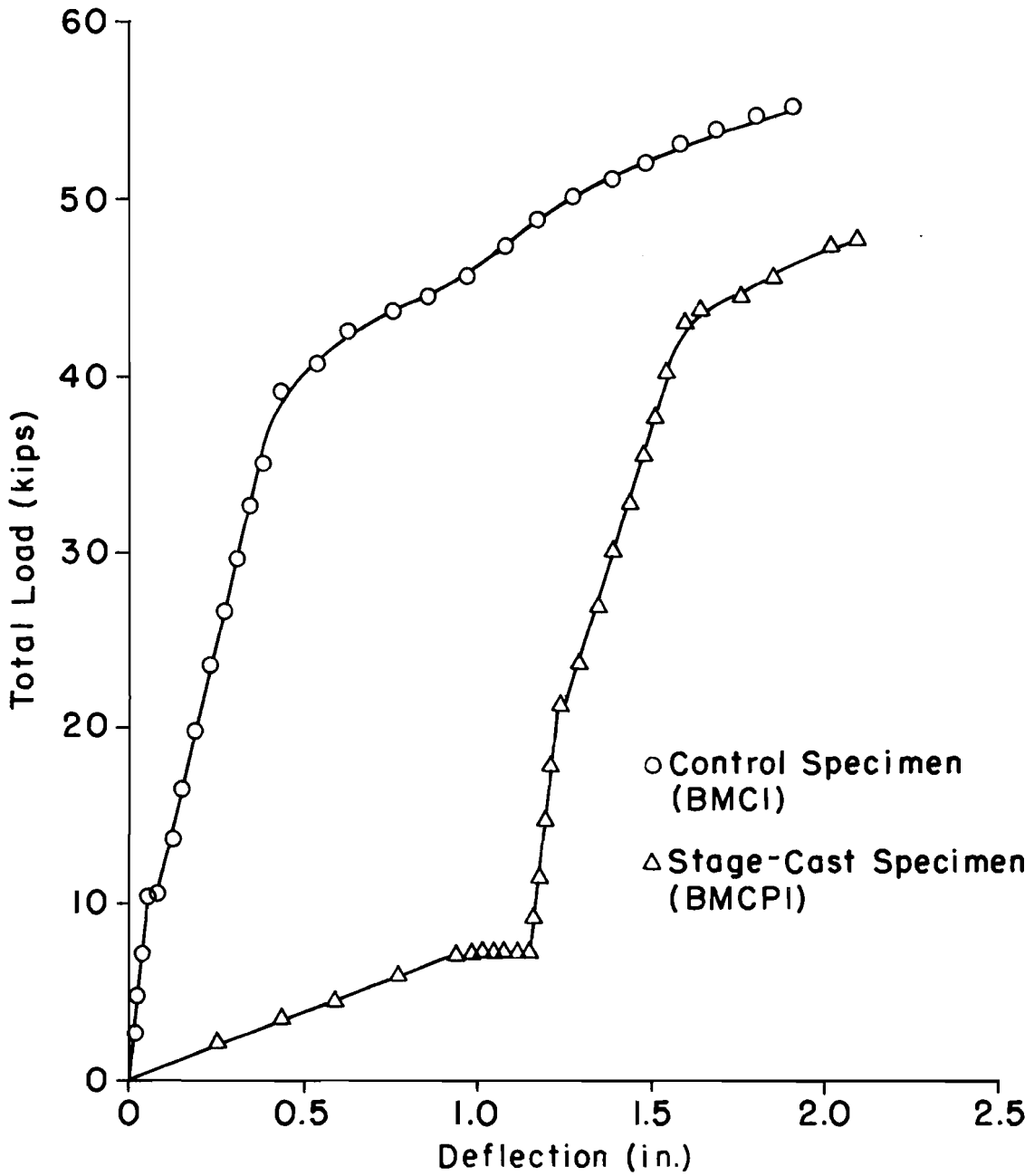

Fig. 3.31 Load-deflection curves for BMC1 and BMCP1, 50-in. cantilever span

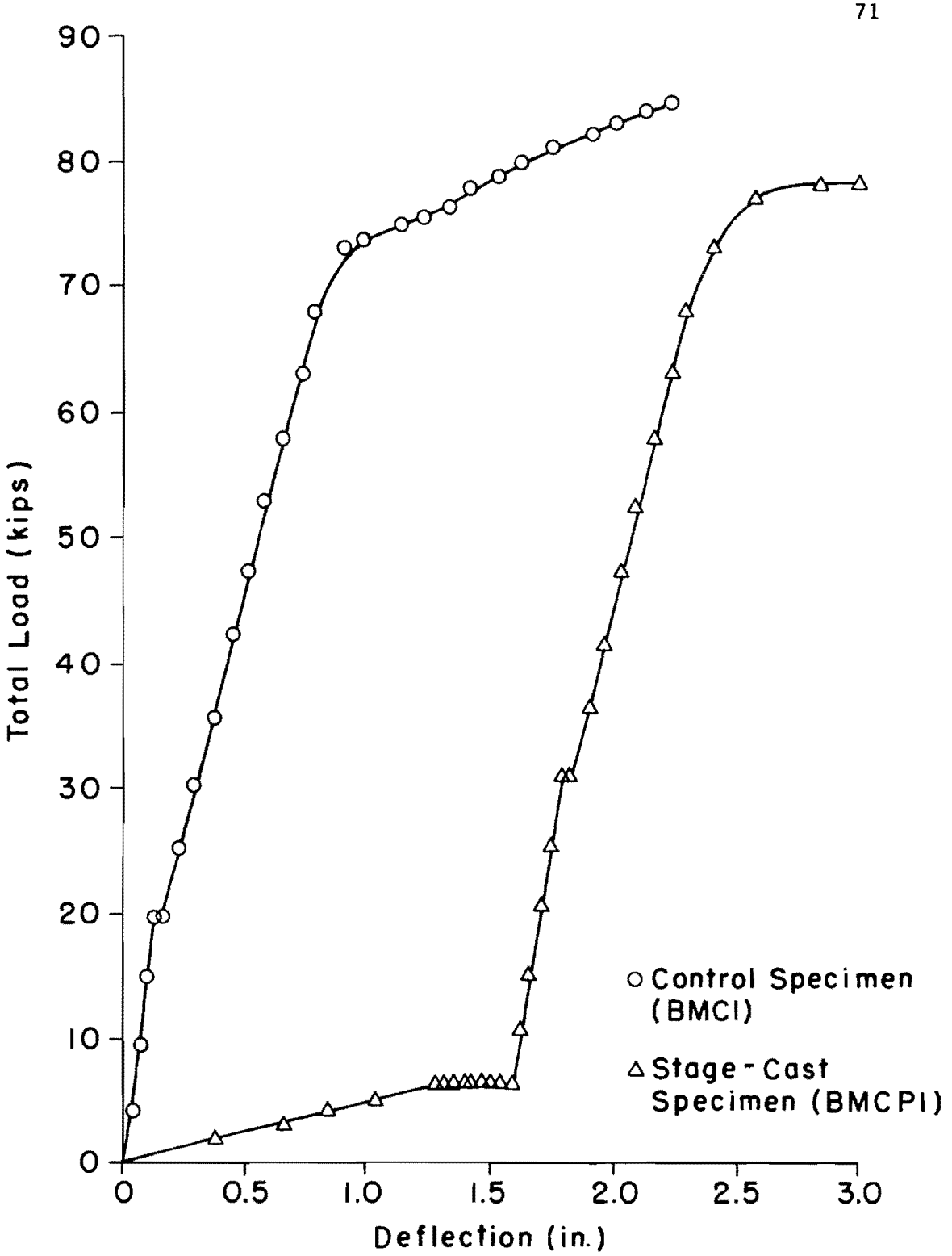

Fig. 3.32 Load-deflection curves for BMC1 and BMCP1, 60-in. cantilever span

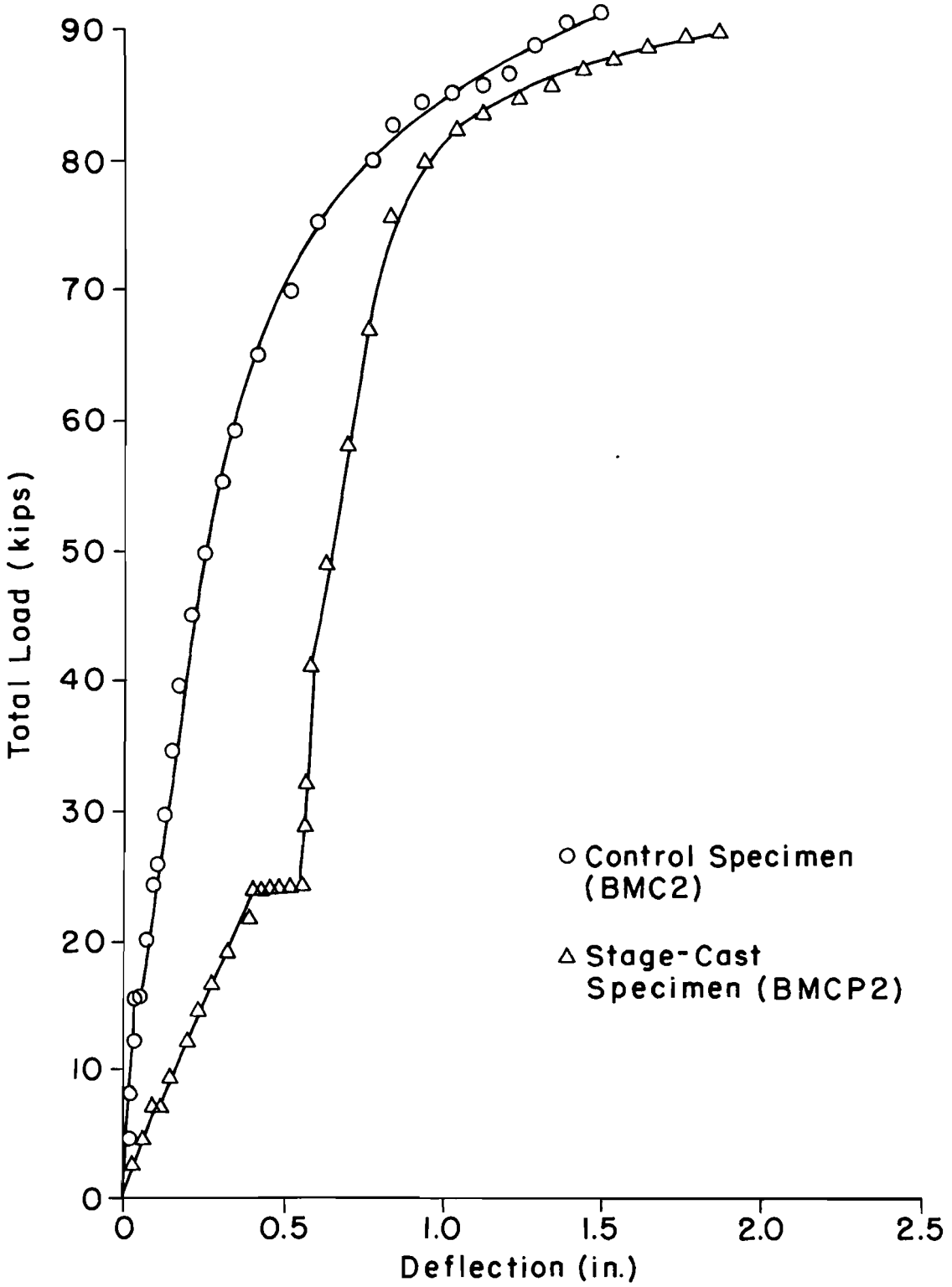

Fig. 3.33 Load-deflection curves for BMC2 and BMCP2, 50-in. cantilever span

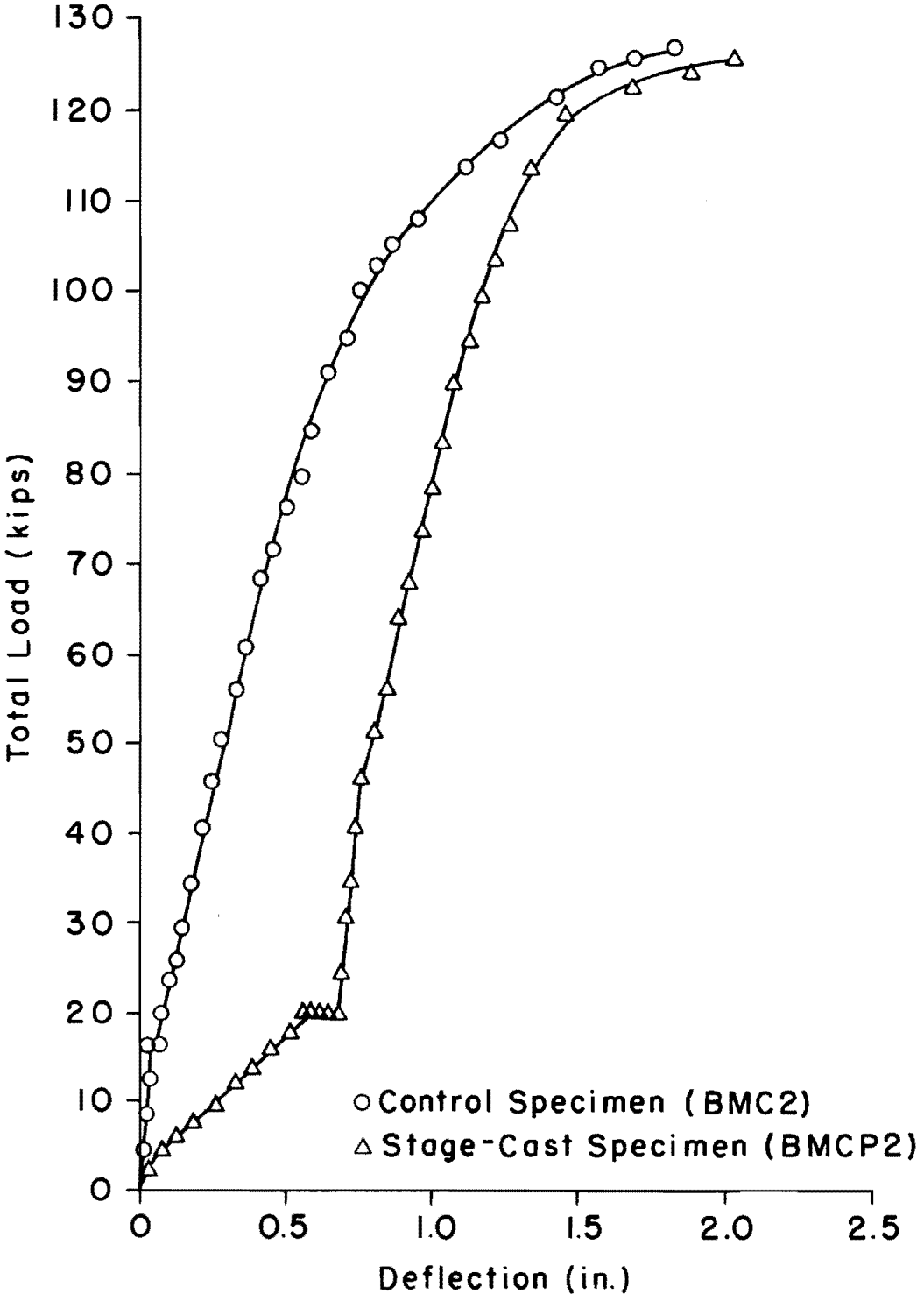

Fig. 3.34 Load-deflection curves for BMC2 and BMCP2, 60-in. cantilever span

than the ultimate strength of monolithic cast thin flanged beams (Figs. 3.31 and 3.32).

Graphs that display force and vertical deformations at the load point for useful range of live load are compared for stage-cast and corresponding monolithic cast specimens in Figs. 3.35 through 3.38. The load ordinates for stage-cast specimens include only the "live" loads that were added after web concrete had set and the beam functioned as a composite member. The corresponding magnitude of flange load was deducted from ordinates of monolithic (control) specimens in order that the force-deformation could be compared.

Thin flange live load response is shown in Figs. 3.35 and 3.36. For both the lightly reinforced 50 in. cantilever and the normally reinforced 60 in. cantilever, the stage-cast specimens were less strong and less ductile than were their monolithic cast companion beams. The yield loads for stage-cast beams were 10 to 15 percent higher than for monolithic cast beams, but the stage-cast beams attained an ultimate curvature only about 60 percent of that reached by monolithic cast beams. The compressive preloading of the thin flanges apparently consumed a significant fraction of the available compressive capacity of these flanges, thereby leading to spalling and crushing failure in the stage-cast members at ultimate live load curvatures much less than those reached by monolithic cast members. The effective stiffness of stage-cast members was virtually identical to that of the monolithic cast members.

The deflection curves of thick flange specimens are shown in Figs. 3.37 and 3.38. With the thicker compression flange, the live load response of the thick flange stage-cast beams revealed more stiffness, a higher yield strength and practically the same strength and ultimate curvature as that observed for the monolithic cast beams. The live load performance of stage-cast beams was either improved or unchanged by the fact of stage-casting of thick flanged beams.

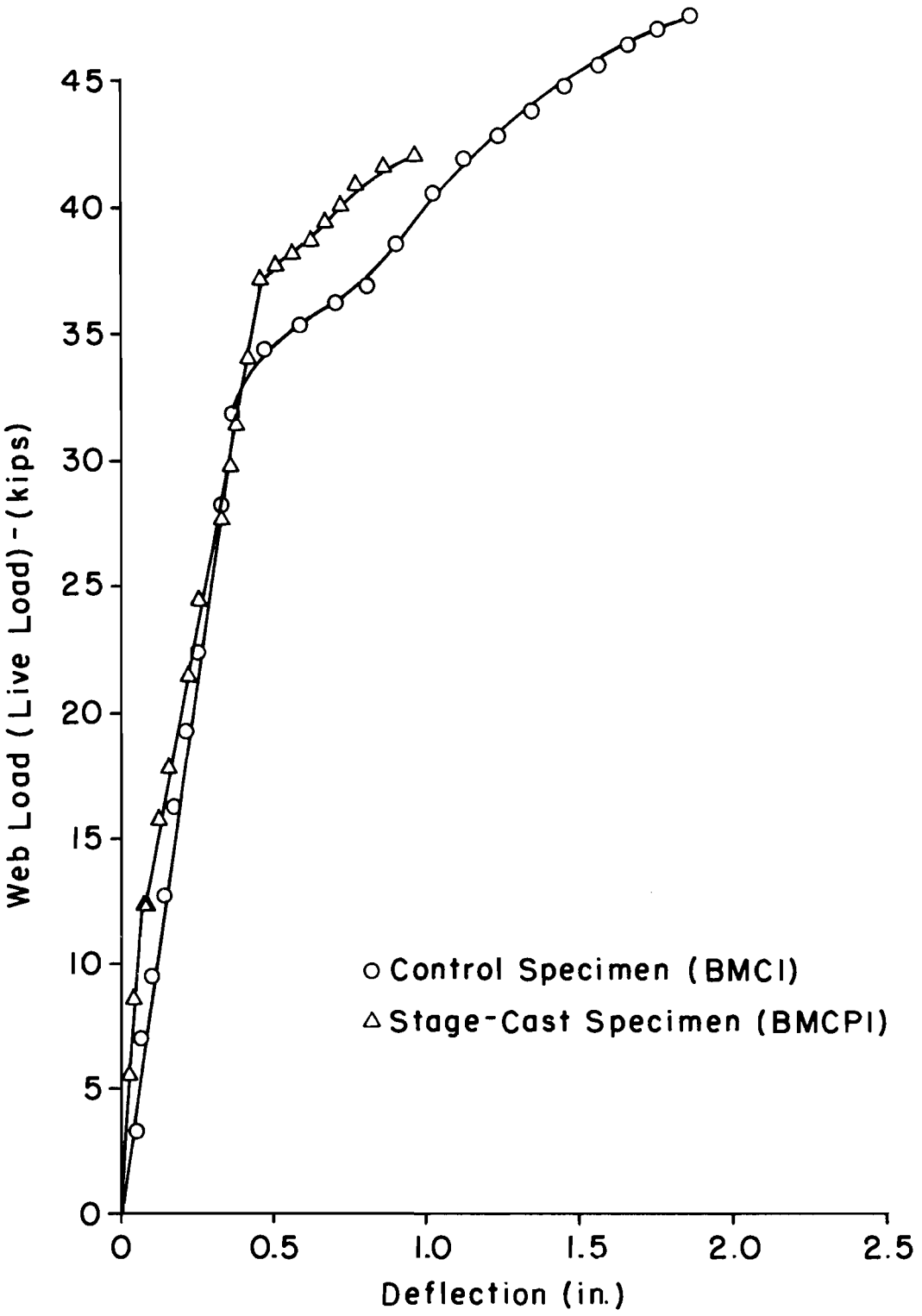

Fig. 3.35 Comparison of live load-deflection curves for 50-in. cantilever span of BMC1 and BMCP1

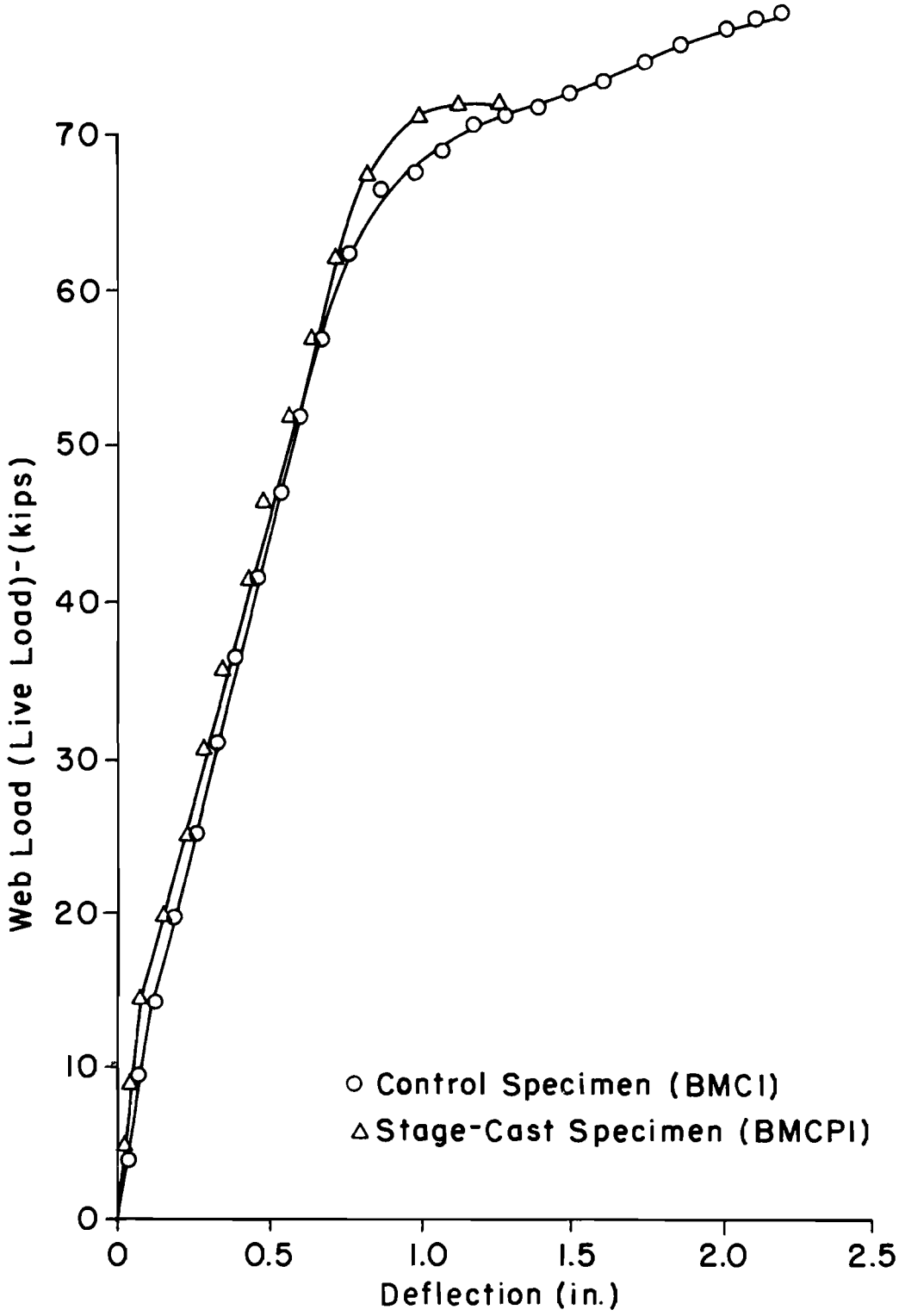

Fig. 3.36 Comparison of live load-deflection curves for 60-in. cantilever span of BMC1 and BMCP1

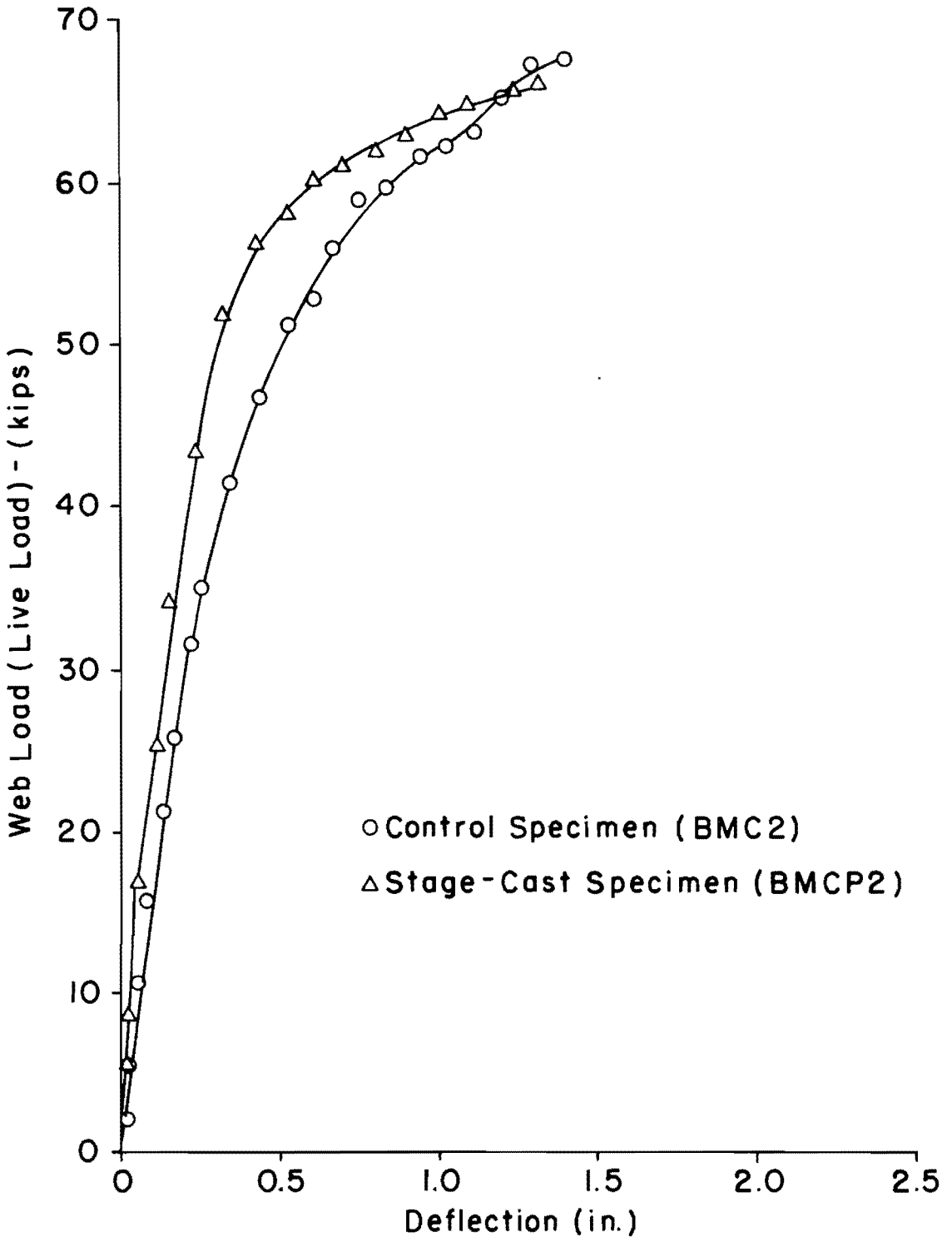

Fig. 3.37 Comparison of live load-deflection curves for 50-in. cantilever span of BMC2 and BMCP2

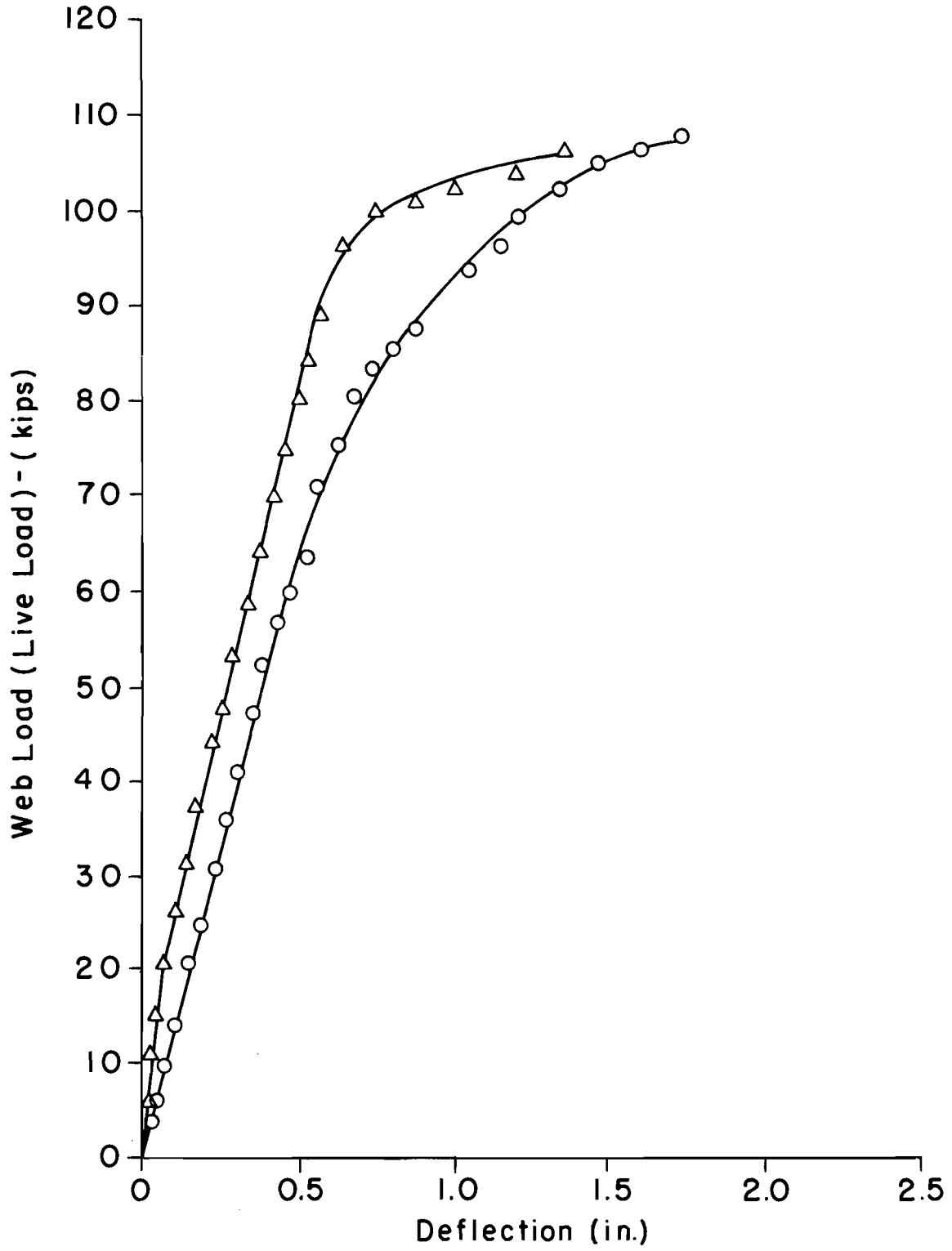

Fig. 3.38 Comparison of live load-deflection curves for 60-in. cantilever span of BMC2 and BMCP2

The performance of thin flanged stage cast beams was either unchanged or inferior to the performance of monolithic cast beams. The relative depth of the stage-cast flange is obviously an important parameter in the design of stage-cast inverted T beams when the flange is to act always in compression. The preloaded strains in the thin flange exceeded 0.1 percent (Fig. 3.19) before the web was cast and subsequent live load was applied. With the high preload in the flange, its capacity to resist live load was reduced approximately 10 percent, and the amount of live load deformation capacity was reduced about 40 percent. The 11 in. thick flange was preloaded to a strain of only 0.05 percent (Fig. 3.20). It exhibited a negligible decrease in live load flexural capacity, and only a 20 percent decrease in deformation capacity. Until more data are acquired, it seems advisable to encourage the use of enough supplementary compressive reinforcement to keep dead load strains in concrete below 0.05 percent.

3.2.3 Cracking. The growth of crack size in cantilever specimens is displayed in Figs. 3.39 through 3.42. Each figure contains graphs of the width of the most prominent cracks for a stage-cast beam and its monolithic companion beam as loads were increased. In general, the loads reached more than 70 percent of the ultimate values before the cracks started rapidly to expand. The data acquired are not adequate to suggest significant differences in the response from stage-cast to monolithic beams, although cracking progressed in more nearly the same size and loading for the thicker flanged specimens than in the thin flanged specimens.

Cracks in stage-cast thin flanged beams became larger at lower levels of service "live" load than in the monolithic thin flanged beams. Crack sizes at the service dead load, service full load, yield load, and ultimate load (last reading before failure) are tabulated in Table 3.6. If the CEB criteria of Table 3.2 were applied as for the positive moment specimens, only the thin flanged cantilever specimens should be in any hazard of developing unacceptable cracks under service loading.

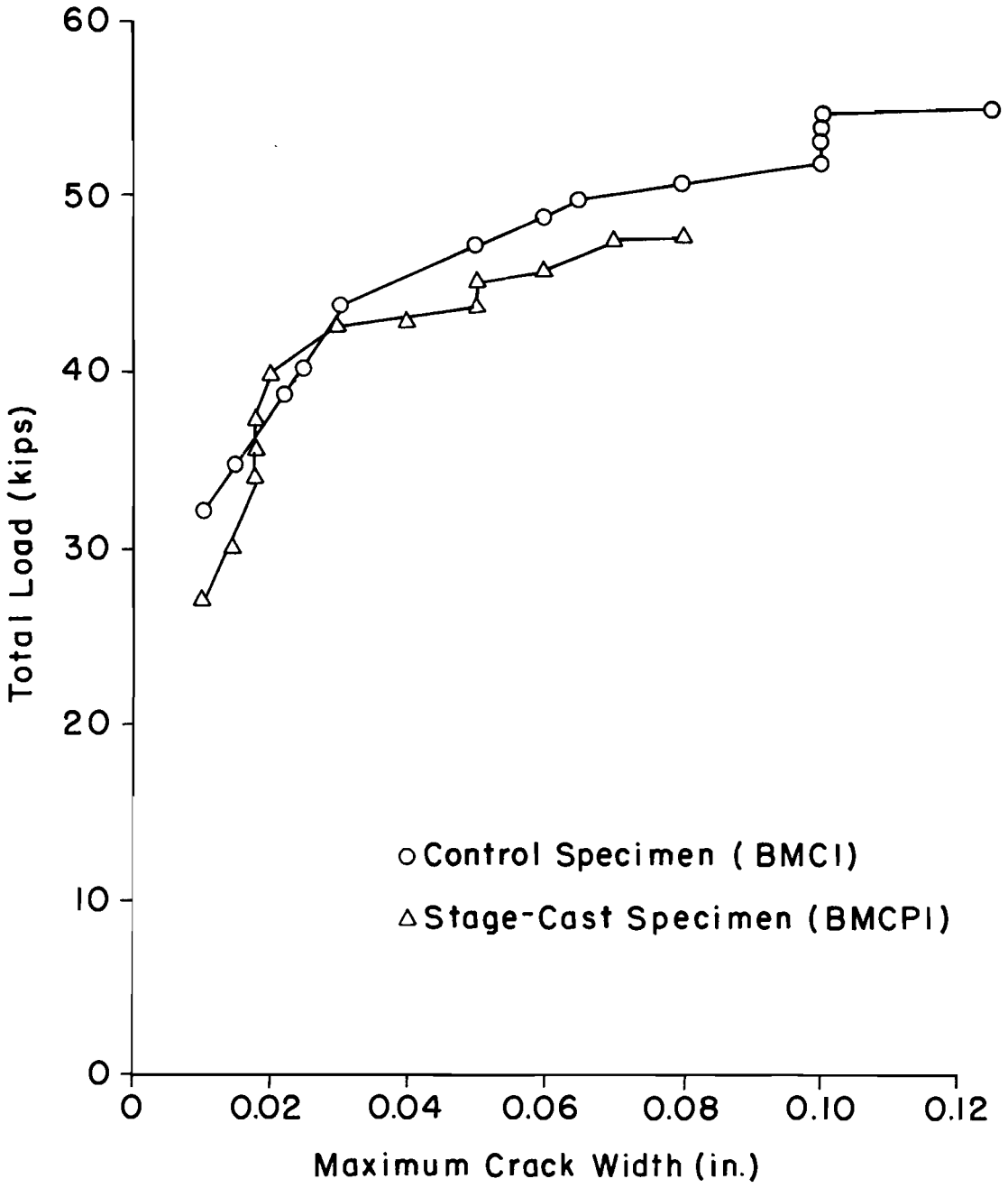

Fig. 3.39 Load-crack size relation for BMC1 and BMCP1, 50-in. cantilever span

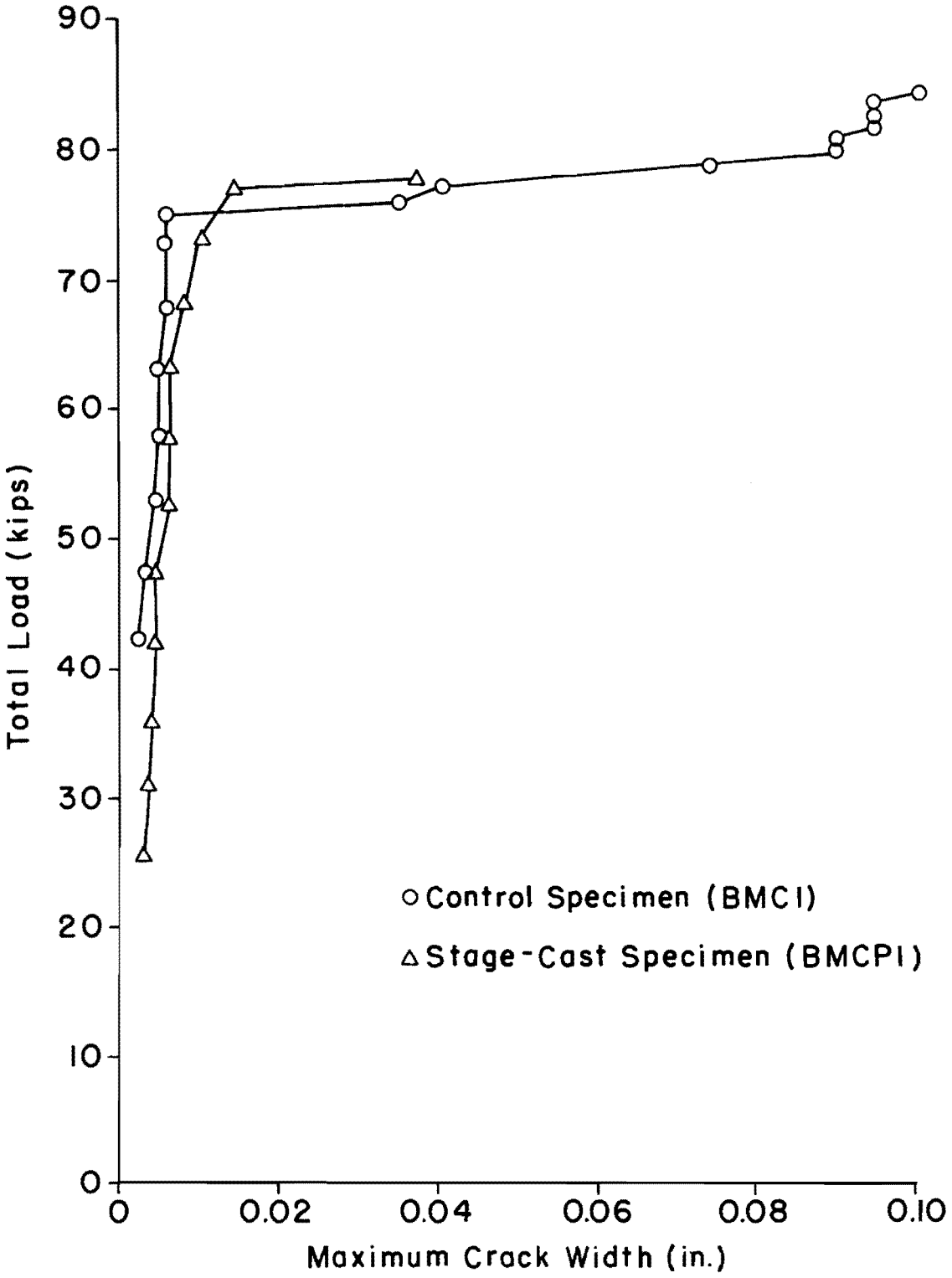

Fig. 3.40 Load-crack size relation for BMC1 and BMCP1, 60-in. cantilever span

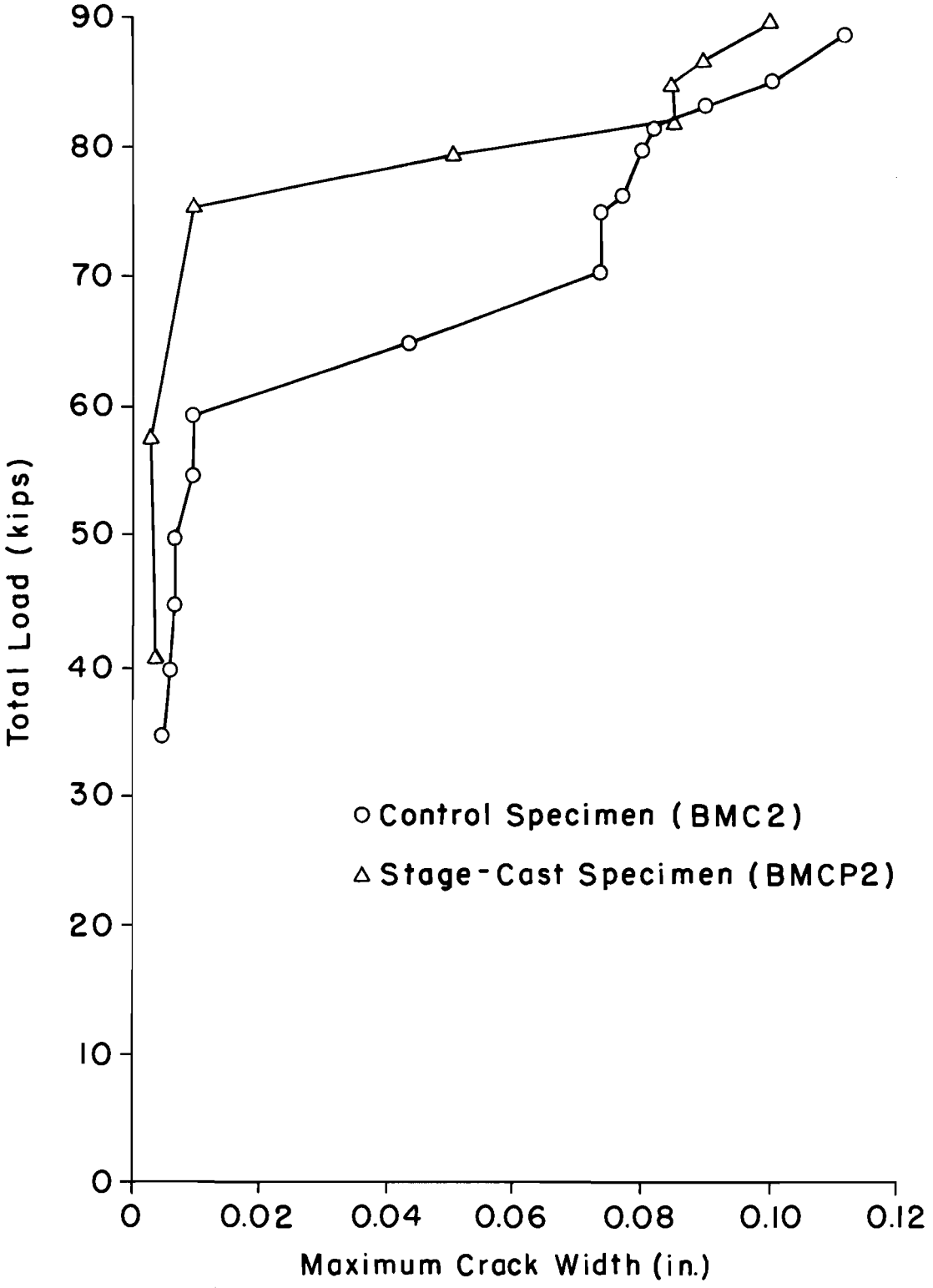

Fig. 3.41 Load-crack size relation for BMC2 and BMCP2, 50-in. cantilever span

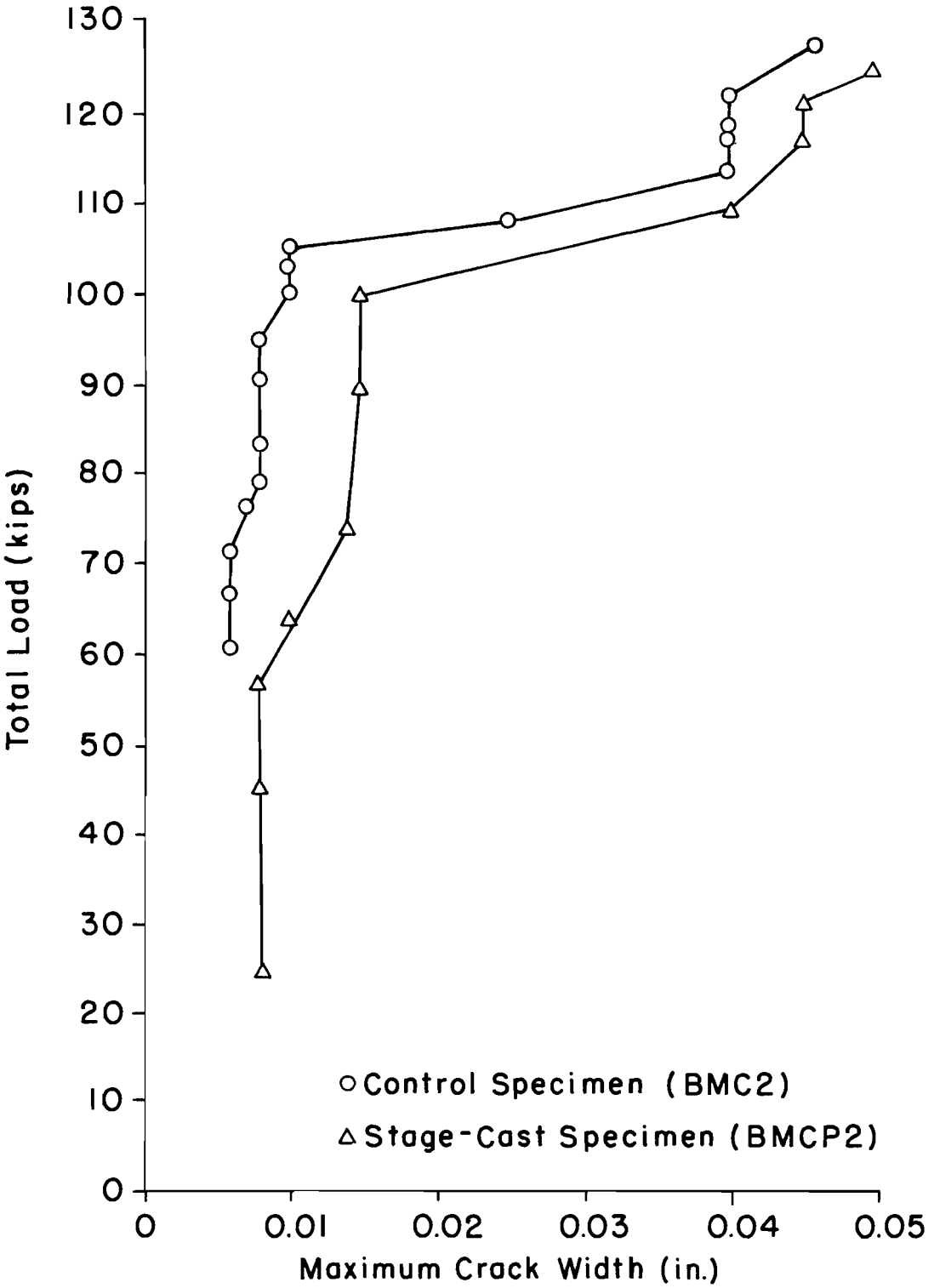

Fig. 3.42 Load-crack size relation for BMC2 and BMCP2, 60-in. cantilever span

TABLE 3.6 MAXIMUM MEASURED CRACK WIDTHS FOR SPECIMENS

Specimen	ρ	Full DL (Zero LL) (kips)	Service Load (from AASHTO Load Factors) (kips)	Yield Load (kips)	Ultimate Load (kips)	Maximum measured crack width at Full DL (Zero LL) (in.)	Service Load (in.)	Yield Load (in.)	Ultimate Load (in.)
BMC1 (50)	0.0029	7.2	18.4	35.3	55.1	< 0.001	0.006	0.015	0.120
BMCP1 (50)	0.0029	7.2	18.4	40.2	47.9	0.005	0.017	0.045	0.080
BMC1 (60)	0.0078	6.0	33.3	68.2	84.6	< 0.001	0.006	0.015	0.100
BMCP1 (60)	0.0078	6.0	33.3	68.1	77.1	0.006	0.015	0.027	0.038
BMC2 (50)	0.0023	24.0	41.5	65.4	91.5	0.002	0.007	0.043	0.110
BMCP2 (50)	0.0023	24.0	41.5	76.0	90.0	0.005	0.008	0.012	0.100
BMC2 (60)	0.0062	20.0	53.5	105.0	128.8	< 0.001	0.010	0.025	0.046
BMCP2 (60)	0.0062	20.0	53.5	120.0	127.0	0.008	0.008	0.045	0.050

On the basis of deflection performance and cracking, the stage-cast thin flanged cantilever specimens did not function as well as did their monolithic cast counterparts, but the thick flange stage-cast cantilever specimens seemed to function very much the same as did the thick flanged monolithic specimens.

3.3 Analysis of Strength

An analysis of flexural strength was made for each of the test specimens. All of the steel reinforcement A_{s1} in the tension face of each beam reached strains in the order of 1 percent, and all of the steel reinforcement A_{s2} in the top edge of the flanges of the inverted T beams yielded before failure took place. Therefore, a total tensile force equal to the product of each steel area and its yield strength had to be equilibrated by a flexural compression force. It was assumed that a concrete stress of $0.85f'_c$ acted at the extreme fibers of the compression face such that a rectangular stress block depth "a" could be computed for each effective width b of the compression flange.

$$a = \frac{A_{s1}f_{y1} + A_{s2}f_{y2}}{0.85f'_c\, b}$$

Then the ultimate moment could be calculated as the sum of tensile forces and moment arms about the centroid of compression which would be located at 0.5a from the compression face,

$$M_{calc} = A_{s1}f_{y1}(d_1 - a/2) + A_{s2}f_{y2}(d_2 - a/2).$$

Properties of specimens and computed values of flexural strength M_{calc} are tabulated in Table 3.7. The observed values of moment at yielding of steel in the tension face M_{yield}, and the observed ultimate moments M_{test} are listed also in Table 3.7. At the extreme right-hand column of Table 3.7 the ratios M_{calc}/M_{test} are shown.

TABLE 3.7 ANALYSIS OF STRENGTH

Specimen	f'_c ksi	b in.	d in.	A_{s1} $in.^2$	f_{y1} ksi	d_2 in.	A_{s2} $in.^2$	f_{y2} ksi	M_{calc} in.-k	M_{yield} in.-k	M_{test} in.-k	$\frac{M_{calc}}{M_{test}}$
BMS1	4.85	8.25	21.1	1.77	65.5	17.5	0.40	65.5	2596	2681	3159	0.82
BMSP1	4.00	9.05	21.7	1.77	65.5	18.2	0.40	65.5	2664	2063	3099	0.86
BMS2	5.21	8.31	26.0	3.93	60.7	17.6	0.40	65.5	5711	5424	7092	0.81
BMSP2	5.54	7.88	26.3	3.93	60.7	17.9	0.40	65.5	5798	3873	6798	0.85
BMC1 (60)	4.78	22.0	19.4	3.52	60.7	4.6	2.20	60.7	4085	4094	5075	0.80
(50)	4.78	22.0	21.0	1.32	60.7	4.6	2.20	60.7	2042	1764	2753	0.74
BMCP1 (60)	4.78	22.0	19.8	3.52	60.7	4.6	2.20	60.7	4171	4394	4623	0.90
(50)	4.78	22.0	21.3	1.32	60.7	4.6	2.20	60.7	2066	2008	2396	0.86
BMC2 (60)	4.92	22.3	24.4	3.52	60.7	4.6	3.52	60.7	6286	6300	7726	0.81
(50)	4.92	22.3	26.0	1.32	60.7	4.6	3.52	60.7	3672	3269	4577	0.80
BMCP2 (60)	4.92	22.9	26.2	3.52	60.7	4.6	3.52	60.7	6670	7203	7621	0.88
(50)	4.92	22.9	24.7	1.32	60.7	4.6	3.52	60.7	3567	3801	4500	0.79

All calculated values of flexural capacity were less than the test values by at least 10 percent and by as much as 26 percent. Since the basic theory upon which the calculations were based involves mechanisms that are rather insensitive to variations of f'_c and even to small changes of d or b, the higher observed values of flexural capacity must be attributed to an effective steel stress in excess of f_y at the very high strains near 1 percent.

It is significant to note that the largest ratios between M_{calc} and M_{test} were obtained in tests of the stage-cast members. In positive moment specimens, stage-cast beams developed about 5 percent less capacity than did the monolithic cast beams and in negative moment specimens the stage-cast beams resisted about 10 percent less moment than that resisted by identical monolithic cast specimens, except for the very lightly reinforced deep flange test of BMCP2 (50).

The yield moments observed in tests of monolithic cast beams were virtually equal to calculated values of moment capacity, encouraging the conclusion that tensile steel developed higher stress levels before failure was observed. The yield moments of stage-cast members, however, were generally significantly lower than the calculated capacities because the stage-casting procedure "locked in" about 75 percent of the yield stresses before webs were cast and loading was continued. The live load behavior of stage-cast members and their apparent ductility in positive moment flexure from live load was more favorable than that of monolithic cast beams, as has been discussed in Sec. 3.1.5.

Even though it is reassuring to observe that the calculated ultimate moments were never as large as those resisted by test specimens, there is evidence that stage-casting can lead to a capacity lower than the capacity of the equivalent, monolithic cast members. Moments actually resisted before failure during tests were larger than those that had been estimated by calculations because the maximum tension force in steel was larger than the nominal yield load of bars. In spite of stage-casting, all compression regions of beams were sufficiently tough or ductile in

compression to resist the ultimate post-yield tensile forces that actually developed in reinforcement. It can be concluded that stage-casting does not invalidate traditional rectangular stress block theory for concrete in flexure when the stage-cast beams contain ductile reinforcement that strain hardens or resists stresses greater than nominal yield before reaching 1 percent strain.

CHAPTER 4

CONCLUSIONS

On the basis of load tests on eight inverted T-beam specimens, four of which were constructed with flanges that were preloaded before webs were cast, the following answers can be offered to the Chapter 1 questions that motivated the study:

(1) Are crack widths in stage-cast members larger or smaller than crack widths in monolithically cast members?

Crack widths were produced in all stage-cast members before webs were cast, and the cracks remained larger than those of monolithic cast members when loading consisted only of dead load from supported floor or deck stringers. As live loads were added to stage-cast members, the initial cracks increased in size at a somewhat slower rate than corresponding cracks in monolithic cast specimens. At the assumed level of design service loads, the cracks in thin flanged stage-cast beams reached levels that should not be accepted for structures exposed to severe weather. Cracking of thick flanged stage-cast beams developed crack widths no more severe than those that developed in monolithic cast beams under design service loads.

(2) Can a close spacing of cracks in a precast flange propagate and create a closer spacing of cracks in the web of stage-cast beams?

Cracks that developed in stage-cast webs tended to propagate from cracks in the preloaded and cracked flanges, but not all flange cracks propagated into web cracks. Consequently, it can be concluded that the sizes and the spacing of web cracks were influenced little, if any, by stage-casting.

(3) How does stage-casting influence live load flexural stiffness?

Stage-cast beams were roughly twice as stiff as monolithic cast beams when each was acted upon by service live loads that created positive moment. The stiffness of stage-cast specimens was only slightly greater than that of monolithic cast specimens subjected to negative moment. When used as cantilevers, the flexural stiffness of stage-cast inverted T-beams should be considered to be the same as the flexural stiffness of monolithic cast beams.

(4) How does stage-casting affect ultimate load flexural ductility?

The live load ductility of stage-cast positive moment regions was better than the live load ductility of monolithic cast regions of inverted T-beams, but the ultimate curvature and deflection reached before failure was virtually the same for both the stage-cast and monolithic cast positive moment specimens. The same improvement in ductility but unaffected ultimate deflection was observed for the deep flanged specimens subjected to cantilevered loading. The ductility and the ultimate deflection of thin flanged stage-cast inverted T-beams were less than the ductility and ultimate deflection reached by monolithic cast beams.

(5) In the flanges of a negative moment region of an inverted T-beam, does the rectangular stress block analysis of concrete capacity continue to give an accurate estimate of flexural capacity?

When flexural tension reinforcement strain hardens before rupture or reaches stress levels higher than its nominal yield strength before concrete reaches strains near 0.3 percent, the use of the rectangular stress block for analysis of concrete capacity need not be modified for stage-cast beams that are analyzed for failure at the nominal yield stress level of reinforcement.

(6) Should there be a special construction load design condition for proportioning stage-cast inverted T-beams?

No special ultimate load factors should be necessary for construction (dead) loads applied only to the flanges of stage-cast beams,

if the flange thickness is at least 40 percent of the composite depth of the inverted T-beam. Flanges less thick than 40 percent of the composite depth of the stage-cast composite member should be analyzed for deflection and probable crack sizes under construction loading. The larger relative deflections (including creep under sustained loads) of thin flanges makes web forms more difficult to fit to the deflected surface before the web is cast. Unacceptably large cracks caused by construction loads do not close after web concrete hardens.

In general it can be concluded that the positive moment behavior of stage-cast inverted T-beams actually is slightly improved by the process of stage-casting. The negative moment behavior of stage-cast inverted T-beams is virtually the same as the negative moment behavior of monolithic cast beams, if the flange thickness is at least 40 percent of the overall height of the composite member. The negative moment behavior of stage-cast inverted T beams is not as good as that of monolithic cast beams, if the flange thickness is only 27 percent of the overall height of the composite member.

R E F E R E N C E S

1. American Concrete Institute, Building Code Requirements for Reinforced Concrete (ACI 318-71), Detroit, 1971.

2. American Concrete Institute, Commentary on Building Code Requirements for Reinforced Concrete (ACI 318-71), Detroit, 1971.

3. Ferguson, P. M., Reinforced Concrete Fundamentals, Third Edition, John Wiley & Sons, Inc., New York, 1973, pp. 12-13.

4. Timoshenko, S., and Goodier, J. N., Theory of Elasticity, Second Edition, McGraw-Hill Book Co., Inc., New York, 1951, pp. 166-171.

5. Department of Civil Engineering, The University of Missouri, "Structural and Economic Study of Precast Bridge Units: Instrumentation," Technical Report No. 1, Cooperative Research Project, Engineering Experiment Station, Columbia, 1957, pp. 6-16.

6. ACI-ASCE Committee 333, "Tentative Recommendations for Design of Composite Beams and Girders for Buildings," Journal of the American Concrete Institute, Vol. 32, No. 6, December 1960, pp. 609-628.

7. Badoux, J. C., and Hulsbos, C. L., "Horizontal Shear Connection in Composite Concrete Beams under Repeated Loads," Journal of the American Concrete Institute, Proc. V. 64, No. 12, December 1967, pp. 811-819.

8. Grossfield, B., and Brinstiel, C., "Tests of T-Beams with Precast Webs and Cast-in-place Flanges," Journal of the American Concrete Institute, Proc. V. 59, No. 6, June 1962, pp. 843-851.

9. Hanson, N. W., "Precast-Prestressed Concrete Bridges: (2) Horizontal Shear Connections," Journal of the PCA Research and Development Laboratories, Vol. 2, No. 2, May 1960, pp. 38-58.

10. Ozell, A. M., "Behavior of Single-span and Continuous Composite Prestressed Concrete Beams," Journal of the Prestressed Concrete Institute, Vol. 2, No. 1, June 1957, pp. 18-31.

11. Revesz, S., "Behavior of Composite T-Beams with Prestressed and Unprestressed Reinforcement," Journal of the American Concrete Institute, Vol. 24, No. 6, February 1953, Proc. V. 49, pp. 585-592.

12. Saemann, J. C., and Washa, G. W., "Horizontal Shear Connections between Precast Beams and Cast-in-Place Slabs," Journal of the American Concrete Institute, Proc. V. 61, No. 11, November 1964, pp. 1383-1409.

13. Broms, B. B., "Crack Width and Crack Spacing in Reinforced Concrete Members," Journal of the American Concrete Institute, Proc. V. 62, No. 10, October 1965, pp. 1237-1256.

14. Comité Européen du Béton, Bulletin d'Information No. 24, Paris, 1960.,

15. Gergely, P., and Lutz, L. A., "Maximum Crack Width in Reinforced Concrete Flexural Members," Causes, Mechanism, and Control of Cracking in Concrete, SP-20, American Concrete Institute, Detroit, 1968, pp. 1-17.

16. Hognestad, E., "High Strength Bars as Concrete Reinforcement, Part 2: Control of Cracking," Journal of PCA Research and Development Laboratories, Vol. 4, No. 1, January 1962, pp. 46-62.

17. Husain, S. I., and Ferguson, P. M., "Flexural Crack Width at the Bars in Reinforced Concrete Beams," Research Report No. 102-1F, Center for Highway Research, The University of Texas at Austin, June 1968.

18. Hognestad, E., "A Study of Combined Bending and Axial Load in Reinforced Concrete Members," Bulletin No. 399, University of Illinois Engineering Experiment Station, Urbana, November 1951.

19. Hognestad, E., Hanson, N. W., and McHenry, D., "Concrete Stress Distribution in Ultimate Strength Design," Journal of the American Concrete Institute, Proc. V. 52, December 1955, pp. 455-479.

20. Mattock, A. H., Kriz, L. B., and Hognestad, E., "Rectangular Concrete Stress Distribution in Ultimate Strength Design," Journal of the American Concrete Institute, Proc. V. 57, No. 8, February 1961, pp. 875-928.

21. Ramaley, D., and McHenry, D., "Stress-Strain Curves for Concrete Strained Beyond Ultimate Load," Laboratory Report No. SP-12, U. S. Bureau of Reclamation, Denver, 1947.

22. Whitney, C. S., "Plastic Theory of Reinforced Concrete Design," Journal of the Structural Division, ASCE, Trans. V. 107, 1942, pp. 251-326.

23. Kaar, P. H., "High Strength Bars as Concrete Reinforcement: Part 8: Similitude in Flexural Cracking of T-Beam Flanges," Journal of the PCA Research and Development Laboratories, Vol. 8, No. 2, May 1966, pp. 2-12.